UNIVERSITÀ DEGLI STUDI DI PADOVA

Dipartimento di Agronomia, Animali, Alimenti, Risorse naturali e Ambiente

Dipartimento del Territorio e Sistemi agroforestali

Laurea magistrale in Scienze e Tecnologie Agrarie

Application of precision agriculture techniques for the differential management of a peach orchard

Relatore

Prof. Luigi Sartori

Correlatore

Prof. José A. Martínez-Casasnovas

Laureanda

Elisa Daniele

Matricola n.1106594

ANNO ACCADEMICO 2015-2016

Index

List of Tables

List of Figures

Abstract

The objective of this work was to investigate the application of precision agriculture techniques in orchard management. For that, a case study in a peach orchard (*Prunus persica*, var. Patty) located in the Lleida province (Catalonia, Spain) was carried out.
To analyze the existence of within-field spatial variability, two types of data were acquired: soil apparent electrical conductivity (ECa) and a multispectral airborne image (0.25 m/pixel). ECa was acquired by means of an on-the-go resistivity sensor (Veris 3100) at two different depths: Shallow (0-30 cm) and Deep (0-90 cm). ECa values were standardized at the reference temperature of 25 ºC. Soil samples were collected in 40 points also at two different depths (0-30 cm and 30-90 cm). Only the samples of the first horizon were analyzed because of time limitation. The properties analyzed were pH, electrical conductivity, equivalent calcium carbonate, cation exchange capacity, organic matter, water retention capacity (WRC) at -33kPa and at -1500kPa, clay, coarse silt, fine silt, coarse sand, fine sand, total silt, total sand. From the multispectral aerial image, the NDVI was calculated and averaged per tree. In addition, the trunk diameter was measured and the number of fruits per tree was counted in selected trees, as indicators of vigor and yield to analyze the relationship with NDVI. Simple linear regression and ANOVAs analysis were carried out to determine the relationships between EC25 or NDVI values and zones (2 or 3 zones) with soil properties, and also between NDVI and the measured vigor and yield parameters.

The results showed that soils were rich in calcium carbonate, the CEC and organic matter were low to moderate and with low WRC, indicating the need of irrigation for fruit trees growing. The most frequent soil texture was loam, clay loam or silty clay loam. Some soils were lightly saline. Shallow and deep EC_{25} values were highly correlated between them, but their spatial distribution seemed to have a relationship with former landforms, which were altered by land levelling works. Instead the spatial distribution of the NDVI seemed to follow a gradient from the south to the north of the plot. There was a positive and significant correlation of the shallow and deep EC_{25} with the $CE_{1:5}$ (p-value < 0.01) and with the WRC at -1500 kPa (p-value < 0.05). The EC_{25} values also showed a negative correlation with the coarse sand fraction. The soil depth also showed a positive significant correlation with the shallow and deep EC_{25}. Per zones, 2 zone EC_{25} maps would be better

than the 3 zone maps to distinguish areas with different soil properties. NDVI performed differently than EC_{25} with respect the relationship with soil properties. In this case, only the textural fractions coarser than clay were correlated. The CEC also showed a certain positive tendency. NDVI was positively correlated to trunk diameter, tree canopy area and the number of fruits, but the NDVI. However, other expected relationships, as the one between EC_{25} and clay content, were not found. This could be probably due to the mask effect of the salts in the ECa signal.

Because of the lack of relationship between EC_{25} and NDVI, two types of management zones were proposed. In any case, 2 zones of EC_{25} or NDVI were better than 3 zones, because one of the 3 is always ambiguous. The Shallow EC_{25} zones would serve mainly to improve the water retention capacity through amendments with organic matter and more frequent irrigation; and to improve natural drainage. NDVI zones would serve as reference to regulate tree vigor and yield through different actions as pruning, growth regulators or fruit thinning.

Acknowledgements

Thanks to University of Lleida, its AgroICT and Department of Environment and Soil Science, for this opportunity of work and hospitality.

1. Introduction and objectives

The present work is intended as a contribution to the application of precision agriculture technologies in the fructiculture sector. It tries to call the attention of this sector because precision agriculture, or site-specific crop management, is widely used in field crops but is not so extensively applied in fruit tree growing yet.

Precision agriculture is a quite recent farming management strategy based on observing, measuring and responding to inter and within-field crop variability. From the beginning (approximately during the early 1990 decade), it has been mainly devoted to arable crops and viticulture, and much less to fructiculture. Maybe, this later application in fructiculture has been determined by varietal and cropping specificities, which do not make them applicable on a large scale. Another reason may be that, although data collection is relatively simple, data processing and interpretation up to a meaningful product to the grower is not so easy.

In Europe, there are areas where fructiculture is the main agricultural sector and where modern precision agriculture techniques are not extensively used yet. Nevertheless, these techniques could play an important role in the near future to increase competitiveness and quality.

According to Eurostat[1], the Mediterranean countries constitute the main fruit production area within Europe. In particular Italy, Spain and Greece are the main producers of peaches, with a total 2619 M tones, out of a total of 2894 M tones produced in Europe. In addition, Italy and Spain are the two most important and competitive countries, that dominate the trend of the European Union fresh fruit exports. In fact, Spanish and Italian exports account for about 45% of the total European fruit production, both in volume and in value in the last decade. In this respect, Spain has increased its exportations to an annual rate of 1.2 % and Italy by 2 % (Palmieri and Pirazzoli, 2013).

The present study was carried out in a peach orchard located in the area of Lleida (Catalonia, NE Spain). The province of Lleida, with a total surface of about 30200 ha

[1]Source: http://ec.europa.eu/eurostat/statistics-explained/index.php/Agricultural_production_-_crops#Fruit

dedicated to fresh fruit production, constitutes the major concentration of sweet fruit production in Spain, and one of the most important in Europe as well (Pascual et al., 2006). In particular, the County of Segrià (with Lleida city as capital of the County) is the main area in the province for sweet fruit growing (Table 1). It is part of the Ebro basin, which is a morphologically flat region and with semi-arid climate. Over the years, irrigation canals to combat aridity have been built, making possible the development and expansion of irrigated agriculture. Segrià's economy has traditionally been based on agriculture and livestock, with a very important specific weight of the fruit sector.

	Lleida municipality	Segrià county	Catalonia
Cultivated land (ha) by type of crop (2009)			
Herbaceous crops	5991	42846	51115
Fruit trees	3603	28459	110819
Olives	328	11229	101236
Vines	2185	2228	61391
Others	14	256	7829
Total	12121	85018	792425
Farm by livestock ownership (2009)			
Without livestock	815	4852	47172
With livestock	161	1122	13667
Total	976	5974	60839

Table 1. Agriculture and livestock in Lleida (municipality), Segrià and Catalonia, years 2009 (http://www.idescat.cat).

The consolidation of the region as prosperous agricultural area was mainly due to changes in the 1960s: the abandonment of traditional dry farming and the starting of fruit-growing thanks to the introduction of irrigation, birth of the first fruit cooperatives, growing demand for fruit (both interior and exterior), generalization of modern use of technology resources during the 1970s and 1980s, and also mechanization systems, training systems, pruning and irrigation. In this way agriculture was integrated into capitalist structures, moving from a subsistence economy to a market economy.

In 2009, the agricultural surface of the Segrià was 139600 ha, with 53170 ha under irrigation. The area devoted to sweet fruit growing was 23915 ha (Statistical Institute of

Catalonia, IDESCAT): mainly pear, apple and peach. In addition, some of the surrounding counties (Pla d'Urgell, Urgell, Noguera and Garrigues), also have substantial extensions of sweet fruit tree plantations, as well as the bordering regions of Aragon.
Other data confirms the importance of Lleida as fruit production region in Spain (Table 2). Lleida is the first Spanish province in pip fruit production (apple and pear) and one of the first in stone fruits (nectarine, peach, and apricot) (Table 2) (Pascual et al., 2006).

	Lleida province	Catalonia
Pear	9137	9659
Apple	6022	8441
Peach and nectarine	13523	16362
Others	1539	3467
Total fresh fruit	30221	37929

Table 2. Agricultural surface (2014) in Lleida (province) and Catalonia (ha). Source: Ministry of Agriculture, Livestock, Fisheries and Food.

Besides this, Lleida has established itself as a city of the area of fruit production with a significant presence of training centres, research and technology transfer related to agriculture and sits one of the largest agricultural areas of the Spanish State (Pascual et al., 2006).

As stated above, the practice of precision agriculture in fructiculture is still scarce. As a crop management concept, precision agriculture can increase crop yields and benefits, reducing at the same time environmental impacts (Stafford, 2000). At present, precision agriculture is considered the set of key advanced technologies that will promote agriculture, in a similar way as in the past three decades, in which global agriculture has made tremendous progress in expanding the world's supply of food (World Resources Institute, 1998).

The fruit orchards usually present spatial variability and, because of that, there are precision agriculture techniques that could help to make fructiculture more productive and competitive. In this respect, several applications in different contexts related to precision plant management have been already reported: irrigation, spraying, inter-row

management, pest monitoring, thinning, fruit growth control, etc. For example, thanks to the development of specific fruit growing curves, by monitoring the growth by means of sensors is possible to identify altering situations from the ordinary fruit development. Also, the prior optical verification of the fruit load can be useful to determine the intensity of subsequent thinning. These issues concern both, researchers and producers, in order to gather information for decision-making. Nevertheless, the success of these actions requires a big renovation of management techniques, with systematic involvement of technicians and producers themselves.

Other applications of precision agriculture techniques are the ones concerning the soil and vigour variability within the fruit tree plantations. Information on the spatial variability of soil properties and/or structural characteristics of trees (height, width, volume, leaf area, etc.), may have innumerable applications in orchard management: application of pesticides, irrigation, fertilization, pruning techniques, etc. Nevertheless, as already stated, there are still few experiences or applications of these types in fructiculture.

According to the above arguments, the main objective of the thesis was to explore some of the possibilities of precision agriculture techniques to improve the management of peach plantations on the basis of within-field variability. In the present work, this variability is characterized by means of soil and vegetation vigor sensing. The management zones based on this study will be oriented to improve fertilization, pruning and drainage.

In this respect, the specific objective of the MSc thesis was to analyze the applicability of apparent electrical conductivity mapping and/or vegetation indices from detailed remote sensing images to identify differential management zones in fruit tree plantations. This was carried out in a reference peach orchard of the fruit growing area of Lleida.

The results and conclusions of this study could benefit not only the fructiculture of Lleida or other parts of Spain, but also the fructiculture of other production regions such as in Italy, where similar situations of soil types, production systems (plantation patterns, irrigation systems and fertilization, among other) exist.

This work was made under the frame of a research project of the National Plan of Research, Development and Innovation funded by the Spanish Ministry of Economy and Competitiveness (project AGL2013-48297CR2-2R).

2. Scientific background

The present work was based on the use of apparent electrical conductivity and vegetation vigor mapping from multispectral airborne images, to map soil properties and to understand the behavior of tree plantations according to soil and terrain variability. Because of that, the scientific background was related to these fields of research within the precision agriculture context.

2.1. Apparent electrical conductivity surveys (ECa) and mapping

Spatial maps of soil properties are invaluable in agriculture for assessing soil quality, planning land use, and determining the suitability of cropping patterns. However, soil maps are costly and difficult to produce. In addition, detailed soil maps for use in precision agriculture, usually do not exist. Normally, the available detailed scale is 1:25000, but it is still not detailed enough to be used in within-field differential management. As an alternative to traditional soil survey methods, mapping of apparent electrical conductivity (ECa) is becoming a technique used to map the spatial variability of soil properties at field scale, being at present a key technique in precision agriculture.

The basic elements of a field-scale ECa survey for application into site-specific crop management include: (i) ECa survey design, (ii) georeferenced ECa data collection, (iii) soil sample design based on georeferenced ECa data, (iv) soil sample collection, (v) physic-chemical analysis of soil properties, (vi) if soil salinity is a primary concern, development of a stochastic and/or deterministic calibration of ECa to soil sample-determined salinity, as determined by the electrical conductivity of the saturated extract (ECe), (vii) spatial statistical analysis, and (viii) determination of the dominant soil properties influencing the ECa measurement at the site of interest (Corwin and Lesch, 2005).

Recent advances in computers, global positioning systems (GPS) and large-scale low-cost soil sensors, that can generate position-referenced data, offer new opportunities for mapping heterogeneous patterns and properties in soils (Johnson et al., 2005). With the development of soil sensors, moreover, data can be obtained without disturbing the soil

and with higher spatial resolution than that obtained through manual or laboratory methods. ECa can be used as a proxy for the relative spatial variability of the prevailing soil properties and provides a simple and reliable tool for characterizing the spatial variation within fields (Bronson et al., 2005; Corwin and Lesch, 2005; McCormick et al., 2009; Moral et al., 2010).

There are two types of sensors to map the soil apparent electrical conductivity: the electromagnetic induction sensors and the resistivity sensors. A soil electromagnetic induction sensor, in fact, is an indirect soil sensing technique that, linked to a GPS, allows measurement of soil electrical conductivity ECa by inducing an electric current in the soil (Viscarra et al., 2011).

On the other hand, electrical resistivity sensors (ER) introduce an electrical current into the soil through current electrodes. The difference in current flow potential is measured at electrodes that are placed near the current flow (Figure 1). Schlumberger in France and Wenner in the United States (Burger, 1992; Telford et al., 1990) developed these methods in the second decade of the 1900s for the evaluation of ground ER.

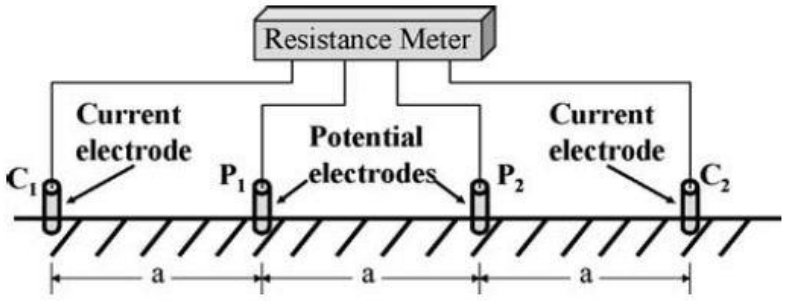

Figure 1. Scheme showing the electrical resistivity method with an array of four electrodes: two current electrodes (C1 and C2) and two potential electrodes (P1 and P2), (Modified from Rhoades and Halvorson 1977). When electrodes are equally spaced at distance "*a*", as shown, the electrode array is called a Wenner array.

The electrode configuration is referred to as a Wenner array. Four electrodes are equidistantly spaced in a straight line at the soil surface, with the two outer electrodes serving as the current or transmission electrodes and the two inner electrodes serving as the potential or receiving electrodes (Figure 1; Corwin and Hendrickx, 2002). The depth of penetration of the electrical current and the volume of measurement increase as the

inter-electrode spacing increases. There are additional electrode configurations that are frequently used, as discussed by Dobrin (1960), Telford et al. (1990) and Burger (1992).

This technique suggests that ECa measured by resistivity sensor at two depths (0-30 cm and 0-90 cm) provides an indication of the heterogeneity of the soil profile, proving to be a useful tool for the delineation of pedologic discontinuities and for detailing the inventory of the field-scale soil stratigraphy.

According to Hanson and Kaita (1997), a linear relationship exists between soil moisture and apparent electrical conductivity for each level of soil salinity over the range of measured soil moistures. In fact, apparent soil electrical conductivity is influenced by soil salinity, but also by water and organic matter content, texture and bulk density (Corwin and Lesch, 2005a). Another important factor influencing ECa is temperature (section 4.3.4).

According to King et al. (2005), in saline soils, the biggest contributor to electrical conductivity can be the solute concentration. Rhoades and colleagues primarily conducted research in this sector in the 1970's at the USDA-ARS Salinity Laboratory in Riverside. Soil salinity refers to the presence of major dissolved inorganic solutes in the soil aqueous phase, which consist of soluble and readily dissolvable salts including charged species (Na^{+}, K^{+}, Mg^{+2}, Ca^{+2}, Cl^{-}, HCO_3^{-}, NO_3^{-}, SO_4^{-2} and CO_3^{-2}), non-ionic solutes, and ions that combine to form ion pairs.

Historically, five methods have been developed for determining soil salinity at field scales: (i) visual crop observations; (ii) the electrical conductance of soil solution extracts or extracts at higher than normal water contents; (iii) in situ measurement of electrical resistivity (ER); (iv) non-invasive measurement of electrical conductance with electromagnetic induction (EM) or electrical resistivity (ER); and most recently (v) in situ measurement of electrical conductance with time domain reflectometry (TDR). In this work was used the third, to obtain ECa.

Because electrical conductivity of the saturation extract (ECe (dS/m)) has been the standard measure of salinity used in all soil salinity studies, a finally relation between

ECa and ECe is needed to relate ECa back to ECe. Over the past decade, research has been directed at developing reliable and efficient conversion techniques from ECa back to ECe (section 4.3.4).

Instead, under non-saline conditions, in fact, soil texture (more specifically clay content and low concentrations of dissolved electrolytes) and soil water content (SWC) are the two predominant factors influencing ECa (Doolittle and Brevik, 2014), such as several studies have demonstrated (Domsch and Giebel, 2004; Sudduth et al., 2005; Saey et al., 2009a; Martínez et al., 2012).

For example, it has been demonstrated that, while the magnitude of temporal ECa measurements varies with soil moisture and temperature, generally the spatial patterns of ECa remain constant. This finding of temporal stability is essential to successfully use ECa mapping as a basis for soil-sampling and mapping in precision agriculture (Johnson et al., 2005; Brevik et al., 2006).

Because ECa is among the most useful and easily obtained spatial properties of soil that affects crop productivity, it has become a popular tool for characterizing field variability to support site-specific soil management (Guo et al., 2012; van Meirvenne et al., 2013; Bonfante et al., 2015).

Another aspect to remember is that ECa techniques may prove to be more effective when the soil profile is moist and it less effective during dry periods.
It is essential to know that in most cases ECa measurements are not sufficient to describe the spatial distribution of all soil properties influencing yield, because ECa are dominated by one or two soil properties (Johnson et al., 2005). Often, in such cases other types of ancillary information can be used to complement ECa (Gomez et al., 2008; Zhang et al., 2012).

Finally, although some studies have shown a general relationship between yield and ECa, this only indicates that the factors contributing to soil fertility are also those that lead to high conductivity.

While ECa measurements may be more directly dependent on certain physical soil properties, yield is more likely to be an integrated response to those "characteristics" that are most important for crop growth (King et al., 2005). It is due to the complex interaction of biological, anthropogenic, and meteorological factors that influence yield beyond soil-related factors, thereby confounding results (Corwin and Lesch, 2003).

In this work, spatial measurements of ECa were used to create maps and to establish a soil sample design (section 4.3.5).

2.2. Vegetation vigor mapping from multispectral airborne images

In the late 1970s and early 1980s, Tucker and co-workers showed that green vegetation can be monitored through its spectral reflectance properties. Then, the availability of the first satellite Landsat images from 1972 impulsed the use of remote sensing to monitor the vegetation vigor. Since then and up to the present, remote sensing (multispectral satellite, airborne or drone images) comprises another interesting field of research in agriculture.

Spectral vegetation indices (or crop vigor indices) are constructed from information obtained from multispectral images (spectral reflectances at different wavelengths, specifically in the blue, B, green, G, red, R and near infrared, NIR, bands). The most frequent indices used in precision agriculture are based on the reflectance of the plant in the red (0.6-0.7 μm) and near infrared (NIR) (0.7-1.3 μm). When a plant is actively growing (healthy and not under stress), it absorbs the red and reflects the near infrared. Conversely, when a plant is not in a growth phase, or when it is stressed, it absorbs the NIR and reflects the red. This has leaded to create different ratios or indices (vegetation indices) such as the PCD (Plant Cell Density), the PVR (Photosynthetic Vigor Ratio) and the most commonly used index by far, the NDVI (Normalized Difference Vegetation Index) (Johnson et al., 2003) (Equation 1). The PCD is calculated as the ratio of near infrared to red reflectance (NIR/R).

Equation 1

$$\mathbf{NDVI} = \frac{(\mathbf{NIR}-\mathbf{R})}{(\mathbf{NIR}+\mathbf{R})}$$

The NDVI has become the most popular indicator for studying vegetation health and crop production, because is indicative of the photosynthetical activity of the green vegetation

(Rouse et al., 1974). It has proven to be sensitive to variations in aboveground biomass (Boelman et al., 2003) and leaf area (van Wijk and Williams 2005; Street et al., 2007).

Correlation of these indices with certain structural or physiological characteristics of the vegetation is, in general, satisfactory. Thus for example, the LAI (Leaf Area Index), the presence of nutritional deficiencies, the water stress status or the health disorder status (incidence of pests or diseases) can be inferred based on calculation of the NDVI or other narrow-band hyperspectral vegetation indices sensitive to chlorophyll content.

Specifically, the high reflectivity which a vigorous and healthy trees present in the near infrared band in comparison to one of poor vigor or subject to adverse conditions (water stress), enables detection of these differences. Thus, the use of this data enables differentiation within the orchards of areas of different vigor.

Interest in estimation of orchard vigor (or leaf density), through the use of local or remote sensors, is due to the influence that may have in the orchard production. However, full understanding of the orchard-production-quality interrelationship requires more research into the linkages between, for instance, remote sensed vegetation indices and fruit-production-quality parameters.

The use of the normalized difference vegetation index (NDVI) acquired from airborne and satellite sensors addresses this need, as it is widely used as a tool for detecting and quantifying spatial and temporal dynamics of tundra vegetation cover, productivity, and phenology.

3. Study area description

3.1. Location of the study area

The present research was carried out in a commercial peach tree plantation located in the municipality of Aitona (Lleida, Catalonia, NE Spain) (Figure 2).

From the physical point of view, the study area is located in the central part of the Tertiary Ebro Depression, at the left bank of the River Segre. The study plantation is just to the south of the Utxesa reservoir. This reservoir actuates as regulator of the water of the Seròs Channel, which gives water to a hydroelectric power station located in Seròs. The study area is also located within the limits of the "Secans del Segrià i Utxesa" (rainfed land of Segrià and Utxesa), which belongs to the Natura 2000 network. In the study field, the irrigation water is pumped from the river Segre and stored in a local reservoir.

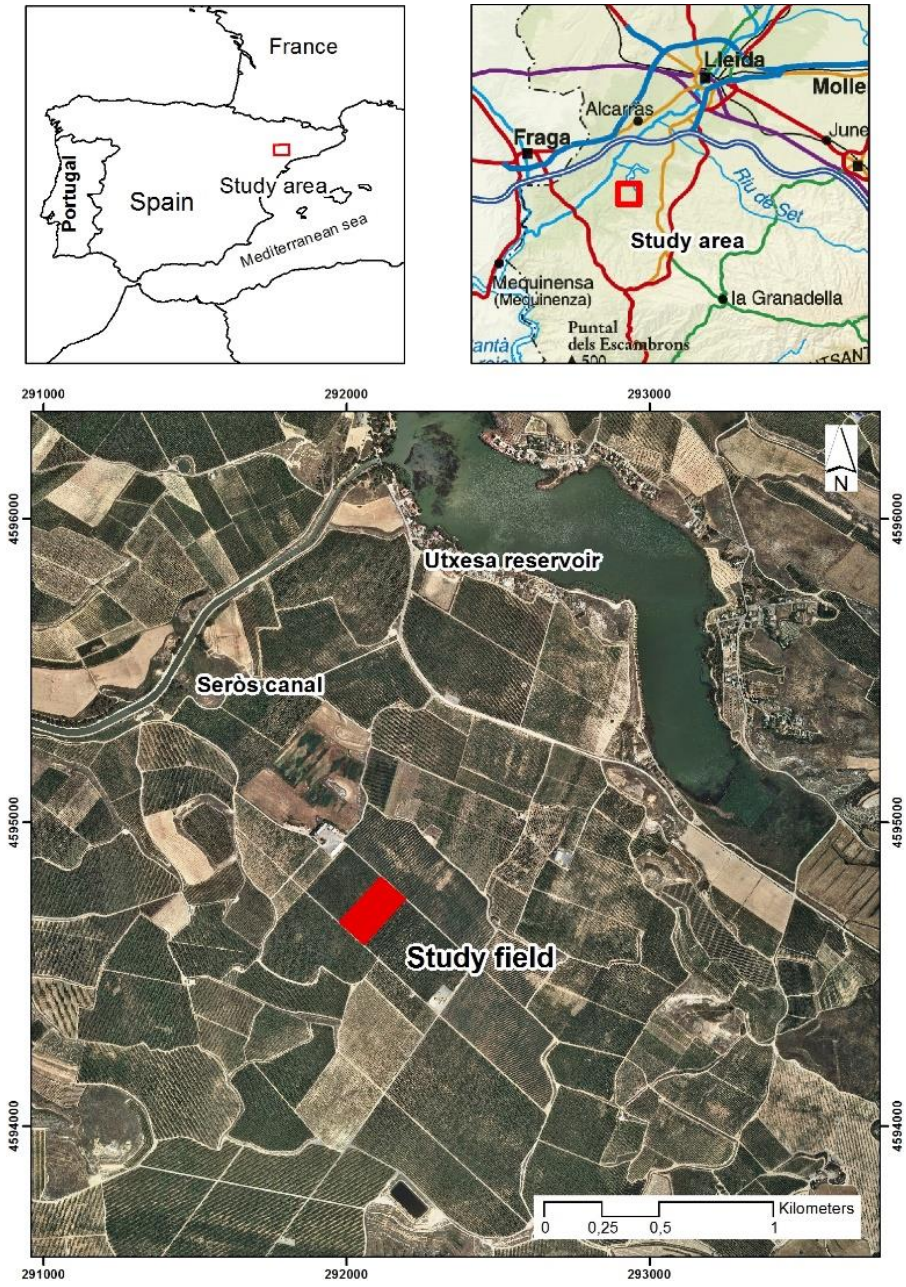

Figure 2. Location of the study area. Source: Own preparation based on images from the Cartographic and Geologic Institute of Catalonia.

The area has an undulating relief, with different valley bottoms (Figure 3). However, the current morphology is not genuine. It is the result of land clearing and levelling carried out before the setting the current plantations.

Figure 3. Present relief in the study area. The relief is undulated with alternate of valley bottoms.

This transformation started in the 1980 decade (Figure 4). Previously, the relief of the area was characterized by the presence of low hills and crops in terraces protected with stone walls (Figure 4).

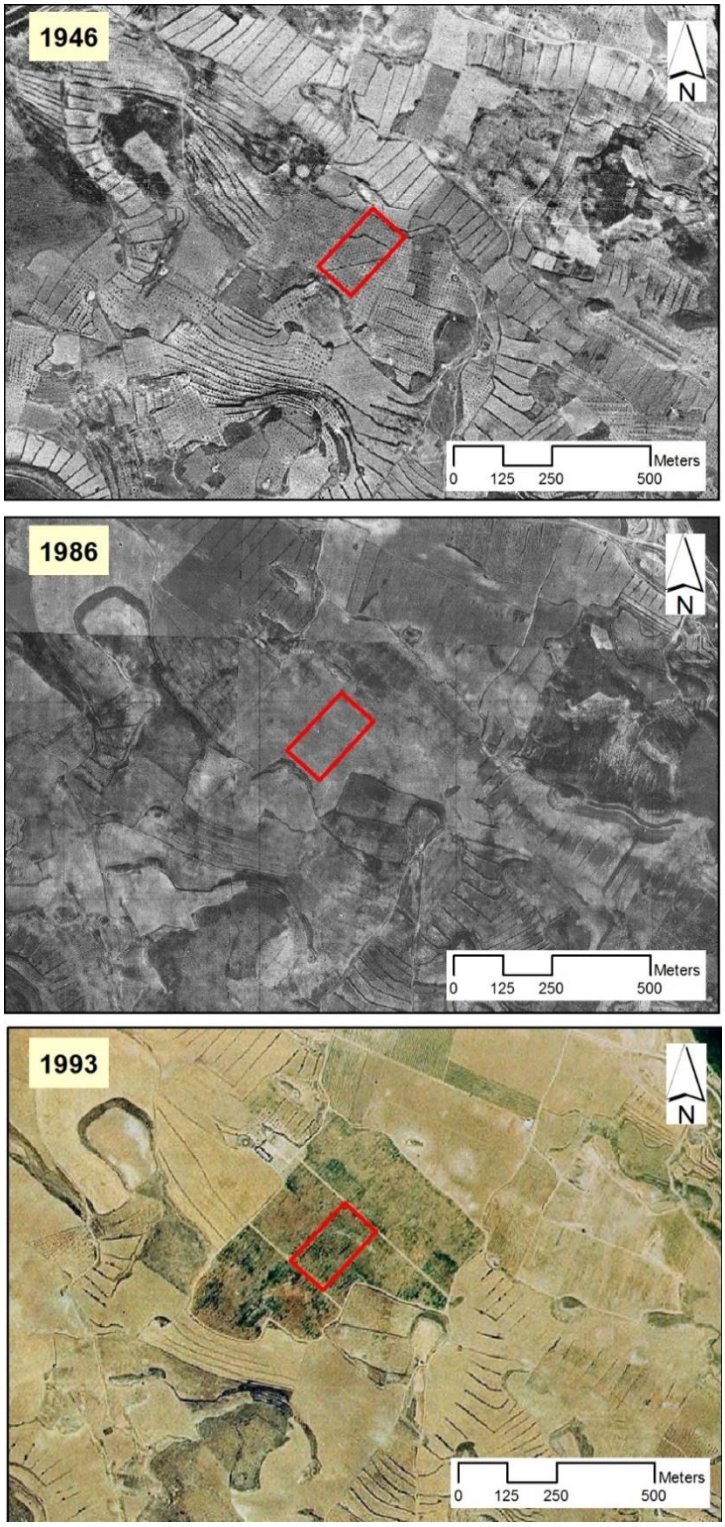

Figure 4. Comparison of former relief and landforms (1946) after the beginning of land transformation. The red rectangle represents the location of the study plot in the present study. In 1946 the landscape was characterized by infilled valley bottoms and terraced slopes. In 1986 it can be observed the elimination and land movements of some terrace banks to enlarge fields. In 1993 new irrigated orchards appear in the image, which marks the starting of the huge transformation of the area into fruit tree plantations. Source: Own preparation based on images from the Cartographic and Geologic Institute of Catalonia.

The present topography is represented in Figure 5 by the 5 m interval contours from the topographic map of Catalonia. The elevation ranges from 156 – 167 m, with an average of 161.30±2.24 m. The slope is gentle or moderated, with an average of 5.33±2.07 %.

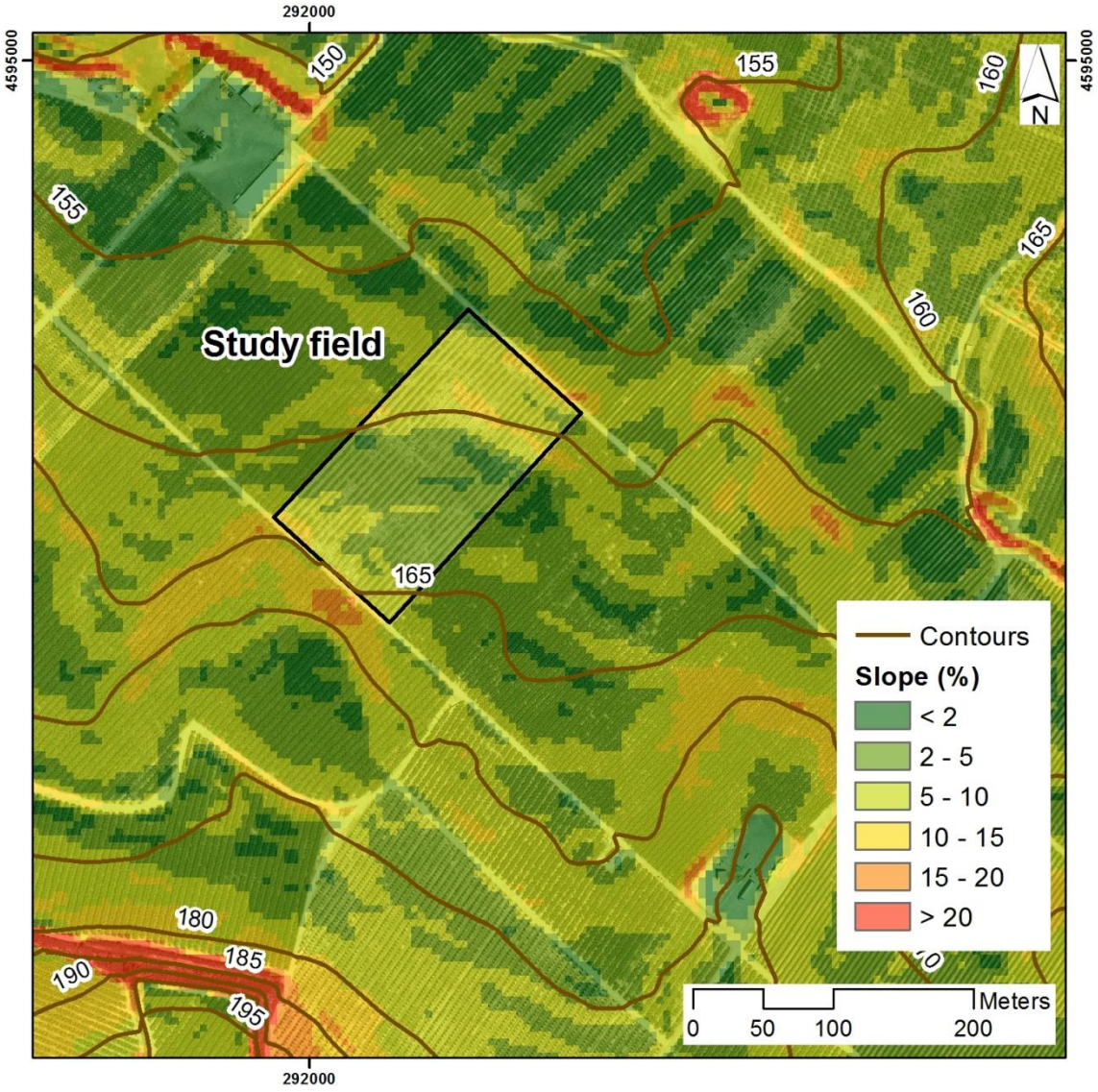

Figure 5. Topography of the study plot and the surrounding area. The contours have an interval of 5 m. Also slope (%) is shown in different classes. Source: Own preparation based on data from the Cartographic and Geologic Institute of Catalonia (Topographical map 1:5000) and the National Cartographic Institute (MDE 5 m from Lidar data).

The company owner of the property (Frutas Espax) was founded in 1977 and is family-owned. At present has become a benchmark in the fresh fruit sector, with a huge expansion and more than 1000 employees on its staff during the harvest.

The total production of the farm is, approximately, 60000 t/year. The main fruits produced in the farm are nectarine, peach, flat peach, flat nectarine, pear, apple and cherry. The entire process is carried out by means of integrated production, environmentally friendly without the use of aggressive products. The fruit production is mainly for export, being Germany, UK, Italy and France the main destinations.

3.2. Climate characteristics

The climate in the Segrià County is Mediterranean continental dry, with an irregular rainfall distribution along the year and a low total annual. Specifically, there is a lack of rainfall during the summer period, thus being an arid season. The maximum precipitation occurs in spring, mainly in the north of the region, while in the centre and the south, where the study area is located, the rainfall peak occurs in autumn. The thermal regime is hot in summer and cold in winter, so that high thermal amplitude is generated. The frost period occurs between the months of October to March (Meteorological Service of Catalonia). The most representative weather station of the "Xarxa d'Estacions Meteorològiques" (Meteorological Service of Catalonia) for this study is located in the same municipality of Aitona (XYZ UTM coordinates 288096. 4596129. 97) (Table 3 and 2; Figure 6).

	JAN	FEB	MAR	APR	MAY	JUN	JUL	AUG	SEP	OCT	NOV	DEC
Precipitation (mm)	27.54	14.20	30.09	58.25	43.84	30.26	14.51	17.86	36.25	40.49	40.65	14.55
Temperature (°C)	5.38	7.26	10.99	14.33	17.95	22.15	24.74	24.50	20.38	15.29	9.15	5.30

Table 3. Summary of the monthly average precipitation and temperature during the period 2007 – 2014 at the weather station of Aitona (Segrià, Lleida, Spain). (Source: Meteorological Service of Catalonia, www.meteo.cat).

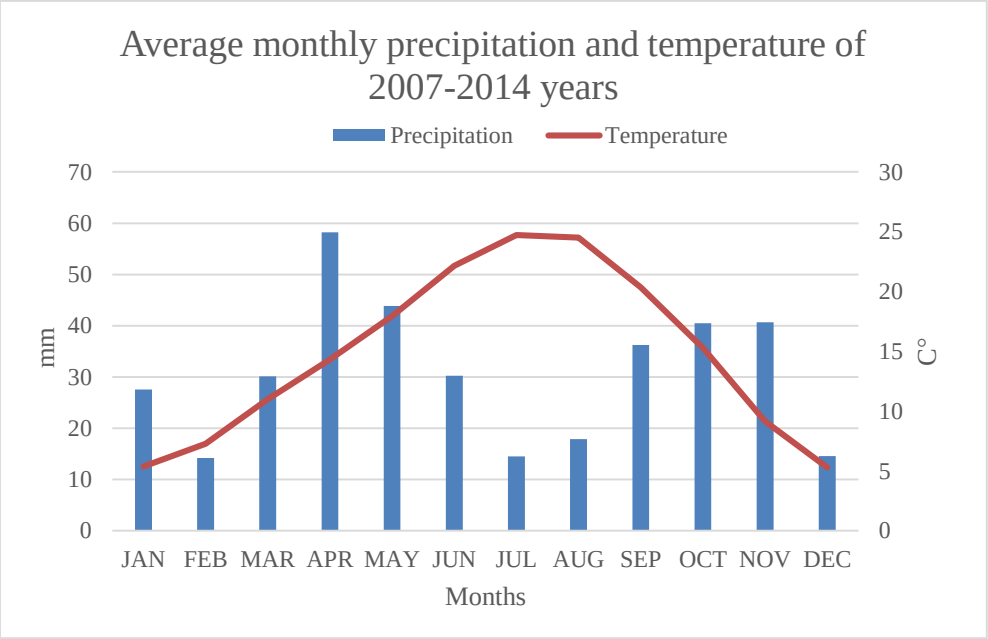

Figure 6. Climograph of Walter and Gaussen in Aitona (Segrià, Lleida, Spain) for the period 2007-2014. It shows the representation of basic climatic parameters: monthly average temperature and precipitation. (Source: Own elaboration with data from the Meteorological Service of Catalonia; www.meteo.cat).

The number of frost days can influence peach blossoming and compromise the fruit sprouting (Table 4, Figure 7). The present year was characterized by a long and unusual period of blossoming, about one month in March, with a very low probability to have some frost days.

	JAN	FEB	MAR	APR	MAY	JUN	JUL	AUG	SEP	OCT	NOV	DEC
Frost days	13.5	13.3	5.4	0.1	0.0	0.0	0.0	0.0	0.0	0.9	7.9	13.1

Table 4. Summary of the monthly average frost day during the period 2007 – 2014 at the weather station of Aitona (Segrià, Lleida, Spain). (Source: Meteorological Service of Catalonia. www.meteo.cat).

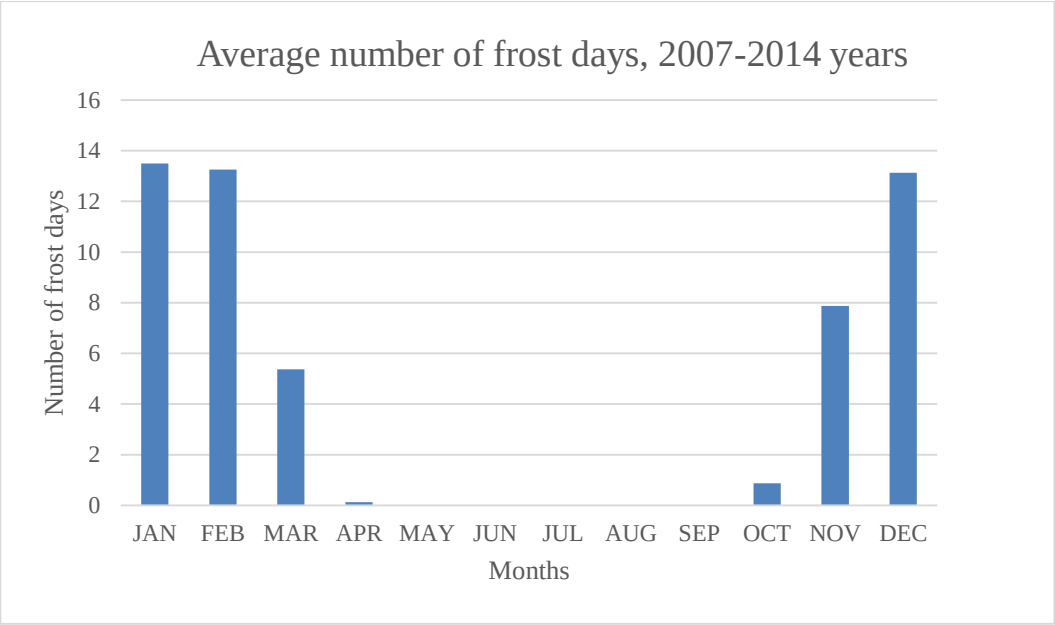

Figure 7. Average number of frost days in Aitona (Segrià, Lleida, Spain) for the period 2007-2014. (Source: Own elaboration with data from the Meteorological Service of Catalonia; www.meteo.cat).

3.3. Lithology

The study area is located in the Central Catalan Depression, which is the name given to the eastern sector of the Tertiary Ebro sedimentary basin. The geological and climatic characteristics of this region along the Tertiary and Quaternary have been the origin of evaporate formations which are widespread in the Depression. They have given rise to a wide typology of soils, with variable content of salts and/or gypsum mainly depending on the type of formation-marine or continental and on geomorphological and climatic changes during the Quaternary.

According to the Geological Map of Catalonia at 1:50.000 (Cartographic and Geologic Institute of Catalonia), there are five main units in area where the study field is located (Table 5 and Figure 8). The first unit (Qco), where the study field is mainly included, corresponds to Quaternary colluvial deposits, which include clays with dispersed angular limestone gravels. The second unit (Qr) corresponds to infilled valley bottoms, composed of deposits of clay loam or silty clay loam texture. The Tertiary deposits around the study field are represented by the units POmcg4, POmcg5 and POmc5. These are marls with sandstone intercalations; clays, silt, marls and fine sandstones; and limestone with

alternate grey and greenish marls. Due to the sedimentary nature of these materials in lacustrine or playa-lake environments, they can content different amount of salts and/or gypsum.

Code	Era	Period	Epoch	Description
Qco	Cenozoic	Quaternary	Holocene	Colluvial deposits; clays with dispersed angular gravels
Qr	Cenozoic	Quaternary	Holocene	Fine deposits in infilled valley bottoms.
POmcg4	Cenozoic	Paleocene	Oligocene	Marls with sandstone intercalations
POmcg5	Cenozoic	Paleocene	Oligocene	Clays, silt, marls and fine sandstones
POmc5	Cenozoic	Paleocene	Oligocene	Limestone with alternate grey and greenish marls

Table 5. Main lithological units in the study area. (Source: Cartographic and Geologic Institute of Catalonia).

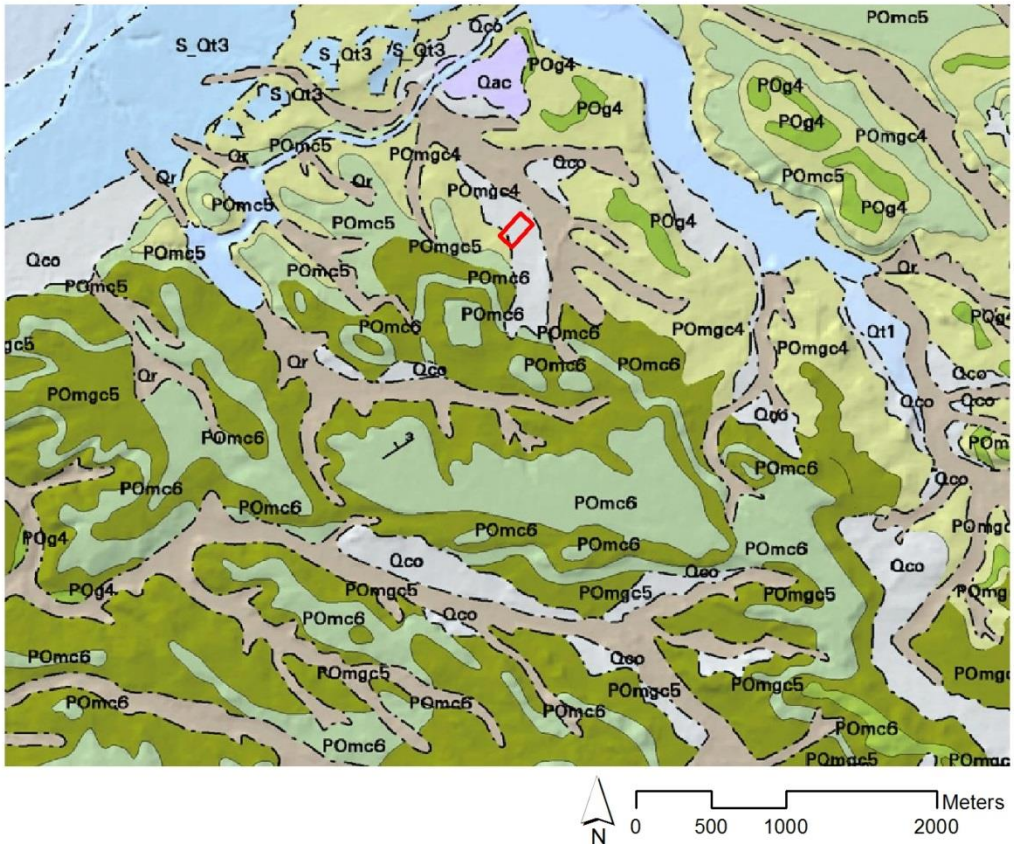

Figure 8. Geological map of the study area. The red rectangle represents the location of the study plot (Source: Own elaboration with data from Cartographic and Geologic Institute of Catalonia).

3.4. Soils

The soils of the study area were mapped by Martínez-Casasnovas et al. (1992) and published by the Cartographic and Geologic Institute of Catalonia in 2010 (Martínez-Casasnovas et al., 2010). The soil survey was conducted to assess the suitability for different agricultural land use types and irrigation, in the frame of the irrigation project of the Segarra-Garrigues canal.

Specifically, the study field is located in the cartographic unit ALC/CMS, which is a complex of soils of the Alcanó and Comes series (Figure 9). Soil series is a level of classification in the USDA Soil Taxonomy classification system hierarchy, which consist of pedons that are grouped together because of their similar pedogenesis, soil chemistry, and physical properties such as soil colour, soil texture, soil structure, soil pH, consistence, mineral and chemical composition and arrangement in the soil profile. These result in soils which perform similarly for land use purposes.

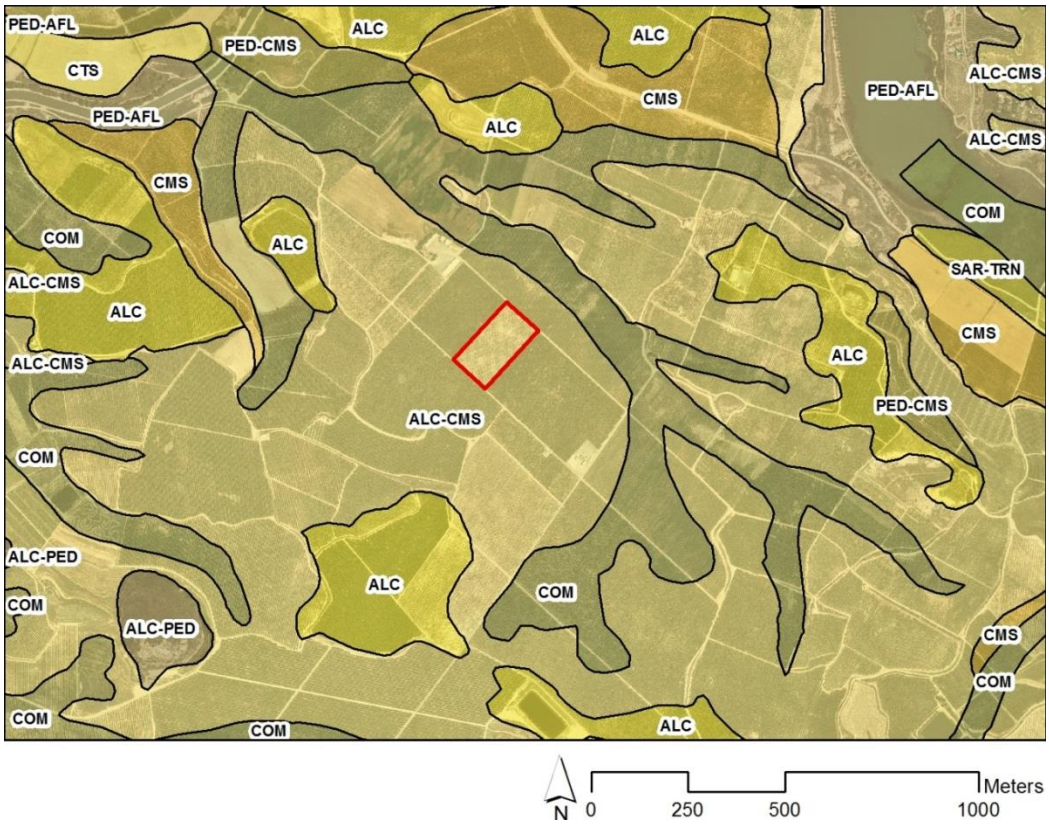

Figure 9. Soil map of the study area. The red rectangle represents the location of the study plot in the present study. The map unit where the study plot is located is a complex of shallow to moderate depth soil of the Alcanó and Comes series (Soil Map of Catalonia 1:25000). (Source: Own elaboration based on data from Martínez-Casasnovas et al., 2010; and the Cartographic and Geologic Institute of Catalonia).

The soils of the Alcanó series are shallow, well drained and of medium texture. They can have frequent limestone coarse elements. These soils developed on limestone of lacustrine origin and are scarcely developed. The typical sequence of horizons is Ap-R (limestone). The Ap horizon has a thickness of 15-40 cm. The texture is loam or silty loam and can present frequent coarse elements. The carbonate calcium content is high and the organic matter content is low. The soils are classified as Lithic Xeric Torriorthent, Loam, mixed (calcareous), thermic (Soil Survey Staff, 2014); or Leptic Regosol (IUSS, 2007).

The soils of the Comes series are moderately depth, well drained and of medium texture. The content of coarse elements is low. They developed on fine colluvial deposits in gentle or moderate degree slopes. The typical sequence of horizons is Ap-Bw-C (Lutite). The thickness of the Ap horizon is 20-40 cm, with a loam or silty loam texture. The calcium carbonate content is high and the organic matter content is low. The Bw horizon has a thickness between 30-60 cm and presents loam, silty loam or clay silty loam texture. The calcium carbonate content is also high. Below the Bw horizon there is a lutite, which usually presents a moderate or high salt content. The soils are classified as Typic Xerorthent, coarse-silty, mixed (calcareous), thermic (Soil Survey Staff, 2014); or Haplic Regosol (IUSS, 2007).

The main properties of the main soil types present in the study area are summarized in Table 6.

Soil properties	Alcanó Soil series	Comes Soil series
Pedogenetic horizons	Ap 2R(k)	Ap
	-	Bw
		C (Lutite)
Depth (cm)	0-30	0-30
	>30	30-60
	-	> 60
pH (1:2.5)	8.3-8.6	8.0-8.6
	-	8.2-8.8
Calcium carbonate equivalent (%)	22-38	21-45
	-	23-50
Organic matter (%)	1.4-2.8	1.0-2.7
	-	0.4-1.8
CIC (cmol (c)/kg)	10-13	5-10
	-	5-10
Clay (%)	15-25	14-28
	-	12-32
Silt (%)	30-54	33-55
	-	39-59
Gravels (%)	5-35	0-15
	-	0-15
Bulk density (kg/m^3)	1250-1500	1300-1600
	-	1400-1600
Gravimetric moisture (-33kPa) (%)	20-26	17-26
	-	19-29
Gravimetric moisture (-1500kPa) (%)	9-12	7-14
	-	6-13
Hydraulic conductivity (m/day)	0.0-3.1	0.3-1.6
	-	0.3-1.6

Table 6. Main analytical properties of the soil series Alcanó and Comes, for 0-30 cm and 30-60 cm.

4. Material and methods

4.1. Study field

The study field had an extension of 2.24 ha. It was planted in 2012 with white peach (*Prunus persica* L.), variety Patty, which is early harvested. The training system was in form of "Catalan" cup or vessel shape, with a plantation pattern of 5x2 m. The trees were irrigated by means of a drip irrigation system (Figure 10).

Figure 10. Image of the study field (in bloom. 01/03/2016). It can be observed the drip irrigation system and the trees training system in form of "Catalan" cup or vessel cup.

4.2. General methodological scheme

The Figure 11 shows a summary scheme of the methodological work flow followed in the present research thesis.

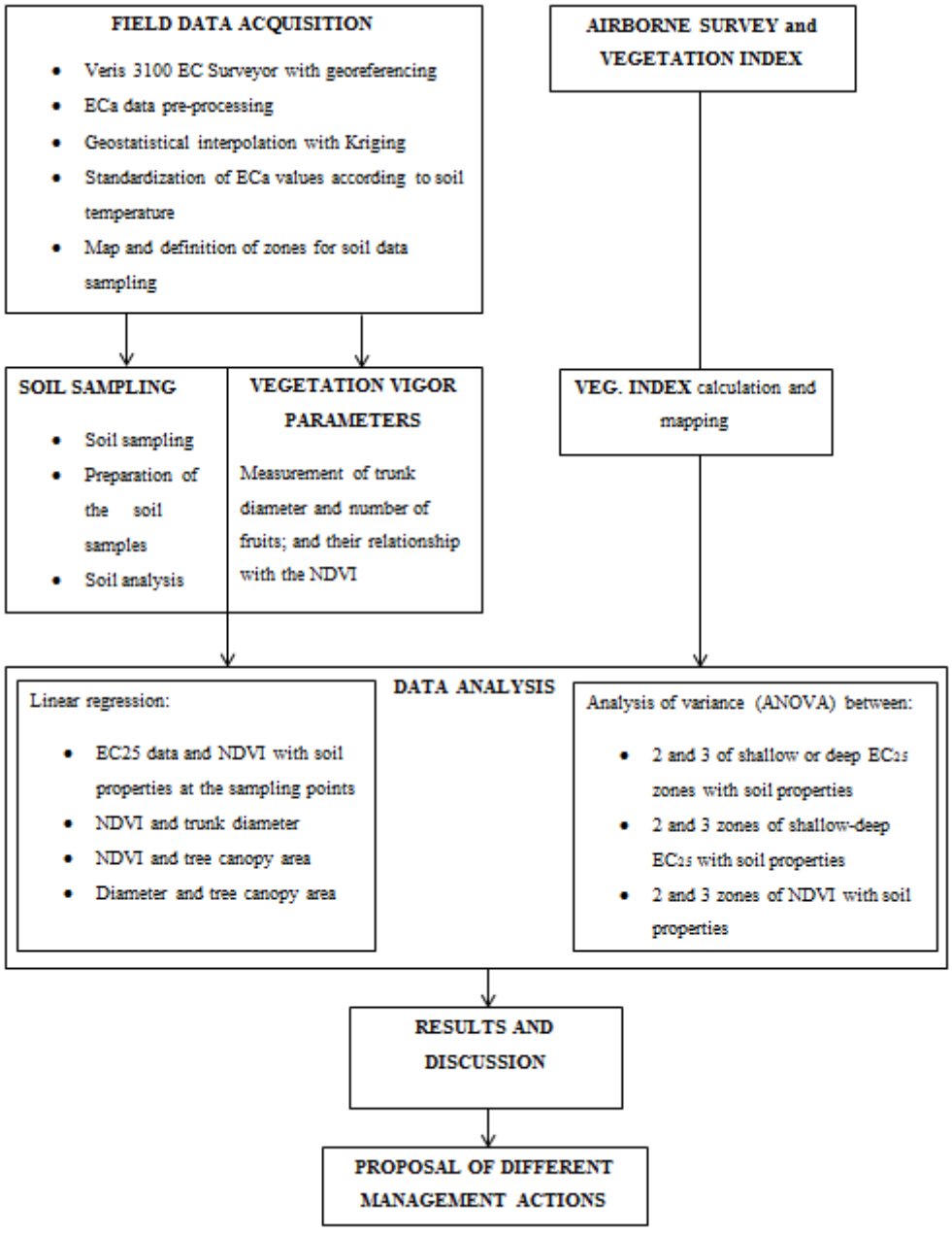

Figure 11. General methodological work flow of the research.

4.3. Apparent electrical conductivity survey and mapping

4.3.1. Veris 3100 Electrical Surveyor

To know the spatial variability of soil properties an apparent electrical conductivity survey was carried out on 01/03/2016. The survey was conducted with a Veris 3100 ECa Surveyor implement (Veris Technologies Inc. Salina, Kansas, USA) (Figure 12).

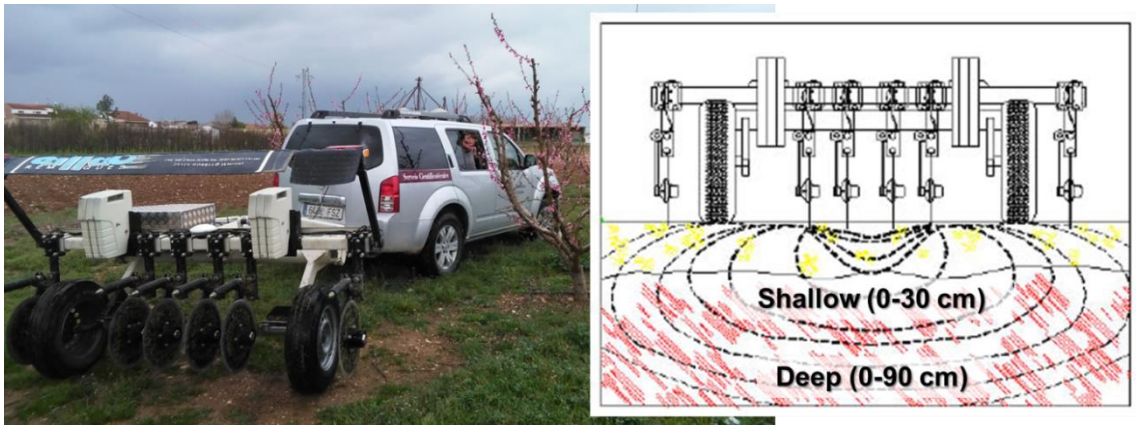

Figure 12. Left: Veris 3100 implement (Veris Technologies Inc.) owned by the University of Lleida for the on-the-go measure of apparent electrical conductivity (ECa). Right: Principals of Veris 3100 ECa data acquisition at two different depths.

Veris 3100 is an implement that is used for the on-the-go soil ECa mapping. With its dual-depth arrays and rugged reliability, it has become one of the most used technologies for EC mappers around the world.

Electrical conductivity is a measure of the ability of a material to transmit (conduct) an electrical charge. Then, geo-referenced soil EC data is a map showing how the various soils in a field differ in their ability to conduct electricity. As the Veris 3100 EC cart is pulled through the field, one pair of coulter-electrodes injects electrical current into the soil, while the other coulter-electrodes measure the voltage drop. While these coulter-electrodes only need to penetrate the soil a few centimetres, the electrical arrays employed by the Veris system investigates the soil to a depth of approximately 90 cm. The Veris 3100 uses two EC arrays to map 30 cm and 90 cm soil depths simultaneously.

The ECa measures are the standard units of measure of bulk soil conductivity. A Siemen is a measurement of a material's conductance, expressing the value in milliSiemens per meter (mS/meter): an Ohm is a measure of resistance, while Siemens are a measure of conductance. (In some scientific literature the electrical measurements of the soil are expressed in resistivity or ohm-meters).

The ECa measurements can be related to soil texture. Heavy clays, with high particle-to-particle contact and high moisture holding capacity are highly conductive. Coarse sands, with limited particle contact and low moisture holding capacity are extremely poor conductors. In the majority of farm fields, the primary ECa response is due to the soil texture variation within the field. In saline areas, the ECa response can be affected by the presence of dissolved salts in the soil's pore water. ECa signals from saline spots are typically much higher than the signals from heavy clays. In those cases, Veris ECa measurements usually reveal the field's soil texture, with saline hotspots clearly visible on the ECa map.

Data was georeferenced by means of a Trimble AgGPS332 GPS with EGNOS differential correction in geographic coordinates WGS84 (EPSG 4326). This GPS receiver was connected to the Veris 3100 data logger by means of a RS232 port.

4.3.2. ECa survey characteristics and data preprocessing

In the study field, the ECa survey was conducted during the bloom of the peach trees (Figure 13).

Figure 13. ECa survey conducted with Veris 3100 in the study field on 01/03/2016.

The Veris 3100 data logger registered a total of 1910 points and generated an ASCII file with the following format: Longitude, Latitude, Shallow ECa, Deep ECa and Elevation.

An example of the first rows of the data acquired by Veris 3100 in the study field is shown here:

```
0,510147   41,478065  99,7  96,4  153,702
0,510142   41,478059  87,0  89,7  153,804
0,510139   41,478055  73,1  78,9  153,815
0,510136   41,478052  72,2  78,4  153,815
0,510132   41,478047  89,6  83,1  153,806
0,510126   41,478042  84,2  84,9  153,808
0,510118   41,478035  69,3  82,1  153,889
0,510109   41,478027  96,5  88,4  154,017
0,510100   41,478018  85,8  86,4  154,082
0,510090   41,478010  91,0  83,6  154,111
0,510079   41,478001  88,5  94,4  154,122
0,510067   41,477992  79,8  88,0  154,098
0,510055   41,477982  77,3  85,5  154,099
...
```

The WGS84 geographic coordinates were then converted to the ETRS89 UTM 31N coordinate system (EPSG 25831), which is the coordinate system that corresponds to the study area and to match other available cartographic data.

The original Veris data file included points along the fruit tree rows and also in the turning lines outside the field (Figure 14).

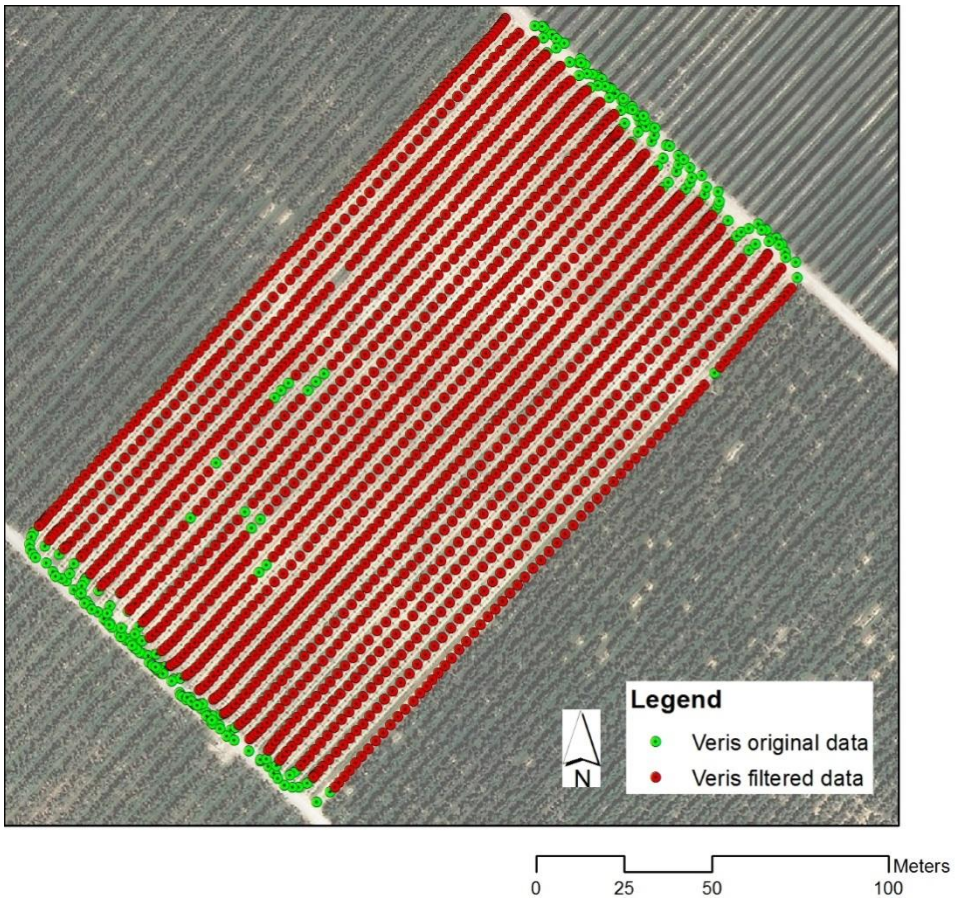

Figure 14. Veris 3100 original data acquired in the study field and data after filtering (turning line points and outliers). The visible green points were the ones that were removed by the filtering process. The red points were the data finally used in the interpolation.

These points outside the field, as well as other outliers, were removed from the original data file. Outliers were considered the points with ECa above or below ±3SD (standard deviations) from the mean, according to the criteria of (Taylor et al., 2007). After filtering, the final set of ECa data used for interpolation to build continuous surfaces of shallow and deep ECa were 1668 points (Figure 14).

4.3.3. Geostatistical interpolation

In the present research a geostatistical interpolation process was considered to map de continuity of the ECa in the study field. This method is based on modelling the so called theoretical semivariogram. In spatial statistics the theoretical semivariogram is a function describing the degree of spatial dependence of a spatial random field or stochastic process. As a concrete example, in the present case study, the semivariogram will give a measure of how much two ECa samples taken in the study field will probably vary depending on the distance between those samples. Samples taken far apart will vary more than samples taken close to each other. In this case, the semivariogram depends only on the distance between sample points, the empirical semivariogram can be computed by pooling data pairs separated by the appropriate distances, regardless of the direction. Such a semivariogram is described as omnidirectional.

In other cases, a property shows different autocorrelation in different directions. Then, the semivariogram depends not only on the distance between sample points but also on the direction. That is, in certain directions, things that are closer to each other may be more alike than in other directions. In those case where in different directions there may be different semivariograms, it is said to exists anisotropy in the semivariogram model.

In the present research, the ECa measurements were interpolated to a 1 m grid by means of ordinary kriging. For that, ArcGIS Geostatistical Analyst 10.3 was used. Previous to the interpolation, a test of data normality was carried out because the kriging is a spatial process that is modelled stochastically as a random function.

Table 7 presents a summary of the tests of normality applied to the Shallow and Deep ECa data.

	Shallow	**Deep**
Num. of points	1668	1668
Max ECa mS/m	226.20	165.80
Mean ECa mS/m	107.11	90.03
Median ECa mS/m	108.25	92.00
Standard deviation	40.33	30.09
Coefficient of variation %	37.65	33.42
Skewness	0.05	-0.17
Kurtosis	2.72	2.63
Variance	1626.51	905.65

Table 7. Summary of the tests of normality for Shallow and Deep ECa data.

According to Table 7, both shallow and deep ECa data seemed to have a normal distribution. This was confirmed by the skewness value < 1 and the kurtosis < 3. Also the mean and the median were similar in both cases.

Once proved the normality of data, the different semivariogram models available in the Geostatistical Analyst wizard of ArcGIS 10.3 were applied in order to select the best model.

The different model's parameters for the shallow and deep ECa modelling are shown in Table 8.

Semivariogram models for Shallow ECa	Partial sill	RMS	Mean standardized	RMSS	Average Standard Error	Nugget	Sill	Spatial correlation
Circular	1028.7	21.4	0.00005	0.85	25.2	470.8	1028.7	31.4
Spheric	1087.1	20.7	0.00040	0.85	24.1	401.2	1087.1	27.0
Tetraspheric	1130.9	20.1	0.00057	0.86	23.2	347.9	1130.9	23.5
Pentaspheric	1164.6	19.7	0.00072	0.87	22.6	307.2	1164.6	20.9
Exponential	1448.7	18.8	0.00092	0.94	19.9	76.0	1448.7	5.0
Rational-Q	1222.7	18.7	0.00092	0.92	20.2	306.9	1222.7	20.1
Hole- effect	673.5	23.3	-0.00260	0.85	27.3	697.6	673.5	50.9
J- bessel	950.3	21.5	0.00130	0.91	23.6	496.4	950.3	34.3
K bessel	1528.0	18.7	0.00069	0.94	19.9	0.0	1528.0	0.0
Stable	1509.8	18.7	0.00057	0.95	19.7	16.7	1509.8	1.1

Semivariogram models for Deep ECa	Partial sill	RMS	Mean standardized	RMSS	Average Standard Error	Nugget	Sill	Spatial correlation
Circular	611.9	15.1	0.00036	0.9	17.3	207.5	611.9	25.3
Spheric	643.8	14.6	0.00040	0.9	16.5	170.8	643.8	21.0
Tetraspherio	653.4	14.2	0.00100	0.9	16.2	154.6	653.4	19.1
Pentaspheric	686.9	13.8	0.00093	0.9	15.3	119.5	686.9	14.8
Exponential	834.8	13.5	0.00022	1.0	13.2	0.0	834.8	0.0
Rational-Q	771.6	12.8	-0.00025	1.3	10.0	50.5	771.6	6.1
Hole- effect	365.4	16.7	0.00320	0.8	20.4	391.8	365.4	51.7
J- bessel	561.6	15.1	0.00130	0.9	16.3	232.8	561.6	29.3
K bessel	835.8	13.4	0.00009	1.0	13.5	0.0	835.8	0.0
Stable	835.6	13.4	0.00009	1.0	13.4	0.0	835.6	0.0

Table 8. Summary of model parameters for the geostatistical interpolation of ECa at shallow and deep depths.

According to Table 8, the best semivariogram model was selected by looking at different criteria: variance value similar to partial sill, lowest root means square (RMS) value, mean standardized closest to 0, root mean square error (RMSE) closest to 1 and the lowest AVG value, which indicates the lowest prediction error. In addition, the spatial correlation (nugget/sill) should be less than 25%. Taking into account these criteria, the exponential semivariogram model was selected to interpolate both data sets (shallow and deep ECa).

In both cases anisotropy in the semivariogram models was considered. As is shown in the semivariogram maps of Figure 15 and Figure 16, the spatial distribution of the semivariance values was clearly not isotropic from the center (sample points close together) to the border of the range (more separated sample points) (the blue lines in the figures show the estimated semivariogram models in different directions). According to that, the semivariance values presented a clear directional distribution in the NW to SE direction, that is the perpendicular direction to the tree grows in which Veris 3100 data were acquired.

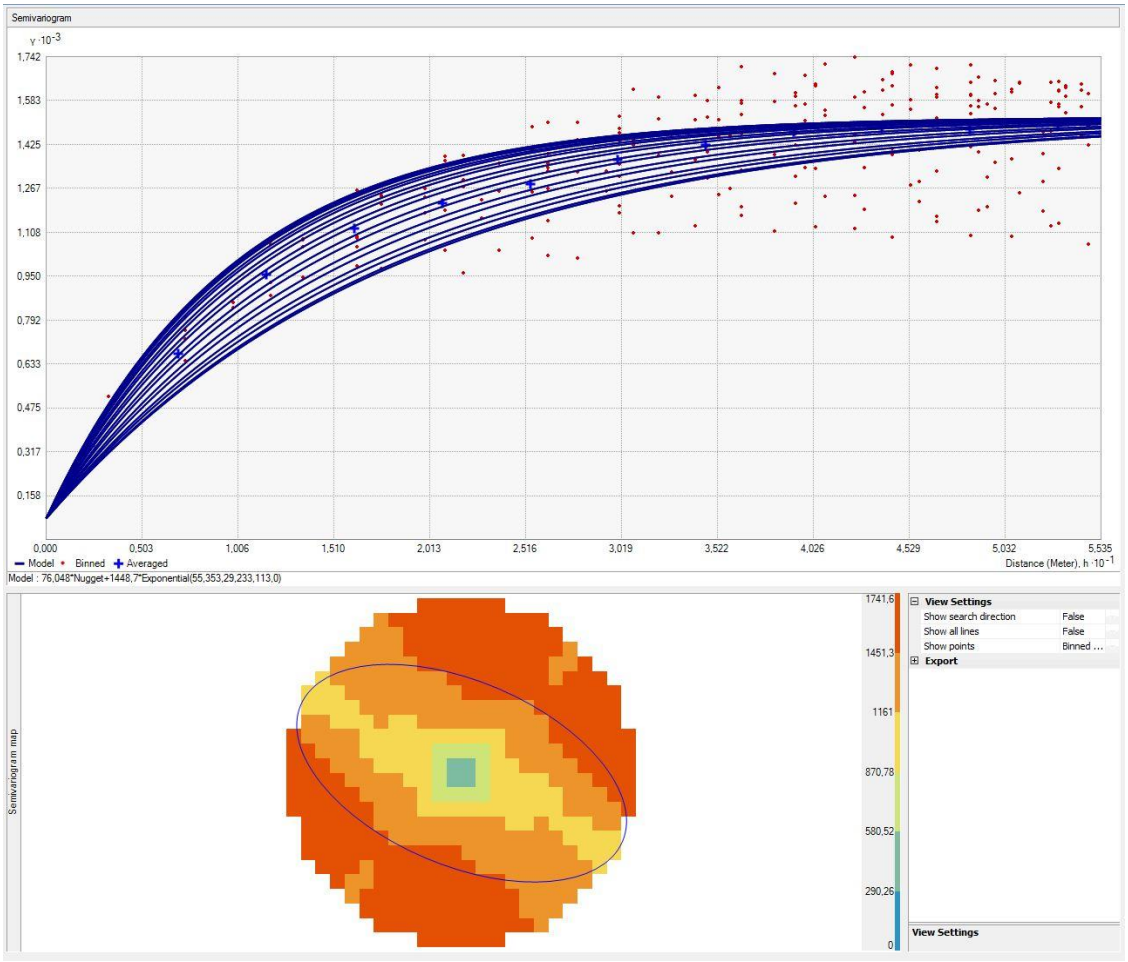

Figure 15. Example of anisotropic exponential semivariogram models considered to interpolate Shallow ECa values. Top: the blue lines in the figures show the estimated semivariogram models in different directions. Bottom: semivariance values at different distances and directions up to the range distance. It clearly shows the anisotropy of Shallow ECa values, mainly in the NW-SE direction.

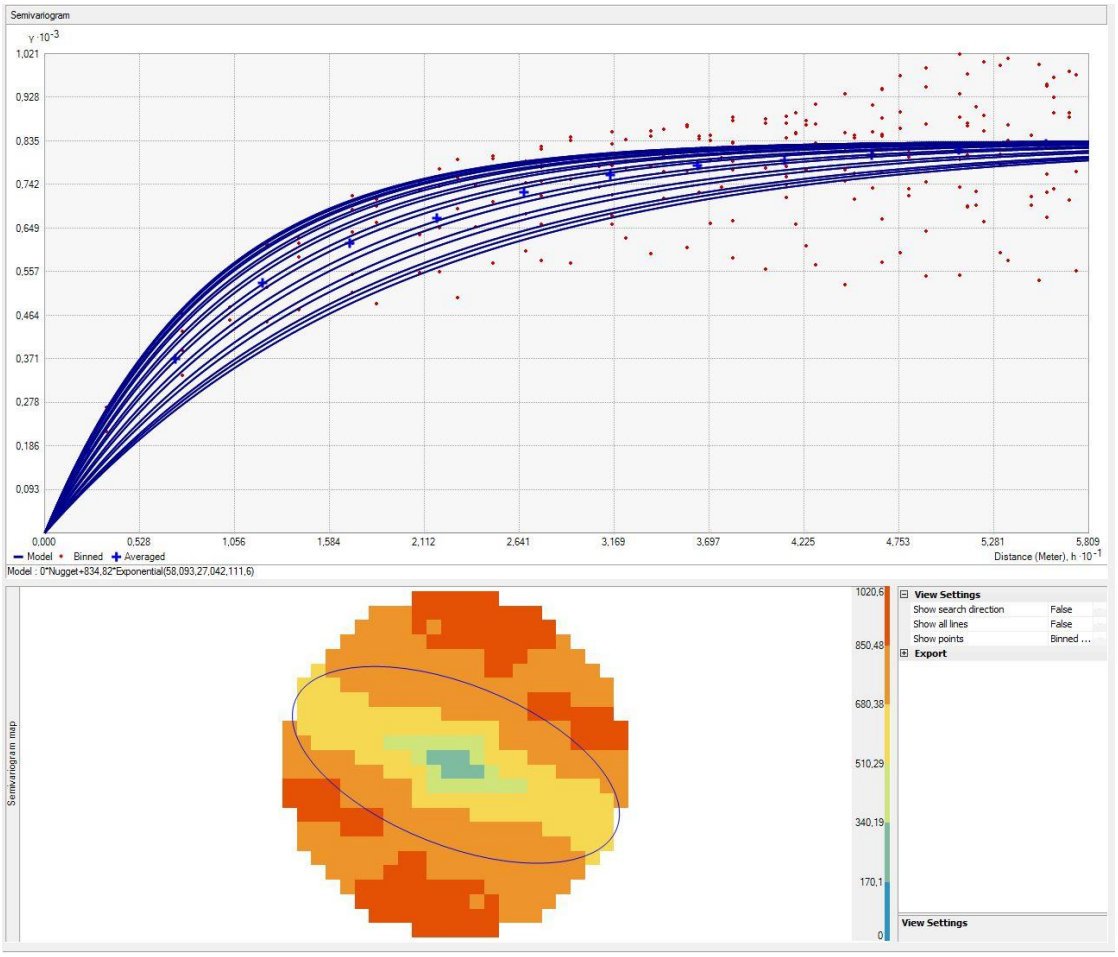

Figure 16. Example of anisotropic exponential semivariogram models considered to interpolate Deep ECa values. Top: the blue lines in the figures show the estimated semivariogram models in different directions. Bottom: semivariance values at different distances and directions up to the range distance. It clearly shows the anisotropy of Deep ECa values, mainly in the NW-SE direction.

4.3.4. Standardization of ECa values according to soil temperature

Soil salinity has been defined and assessed in terms of laboratory measurements of the electrical conductivity of the extract of a saturated soil-paste sample (ECe) at the reference temperature of 25 ºC (Rhoades, 1999). However, in the present work, electrical conductivity was measured by means of an indirect method, that is the electrical conductivity of the bulk soil (apparent electrical conductivity) by means of a resistivity sensor (Veris 3100). A factor influencing ECa is temperature. Electrolytic conductivity increases at a rate of approximately 1.9 % per ºC increase in temperature (Rhoades, 1999; Corwin and Lesch, 2005).

Therefore, for interpretation and comparison purposes of the values, these should be standardized at the reference temperature. The EC (i.e. ECa) measured at a particular temperature, t (in ºC), EC_t, can be adjusted to a reference EC at 25 ºC, EC_{25}, using the below equation (Equation 2) from Handbook 60 (U.S. Salinity Laboratory Staff, 1954; in Rhoades, 1999):

Equation 2

$$\mathbf{EC_{25}} = \frac{\mathbf{f_t \cdot EC_t}}{\mathbf{100}}$$

where, EC_{25} is the electrical conductivity in dS/m at 25 ºC, *ft* is a temperature conversion factor and EC_t is, in this case, the apparent electrical conductivity measured by the Veris 3100 sensor in mS/m at the soil temperature.

According to Corwin and Lesch (2005) and Ma et al., (2010), approximations for the temperature conversion factor (f_t) are available in polynomial forms or other type of equations. In this respect, following the recommendations of Ma et al. (2010), the best equation is the one adjusted by Sheets and Hendrickx (Equation 3), for data acquired between the range of 3-50 ºC:

Equation 3

$$\mathbf{f_t = 0.447 + 1.4034 \cdot e^{-\left(\frac{t}{26.815}\right)}}$$

where f_t is a temperature conversion factor and *t* is temperature at which the ECa is measured.

To compute the temperature conversion factor, the soil temperature at the date of data acquisition was estimated by assuming that soil temperature is related to air temperature. Surface soil temperature is 1-5 ºC higher than the air in the immediate soil surface (Osman, 2013). According to Soil Survey Staff (1975) mean annual soil temperature at 50 cm can be about 1 ºC higher than the mean annual temperature. Taking these relationships into account, in the present work, the soil temperature for the shallow (0-30 cm) was estimated as the average of the air temperature of the previous 10 days to the

ECa survey, for the reference observatory of Aitona (Lleida) (9.5 ºC), +0.5 ºC. In the case of the deep (0-90 cm) the correction factor applied was + 1ºC.

The temperature conversion factors (f_t) considered was: Shallow ECa= 1.413; Deep ECa= 1.395. By applying these conversion factors, the shallow and deep ECa interpolated maps were converted to the standard units of EC_{25} (dS/m at 25 ºC).

4.3.5. Definition of zones for soil data sampling

The EC_{25} maps showed the spatial variability of the EC_{25} property within the study field. These data were used to determine different zones where to sample soils in order to correlate the EC_{25} signal with soil properties.

Following the recommendations of Veris Technologies Application Notes, 5 zones were differentiated to guide soil sampling in the study field. For that, an unsupervised classification was performed, using the shallow and deep layers as input data. This method shows the maximum amount of contrast in the field and does not require subjective judgement to delineate different zones.

Then, 40 sample points were randomly distributed given by the 5 EC_{25} zones. In this way, in each zone 8 sampling points were allocated (Figure 17).

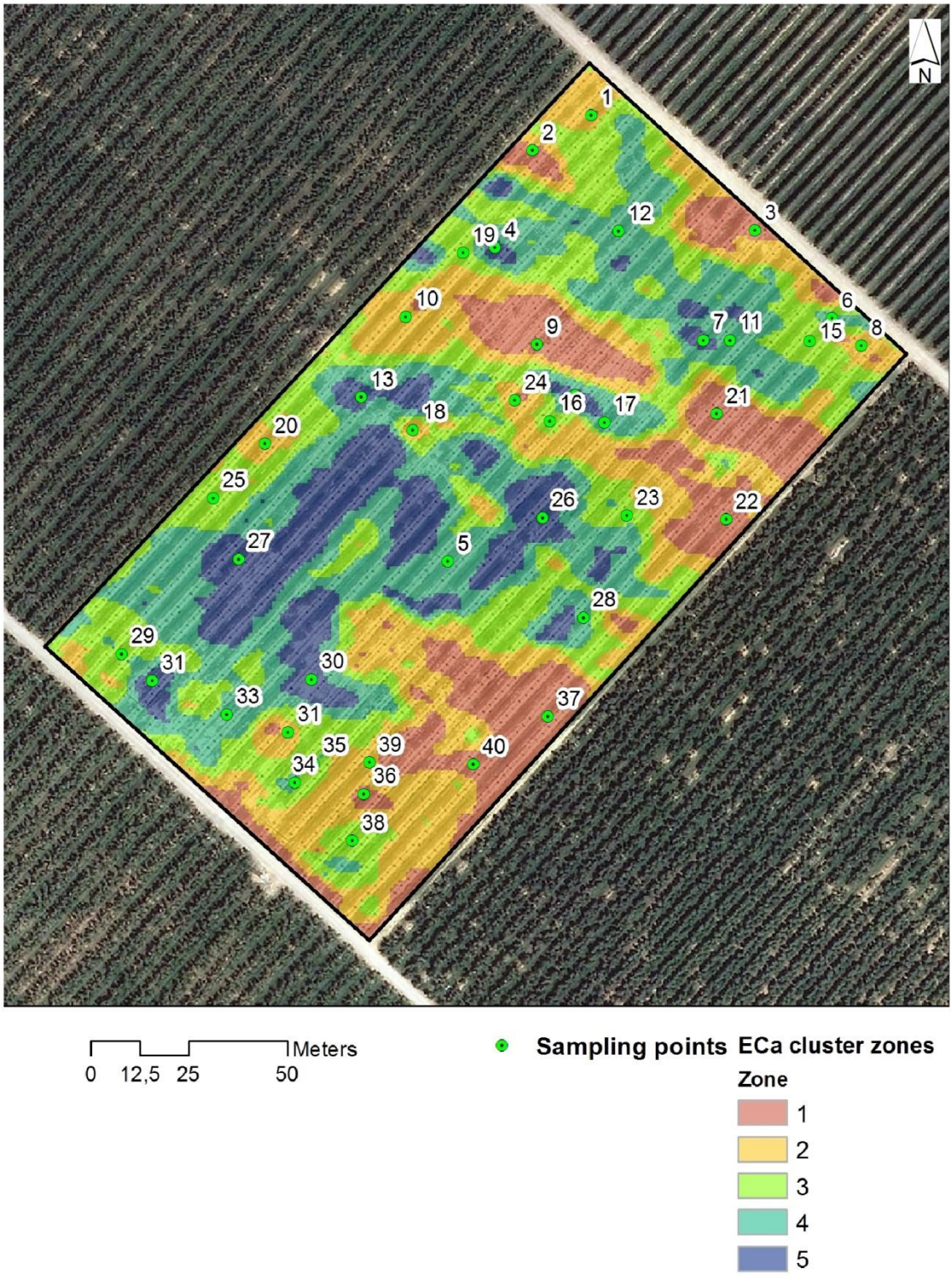

Figure 17. EC_{25} classified in 5 zones according to an unsupervised classification of the Shallow and Deep layers. In each zone 8 soil sampling points were randomly located.

For each zone, the basic statistics are shown in the Table 9 and Table 10.

EC_{25} Zone	EC_{25} min	EC_{25} max	EC_{25} mean	EC_{25} SD
1	0.22	1.21	0.71	0.19
2	0.51	1.92	1.18	0.19
3	0.90	2.11	1.54	0.16
4	1.39	2.63	1.92	0.16
5	1.68	3.02	2.33	0.23

Table 9. EC_{25} basic statistics of Shallow layer.

EC_{25} Zone	EC_{25} min	EC_{25} max	EC_{25} mean	EC_{25} SD
1	0.18	1.12	0.67	0.18
2	0.23	1.58	0.99	0.17
3	0.70	1.79	1.30	0.16
4	0.87	1.97	1.54	0.16
5	1.36	2.29	1.88	0.15

Table 10. EC_{25} basic statistics of Deep values.

4.4. Soil sampling and sample pre-processing

Soils were sampled at the pre-established sampling points using an Eijkelkamp auger hole (Figure 18). The sampling was carried out in two different dates: 07/03/2016 and 14/03/2016. The points were located in the field with the aid of a Trimble Geoexplorer XH GPS, with EGNOS differential correction. The location accuracy was less than 0.5 m. In each point samples were taken at a depth of 0-30 cm and 30-60 cm or up to the limit of the lithic (calcareous rocks) or paralithic contact (lutites).

Figure 18. Right: Soil sampling in the study field by means of an auger hole. Left: Support material for soil sampling (GPS and ECa maps).

The soil samples were processed and analysed by the author of this work in the Soil Laboratory of the Department of Environment and Soil Science (University of Lleida). The preparation process consisted of drying, milling and sieving the samples at 2 mm (Figure 19).

Figure 19. Preparation of the soil samples for chemical and physical analysis.

However, some analysis, such as the equivalent calcium carbonate, organic matter content and Kjeldahl nitrogen, needed a finer soil particle sample. Because of that, a part of each sample was pulverized at Ø< 2mm.

Each sample was signed following the laboratory register. In total, 79 samples were taken and analysed: 40 of first horizon, 39 about the second.

4.5. Soil analysis

Two types of analysis were carried out: chemical and physical. Chemical properties: pH, electrical conductivity (1:5), equivalent calcium carbonate, organic matter content and cationic exchange capacity of cationic interchange. Physical properties: particle-size (texture) and water retention capacity at -33 and -1500 kPa. To analyse the equivalent calcium carbonate and the organic matter, a pulverized soil sample (as described in the previous section).

4.5.1. pH

Soil pH is a measure of the activity of ionized H (H^+) in the soil solution. It was potentiometrically measured in a soil-water dispersion, 1:2.5 ratio (Dirección General de Política Alimentaria, 1986) and was measured with a pH-meter called micropH-2002 (Crison), calibrated with two buffer, of 7.02 pH for the neutral level and 4 pH for the acid.

4.5.2. Electrical conductivity

This is a previous test of salinity in a soil-water dispersion 1:5 ratio, which supposes a rough assessment of soil salinity (Dirección General de Política Alimentaria, 1986). It was determined by means of a standard process of soil-to-water mixture by vacuum filtration (Figure 20) and measured with a Conductimeter GLP 31 (Crison), which was calibrated and set up a 25°C. The results were expressed in dS/m at 25°C.

Figure 20. Filtration in the Electrical Conductivity analysis

4.5.3. Equivalent calcium carbonate

There are different methods for quantitative determinations of total inorganic carbonates: (i) neutralization of the carbonate with acid and back titration of the excess acid; (ii) determination of Ca and Mg in an acid leachate; (iii) dissolution of carbonates in acid and determination of the evolved CO_2 by measuring the volume of the CO_2 (ml) by titrimetry (Buurman et al., 1996)

In this work, the third method was used. This method is named as Calcium Carbonate Equivalent (CCE), because not only calcite is dissolved, but also other carbonates.The carbonate's samples were dissolved in a hydrochloric acid and the CO_2 volume (ml) was measured in a Bernard's calcimeter. The results were obtained as a correlation of this volume with the total amount of carbonates of the control samples.

4.5.4. Organic matter

It was calculated using the Walkley-Black method, according to which soil organic carbonates are oxidized with dichromate in presence of sulphuric acid. Excess oxidant, so the residual dichromate, was titrated again with Mohr's salt. The oxidized organic

matter amount was calculated from reduced dichromate amount (Dirección General de Política Alimentaria, 1986).

The most important parameters were the soil weight and the end-point colour of final reaction. In this work, organic matter content was calculated only for the top horizon samples 0-30. For the second, organic matter content was estimated. The results were expressed as g/100 g.

4.5.5. Cation exchange capacity

It is the measure of the quantity of readily exchangeable cations neutralizing negative charge in the soil (Page et al., 1982). It is usually expressed in milliequivalents per 100g of soil. The analysis included two procedures. Firstly, it was used the "Ammonium acetate method" on percolation tubes with a filter of cotton wool and sand, above which 5g of soil sample were put (van Reeuwijk, 1995) (Figure 21). Then, the sample was percolated with ammonium acetate and the bases were measured in the final percolate. Secondly, a mechanical extractor (K-Jeltec 2200 based on Tecador Technology, Foss-machine), it was used.

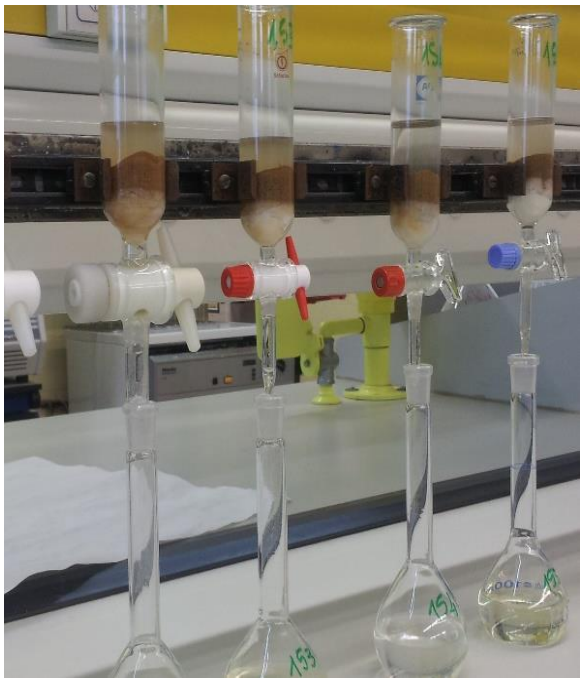

Figure 21. Percolation tubes with a filter of cotton wool-sand and soil sample

4.5.6. Kjeldahl Nitrogen

The Kjeldahl method to quantify the nitrogen included two phases: digestion and distillation. Firstly, the samples were digested in sulphuric acid and hydrogen peroxide with selenium as catalyst, to convert organic nitrogen to ammonium sulphate. The solution was then made alkaline and ammonia was distilled in a specific digest (van Reeuwijk, 1995).

Secondly, the evolved ammonia was absorbed in H_3BO_3. Ammonium borate is formed and is titrated back to H_3BO_3 by titration against standard strong acid HCl (Kalra and Maynard, 1991). The distillation apparatus was K-Jeltec 2200 based on Tecador Technology (Foss-machine)[2].

4.5.7. Particle-size analysis

Particle-size analysis (PSA) is the separation of the mineral part of the soil into various size fractions and determination of the proportion of these fractions (FAO). The analysis comprise: coarse sand (500<Ø<2000 µm), fine sand (50<Ø<500 µm), coarse silt (20<Ø<50 µm), fine silt (2<Ø<20 µm) and clay (Ø<2 µm).
Various systems of size classification have been used to define arbitrary limits and ranges of soil particle size. In this work, the USDA denomination was adopted, but the silt was divided in fine (called also international silt) and coarse silt to have a better classification. Fine silt was determined as the difference between the clay more fine silt and the total clay.

Particle-size analysis requires that the particles are well dispersed in an aqueous solution and all aggregates are disintegrated, with individual particles detached. However, in the present case study, this method did not give satisfactory results because of the presence of soluble salts that prevent a good dispersion, due to the flocculating action of salts (Buurman et al., 1996) (Figure 22). To overcome this problem, a specific pre-treatment (before proceeding with the classic procedure) was done. This is described here below.

[2] Nevertheless, due to the instability of the Kjeldahl Nitrogen in previous analyses of fields similar to the one of the study area and of the analysis device, this property was finally not considered in the study.

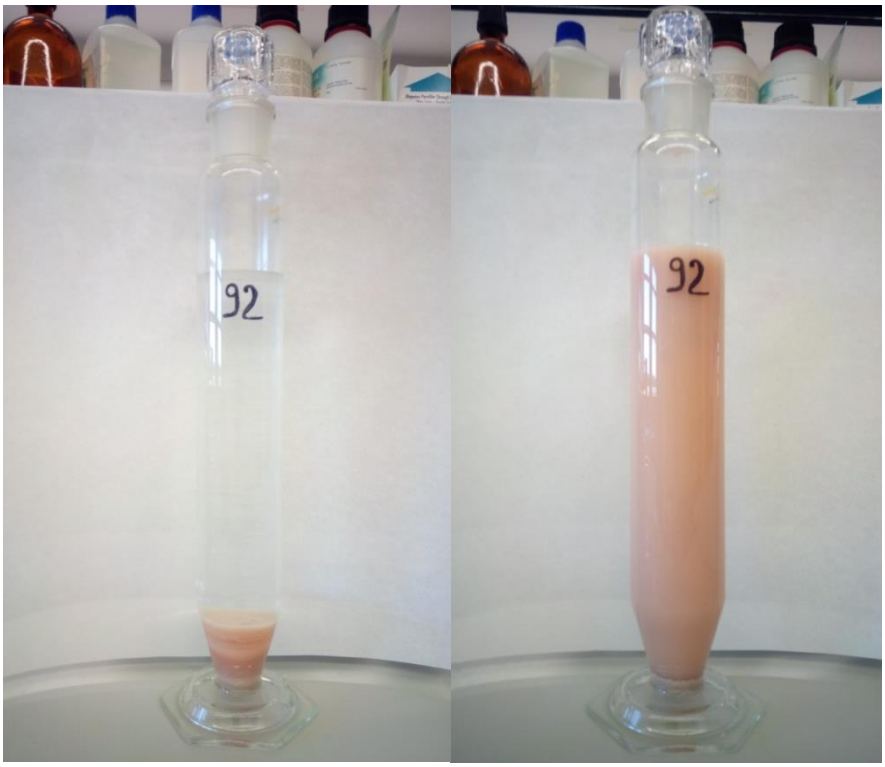

Figure 22. On the left: flocculated soil sample. On the right: no flocculated soil sample after a specific pre-treatment.

- Specific pre-treatment to remove organic matter and soluble salts:

This is a key step in Particle-size analysis in the case of flocculation due to the content of salts or organic matter. To avoid flocculation, the following method was applied. Ten grams of soil were weighed and put in beakers of 1000 ml with 300 ml of deionized water and 20 ml of hydrogen peroxide. The agent used to remove organic matter was H_2O_2. The beaker was put on a thermic hot plate to start the oxidizing action of the peroxide. The procedure lasted until the organic matter was lower than 1%.

If high concentrations of soluble salts caused the flocculation of soil suspensions, at the end of this phase, water and soil are in two different layers. Alkaline salts (sample's soil is typically alkaline and can have a variety of soluble salts including calcium, magnesium chlorides and carbonates), can cause a decomposition of H_2O_2, decreasing its effectiveness as an oxidizing agent for soil organic matter.

The most common procedure to remove soluble salts is to leach the salts with deionized water, when possible beaker's water was decanted without losing soil sample. Then, remnant semi-liquid fraction of soil sample was put in a centrifuge bottle (while the soil solid fraction remained inside the beaker).

Standard laboratory rules of procedure were followed to place each sample bottle in the centrifugal machine (ten minutes with 5000 rpm). When the bottle was drew out from the centrifugal machine, soil-solid and water-liquid layers were definitely separated. The water contained the soil salts and it was again decanted.

The solid soil fractions of the beaker were added to remnant soil in centrifugal bottles and washed with deionized water. At this time, a dispersing agent called Na-hexametaphosphate (HMP) was added. Then, the soil samples including the Na-hexametaphosphate were put for two hours in a shaker machine and then the samples were washed with deionized water up to 1000 ml in a glass sedimentation cylinder (Figure 22).

- Determination of clay and clay more fine silt with "Pipette method" (Buurman et al., 1996).

After the pre-treatment to remove organic matter and salts, samples were ready for determination of the particle-size distribution. For that, the pipet method, which is a direct sampling procedure to determinate clay and clay more fine silt, was applied. The proportions of soil fractions were determined by the sedimentation principle based on Stokes' law, which relates the radius of the particles to the velocity of sedimentation (Kalra and Maynard, 1991). This method consists on taking a small subsample by means of a pipette at a depth *h* and time *t*, according to a specific table on which the selected depths and the specific times depend also on the laboratory temperature.

Finally, at the end of the process, the clay and clay plus silt collected were put in tared pans and dried at 105°C during 24 hours, and consequent weighted.

- Determination of coarse silt, fine sand, coarse sand by the “Sieving method”.

The sample was transferred to top sieve of a nest of sieves arranged from top to bottom as follows: 500 μm, 50 μm, 20 μm (Figure 23). These levels retained coarse sand, fine sand and coarse silt.

Figure 23. Determination of coarse silt, fine sand, coarse sand by different sieves.

Each sand and silt collected were put in tared pans and dried at 105 °C during 24 hours, and consequent weighted.

4.5.8. Water retention capacity

The maximum amount of water that a given soil can retain is called field capacity, whereas a soil so dry that plants cannot liberate the remaining moisture from the soil particles is said to be at wilting point. Available water is that which the plants can utilize from the soil within the range of field capacity and wilting point. Field capacity can be measured in a suction matrix (Richard plate) with a suction pressure of 0.33 kPa (kilo Pascals) and the wilting point with a suction pressure of 1500 kPa (Figure 24) (Buurman et al., 1996).

Figure 24. Soil samples in the pressure plate

It is traditionally expressed as the ratio of the mass of water present in a soil sample to the mass of the sample after it has been dried to constant weight. Also it can be measured as the volume of water present in a unit volume of the sample.

Firstly, each Richard plate was saturated and placed in a pF high-pressure equipment (Figure 25). Secondly, sample's cores were placed in oven (105 °C, 24 hours), where sample's water was removed by evaporation. The difference between wet-pressurized weight and dry weight by oven gave the water retention capacity at both pressures.

Figure 25. High-pressure equipment where Richard plates are collocated.

4.5.9. Gypsum

For some samples on which the sum of sand clay and silt was not 100%, firstly a qualitative analysis of Gypsum was done; secondly it was determinate quantitatively with a physical method using high temperature on witch Gypsum is progressively soluble.

4.6. Vegetation vigor characterization

Vegetation vigour was estimated by two methods: by mapping the Normalized Difference Vegetation Index (NDVI) derived from a detailed multispectral image (0.25 m resolution) and by trunk diameter measurement in 103 sample trees.

4.6.1. Airborne survey and vegetation index

The image was acquired on May 16, 2016 (approximately one month before the harvest) by means of a Digital Multi-Spectral Camera (DMSC) (Specterra Services-Australia). The platform was an aeroplane operated by RS Servicios de Teledetección (Lleida, Spain) (Figure 26).

Figure 26. Aeroplane CESSNA 172S SKYHAWK operated by RS Servicios de Teledetección from the airport of Lleida-Alguaire (Spain), with which the multispectral image for the present study was acquired. The figure also shows the Digital Multi-Spectral Camera used in the survey.

The DMS camera captures four spectral bands of 20 nm width and centred at 450 nm (blue), 550 nm (green), 675 nm (red) and 780 nm (near infrared). The spectral bands were pre-processed by the provider to compensate for miss-registration due to lens distortion (less than 0.2 pixels) and for scene brightness due to the Bi-directional Reflectance Distribution Function (BRDF). Absolute radiometric calibration was not carried out since the purpose of the study was not a multi-temporal analysis of the tree's vigour (Figure 27).

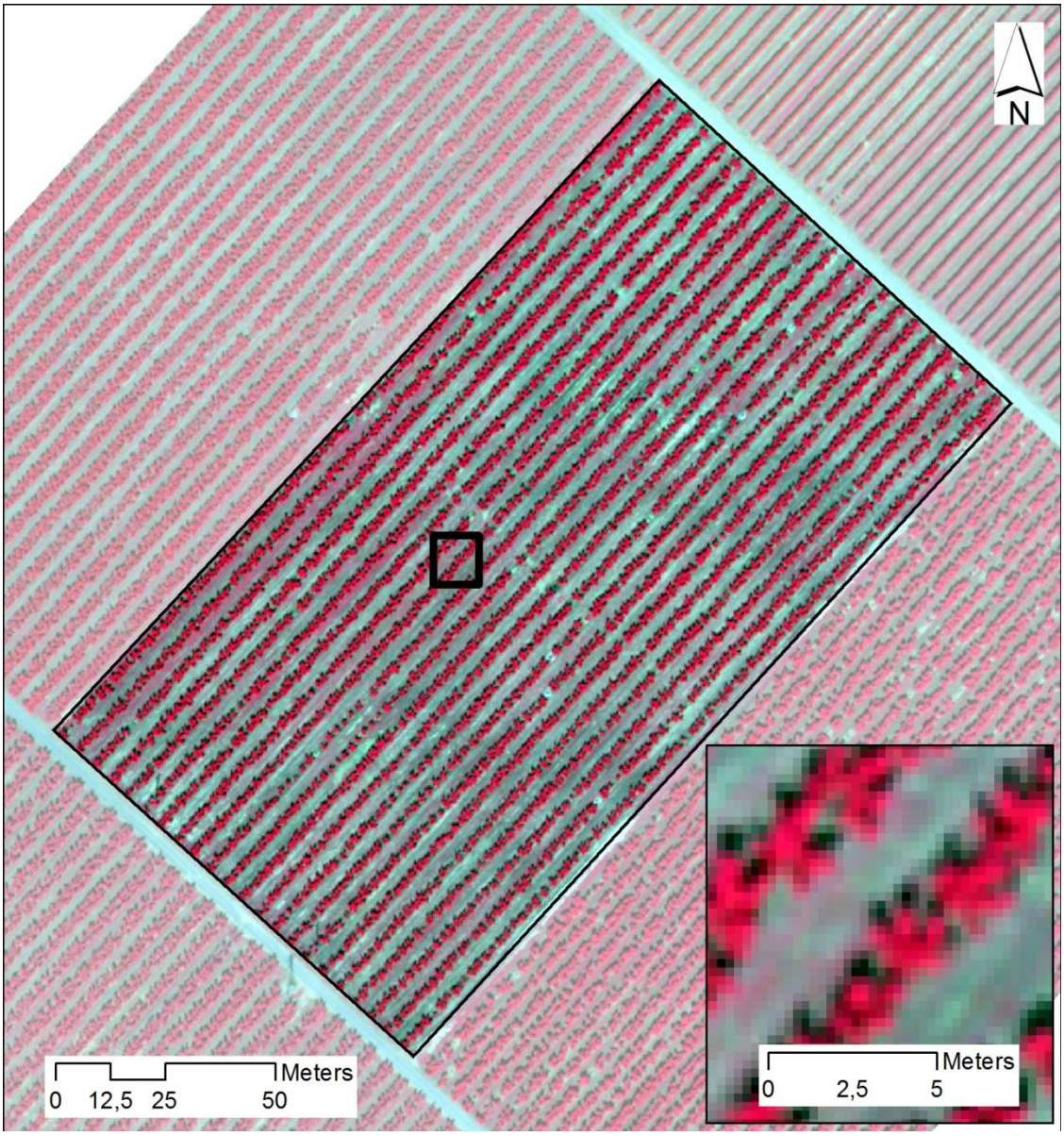

Figure 27. False colour composite (RGB NIR, Red, Green) of the multispectral image acquired on May 16, 2016. The spatial resolution was 0.25 m/pixel.

From the red (R) and infrared (IR) bands, the NDVI was computed according to Equation 1.

Only pixels with presence of vegetation in peach trees were mapped. This was done by applying a threshold NDVI value of 0.50 to the entire NDVI image. Above this threshold weeds were not selected.

The tree NDVI pixels were converted to a mask to define the tree canopy cover. This mask was converted to a polygon layer. Then, in the case of continuous coverage along trees, the polygons were cut in order to individualize each tree as an object. The polygons were used to calculate the NDVI zonal statistics per tree (min, max, mean and standard deviation). These basic statistics were joined to the tree canopy layer and then the polygons were converted to points (at the centroid). The objective was to refer the basic NDVI statistics to the trees represented as points to facilitate further data analysis (e.g. surface interpolation).

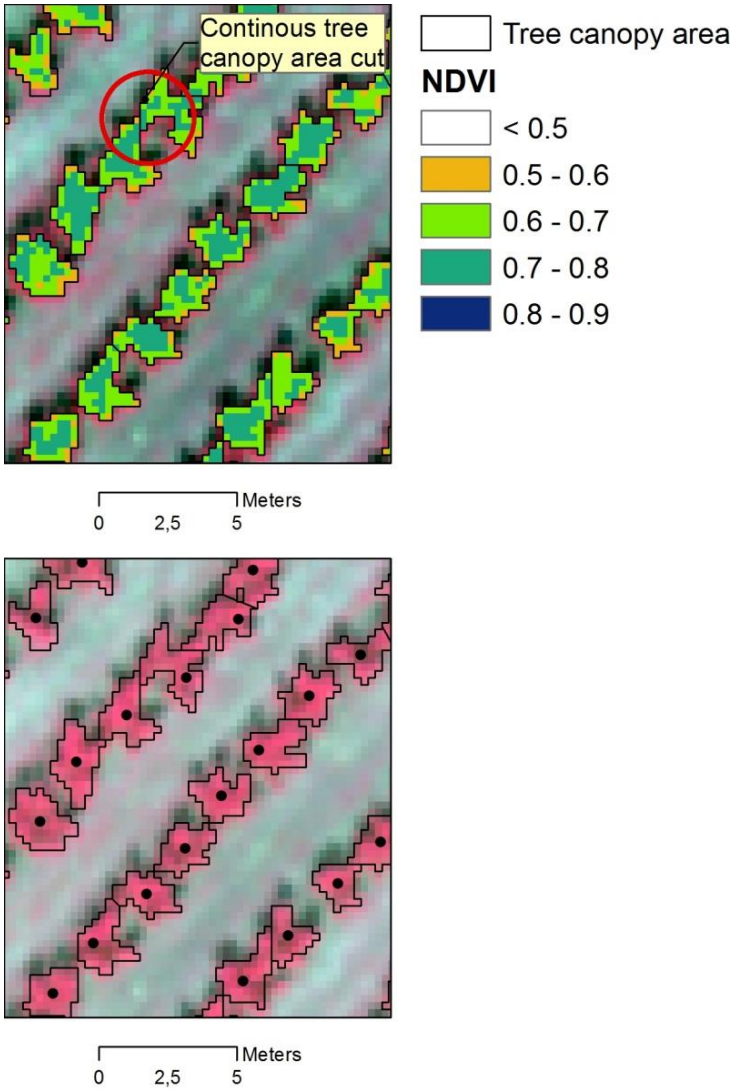

Figure 28. Top: NDVI of the tree canopy cover and NDVI mask converted to polygons. The figure also shows how the continuous tree cover was cut in some cases to have one polygon for each individual tree. Bottom: Tree canopy area represented as polygons and centroids. The points contained the summary statistics of the NDVI per tree.

From the trees represented by their centroids, an ordinary kriging was performed to interpolate a surface with the NDVI continuous spatial distribution. This was done with the objective to later create zone maps (potential management zones) by means of unsupervised classification (clustering). The best semivariogram model adjusted was the exponential (Figure 29), with the parameters listed in Table 11. Particularly relevant in this table is the value of the spatial correlation, which is less than 25, indicating a strong spatial correlation of the variable.

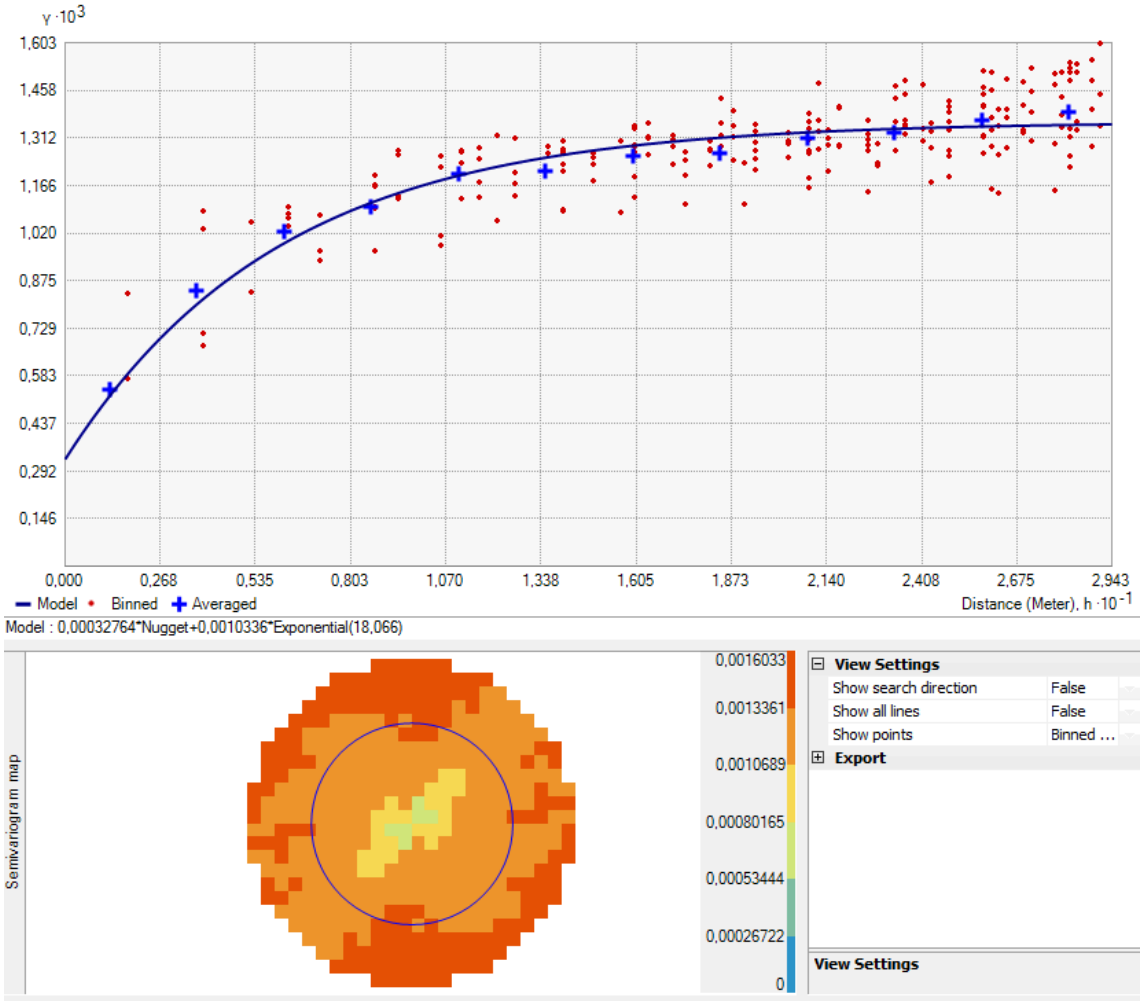

Figure 29. Exponential semivariogram model adjusted for the interpolation of the NDVI surface in the study plot.

Semivariogram models for NDVI	Partial sill	RMS	Mean standardized	RMSS	Average Standard Error	Nugget	Sill	Spatial correlation
Exponential	0.0010	0.027	0.0051	0.98	0.028	0.00032	0.0010	24.24

Table 11. Summary of model parameters for the geostatistical interpolation of the NDVI surface.

4.6.2. Measurement of trunk diameter, number of fruits and relationship with the NDVI

In order to relate the indirect vigor measures by means of the NDVI with real measures indicative of vigor, the trunk circumference and the number of fruits were sampled in 103 peach trees in a regular pattern of 15x15 m. The circumference of the trunk was measure with a measure tape at 25 cm from the soil, before the insertion of the first branches (Figure 30). From the trunk circumference values the diameters were calculated. The survey was conducted on 25/05/2016.

Figure 30. Measure of the trunk diameter by means of a measure tape.

The sample points were overlaid to the tree canopy area layer containing the NDVI basic statistics and a new point layer was created with the aid of ArcGIS (Figure 31). The new point layer contained the measures of the trunk diameter, the number of fruits as well as the NDVI basic statistics of the sample trees.

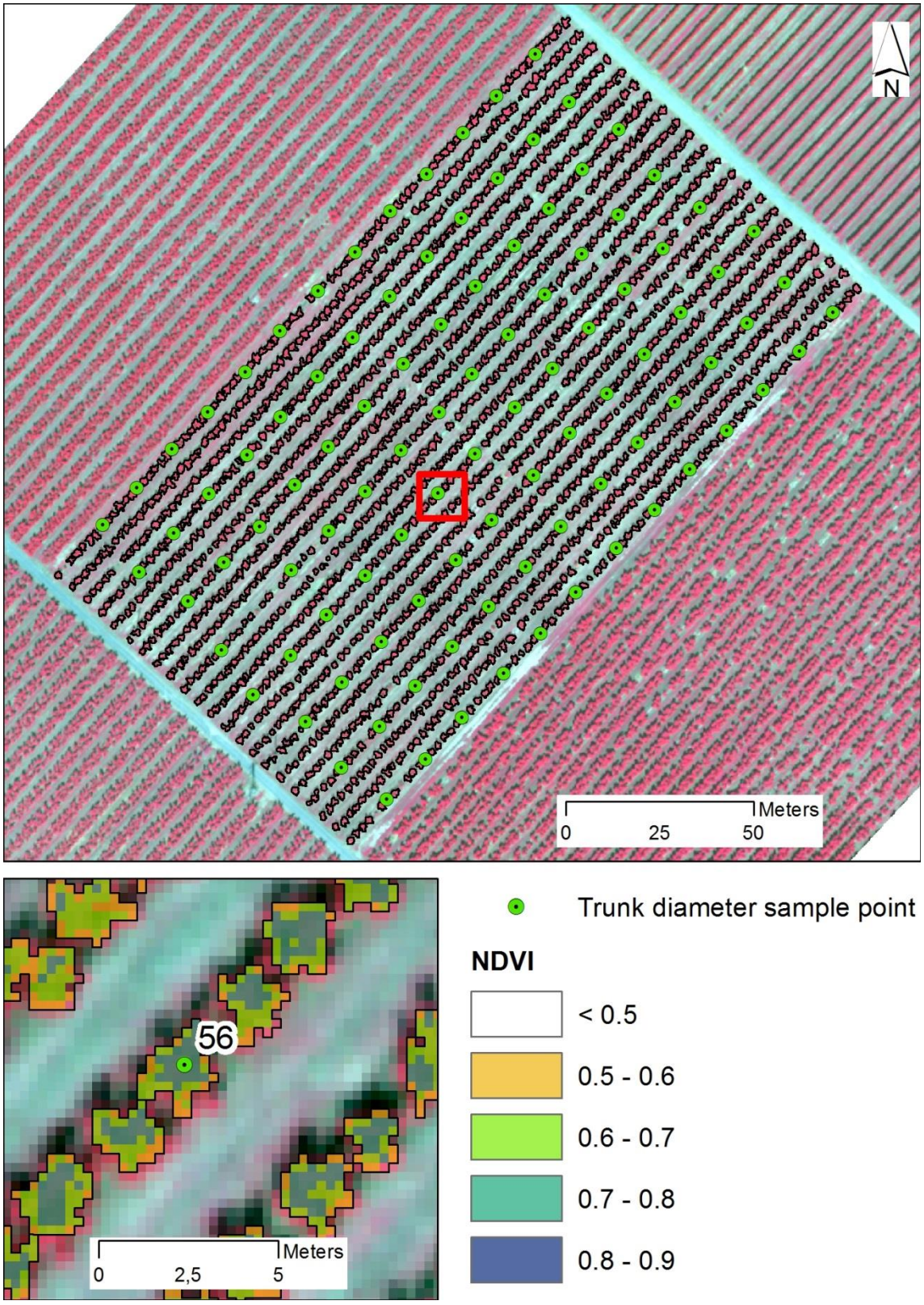

Figure 31. Location of the sample trees where the trunk diameter and number of fruits were measured and counted on 25/05/2016. At each sample tree, the basic NDVI statistics were captured to calculate the relationship between the variables. The sample pattern is (approximately) 15x15 m.

4.7. Definition of differential management zones

In addition to analyse the relationships between the individual properties, possible differential management zones were delineated according to the EC_{25} or NDVI surface values. For that, and in order to classify these properties in different zones, an unsupervised classification method was used. This was the ISODATA algorithm implemented in the Image Analyst of ArcGIS 10.3.1 The ISODATA is a k-means algorithm that uses minimum Euclidean distance to assign a cluster to each candidate pixel in an iterative process (Jensen, 1996), removing redundant clusters or clusters to which not enough samples are assigned. This classifier produces zones which are significantly different.

The following cluster maps were created:

- 2 and 3 Zones of Shallow EC_{25}
- 2 and 3 Zones of Deep EC_{25}
- 2 and 3 Zones of Shallow and Deep EC_{25}
- 2 and 3 Zones of NDVI

4.8. Statistical analysis

Several types of statistical analysis were carried out to describe and analyze the different acquired variables (EC_{25}, soil properties, NDVI and trunk diameter). The software JMP Pro 12 (SAS Institute Inc.) was used.

The following analyses were done:

- Descriptive analysis of variables

- Simple linear regression:
  - EC_{25} data and NDVI with soil properties at the sampling points
  - NDVI and trunk diameter, NDVI and tree canopy area, NDVI and number of fruits, diameter and tree canopy area

- Analysis of variance (ANOVA) of soil properties taking as factors to analyze:
  - 2 and 3 of shallow or deep EC_{25} zones
  - 2 and 3 zones of shallow-deep EC_{25}
  - 2 and 3 zones of NDVI

5. Results and discussion

5.1. Soil properties

Table 12 summarizes the basic statistic parameters of soil properties analyzed in the 40 samples collected in the study field. In this work, only the samples of the first horizon (0-30 cm) were considered[3].

Soil property	Average	SD	Min	Max	CV (%)
$pH_{1:2.5}$	8.20	0.18	7.89	8.89	2.25
$CE_{1:5}$ (dS/m)	1.59	0.87	0.19	3.58	54.41
$CaCO_3$ (%)	33.31	6.29	22.95	52.74	18.88
CEC (meq/100g)	10.35	2.22	6.76	15.26	21.43
M Org (%)	2.16	0.73	1.03	4.46	34.06
WRC -33kPa (%)	22.70	2.78	17.34	29.52	12.24
WRC -1500kPa (%)	12.93	2.35	8.21	19.26	18.14
WRC (%)	9.77	1.46	5.44	13.36	14.96
Clay (%)	23.93	5.84	0.21	32.71	24.38
Coarse Silt (%)	12.32	2.81	4.10	21.12	22.78
Fine Silt (%)	26.46	6.06	16.20	37.90	22.89
Total Silt (%)	38.78	8.86	20.30	59.02	45.67
Coarse Sand (%)	2.52	0.91	1.14	4.90	36.05
Fine Sand (%)	32.23	9.69	16.15	50.49	30.05
Total Sand (%)	34.76	10.60	17.29	55.38	66.10
Depth (cm)	61.15	21.04	30.00	90.00*	34.40

Table 12. Basic statistics of the soil properties analysed for the top soil samples (0-30 cm) and depth for the whole soil profile. (* the maximum measured soil depth was 90 cm, which was the maximum depth reached with the auger hole used for soil sampling).

According to Table 12, the soils of the study area had a basic pH (8.2±0.10). This is typical of soils with high contents of calcium carbonate, as it is the case (33.1±6.29 %).

[3] Due to the time that would be required to analyze 79 soil samples, with all the considered determinations, only the results of the samples of the top horizon were included in the thesis.

It could create problems of ferric chlorosis, which in the case of the study field (and for peach trees) is mended with iron chelates (iron 4.7% + manganese 1% + zinc 0.5%, commercial name Vanguard, information provided by the farmer).

The electrical conductivity ($CE_{1:5}$) had values between 0.19-3.58 dS/m at 25 ºC. The average was 1.59±0.87. These values should be indicating non-saline soils (< 2 dS/m at 25 ºC) or lightly saline soils (2-4 dS/m at 25 ºC). However, these classification ranges refer to salinity in saturated extracts of soil, but not to the 1:5 extract analyzed in this work. Therefore, this interpretation may be not conclusive. In addition, the values should be interpreted depending on the crop that is cultivated. In the present case study, and according to Tanji and Kielen (2002) and Porta et al. (2003), peach orchards are sensitive to the salts, with a threshold value of 1.7 dS/m at 25 ºC in which the plant starts to decrease the yield. In addition, the slope of the regression line with yield (according to Tanji and Kielen 2002) is 21%, which indicates a fast decrease of yield as salinity increases above the threshold. This means that may be there are zones of the field in which trees could be affected by soil salinity. Nevertheless, it could be masked by the effect of drip irrigation (Figure 32).

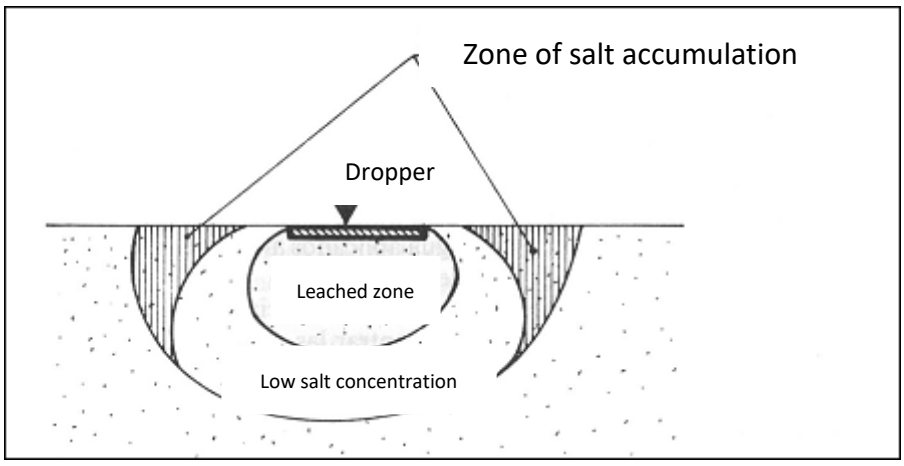

Figure 32. Typical distribution of water and salts in drip irrigation. The water content is higher in the zone closer to the drip and leach the salts to the exterior part of the bulb and the top soil. (Source: http://ocwus.us.es/).

Some field observations confirmed the results about soil salinity. Figure 33 shows a saline patch observed in the upper part of the plot, in an inter-row area. The location of the patch can be viewed in Figure 36. This photograph was acquired after some rainy and windy

days at the end of April 2016, which favoured the action of capillarity. In addition, it can be observed that the bulb zone of the trees is free of salts, as showed in Figure 32.

Figure 33. Saline patch in the study field at the soil sample point num. 30 (03/05/2016). The location of the patch can be observed in Figure 36, which match with an area of high apparent electrical conductivity.

The cation exchange capacity (CEC) is a measure of the total number of negative charges that are available on the surface of soil particles. It is an indicator of the potential of the soil to retain and exchange plant nutrients, by estimating its ability to retain cations (cations = substances which are positively charged). Soils that have a low cation-exchange capacity hold fewer cations and may require more frequent applications of fertilizer than soils that have a high cation-exchange capacity. In the study plot, the average CEC was 10.35±2.22 meq/100g, which according to Ilaco (1985) is low to moderate. From the point of view of fertility, this would indicate that the CEC could be improved by addition of organic matter.

The organic matter content was low or moderate (2.16±0.73 %). This is typical of soils in semiarid areas, with high contents of calcium carbonate.

The average water retention capacity of the top soil horizons was 9.77±1.46 %. If this value is extrapolated to the average depth of the soils (61.15 cm), the WRC would be 58.86±8.79 mm. According to the USDA National Soil Handbook (USDA 1983), these values indicate a very low or low WRC available for the plants (< 64 mm, or up to 127 mm in the case of aridic or xeric soil moisture regime). This indicates the need of irrigation for fruit trees growing.

The most frequent soil texture was loam, clay loam or silty clay loam (Figure 34). Those textures do not represent particular limitations for crop development.

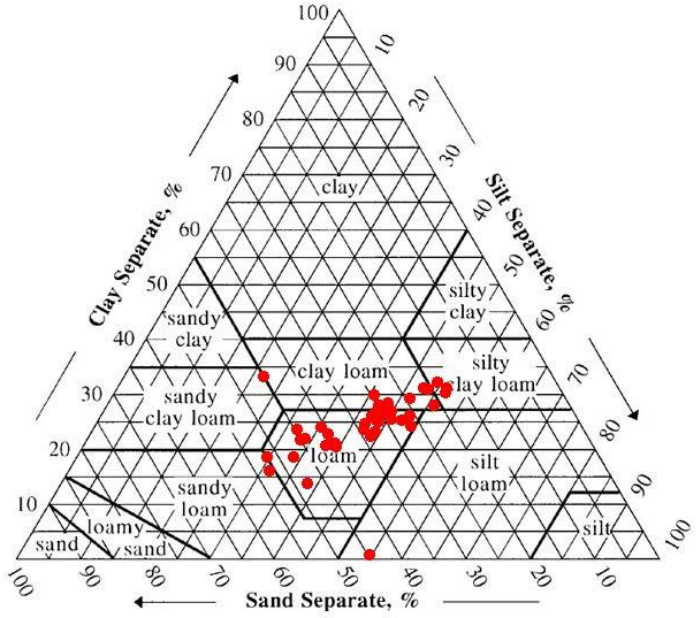

Figure 34. Texture triangle with the distribution of the soil texture class of the 40 samples of the top horizon. (Criteria: USDA Natural Resources Conservation Service – Soils, http://www.nrcs.usda.gov/wps/portal/nrcs/detail/soils/survey/).

Here below, Table 13 shows the correlation coefficients, and their significant level, between soil properties of the top soil samples. The properties with higher correlation between them were the related to CEC, organic matter content, water retention capacity at -33 and -1500 kPa and texture (clay, fine silt and fine sand). These were expected relationships, since the CEC is mainly related to clay and organic matter content. Also

WRC at -33 and -1500 kPa are related to clay and organic matter content, and negative correlated to fine sand and fine silt.

	Soil depth (cm)	$pH_{1:2.5}$	$CE_{1:5}$ (dS/m)	$CaCO_3$ (%)	CEC (meq/100g)	M Org (%)	WRC -33kPa (%)	WRC -1500kPa (%)	WRC (%)	Clay (%)	Coarse Silt (%)	Fine Silt (%)	Coarse Sand (%)
Soil depth (cm)													
$pH_{1:2.5}$	-0,0750												
$CE_{1:5}$ (dS/m)	0,2006	0.1290											
$CaCO_3$ (%)	-0,4773	0.0811	0.0082										
CEC (meq/100g)	-0,0176	-0.1383	0.0400	0.1032									
M Org (%)	0,1082	-0.2647	-0.0732	0.0737	0.7499								
WRC -33kPa (%)	0,0755	-0.3587	0.0769	0.1624	0.7804	0.7453							
WRC -1500kPa (%)	0,1099	-0.3104	0.1876	0.1290	0.7889	0.6022	0.8504						
WRC (%)	-0,0286	-0.1839	-0.1548	0.1018	0.2178	0.4506	0.5364	0.0122					
Clay (%)	-0,0517	-0.3061	-0.0182	0.1841	0.5224	0.4205	0.7819	0.7587	0.2690				
Coarse Silt (%)	0,1009	-0.1182	0.0050	-0.0194	0.3901	0.2420	0.1922	0.2179	0.0158	0.0440			
Fine Silt (%)	0,1451	-0.0608	-0.0005	-0.0283	0.7479	0.5180	0.6084	0.5866	0.2152	0.3177	0.3652		
Coarse Sand (%)	-0,4891	-0.0471	-0.2900	0.2106	-0.0629	0.0191	-0.1332	-0.2101	0.0839	-0.1783	-0.0685	-0.0919	
Fine Sand (%)	0,0164	0.1988	-0.0331	-0.1666	-0.8250	-0.5812	-0.8219	-0.7987	-0.2808	-0.6862	-0.3996	-0.8366	0.0432

p-value < 0.01; p-value < 0.05

Table 13. Correlation coefficients between soil properties of the top horizon (0-30 cm), N = 40.

5.2. Apparent electrical conductivity

Figure 36 shows the results of the electrical conductivity survey carried out by means of the Veris 3100 surveyor. The values have been referred to the standard units of dS/m at 25 ºC. After filtering anomalous values, a total of 1668 points were acquired in the 2.24 ha peach study plot. Shallow EC_{25} and Deep EC_{25} values are presented in the following figures (Figure 35).

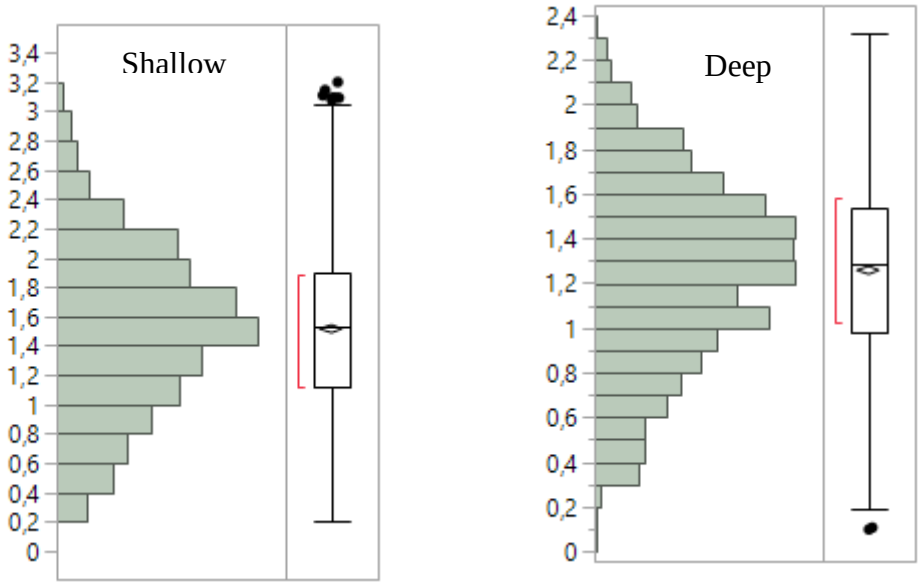

Figure 35. Frequency distribution of the apparent electrical conductivity values acquired by the Veris 3100 sensor. Left: Shallow (dS/m at 25 ºC); right: Deep (dS/m at 25 ºC).

The top soil volume explored by Veris 3100 (Shallow lecture, 0-30 cm) presented higher values than the 0-90 cm volume (Deep lecture): 1.51±0.57 and 1.25±0.42 dS/m at 25 ºC. This can also be seen in the maps of Figure 36, in which EC_{25} data are compared with the same legend.

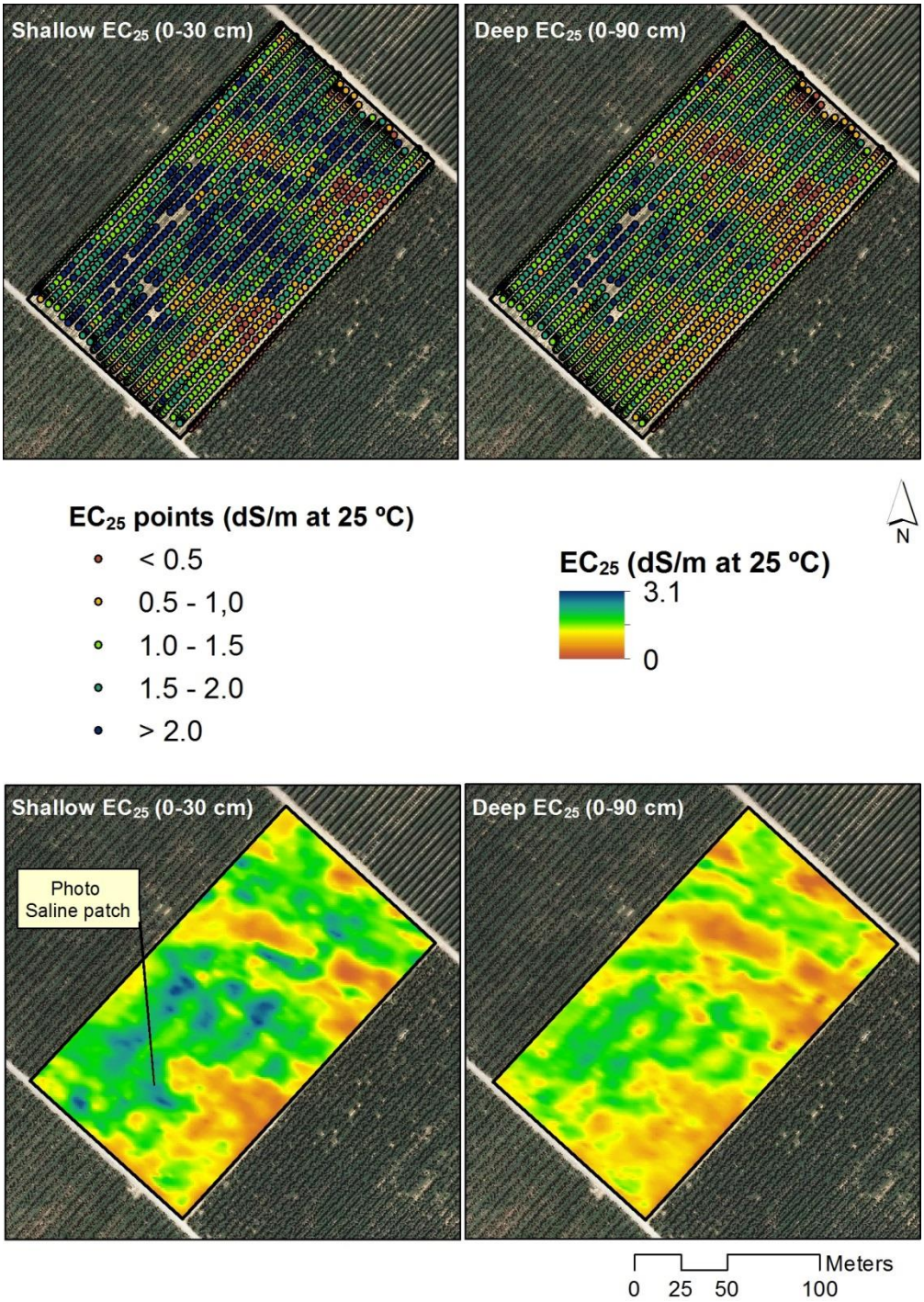

Figure 36. Electrical conductivity points (EC_{25}). Top: Points with Shallow and Deep EC_{25} values. Bottom: Interpolated surface from Shallow and Deep EC_{25} values.

The shallow and deep EC_{25} lectures were highly correlated (R= 0.788). This can be seen in Figure 37, which shows the point cloud of the 1668 acquired points.

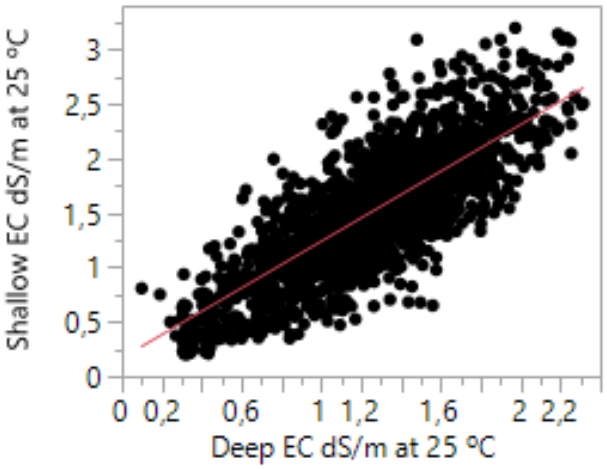

Figure 37. Point cloud of the shallow and deep data acquired by Veris 3100 and referred to the standard units of dS/m at 25 ºC. The figure also shows the adjusted regression line.

The linear regression model between both variables is shown in Equation 4:

Equation 4

$$\textbf{Shallow } \mathbf{EC_{25}} = 11.93 + 1.057 \textbf{ Deep } \mathbf{EC_{25}}$$

P-value < 0.0001 and R^2= 0.622

The spatial distribution of the shallow and deep apparent electrical conductivity seems to have a relationship with former landforms and/or type of soils in the study area. As described in section 3.1 (study area), land levelling works were carried out in this area to remove stone terraces to create larger fields. This can be seen in Figure 38. This figure shows the comparison between the location of the old stone terraces in 1946 and the apparent electrical conductivity survey carried out in the present research. Lower EC_{25} values seem to follow the pattern of the lower part of the terraces, which were filled with marls and calcareous rocks. Between the terraces there are higher EC_{25} values, probably due to deeper soils. In the highest part of the field (SE), there were mainly low EC_{25} values, probably due to the higher slope degree of this zone and lower soil depth.

Another interesting interpretation of the pattern of spatial variation of shallow and deep EC_{25} is that the high relationship between them would indicate that the pattern of top soil does not vary in relation to the pattern of deeper layers, i.e. soil varies in a homogeneous manner in depth.

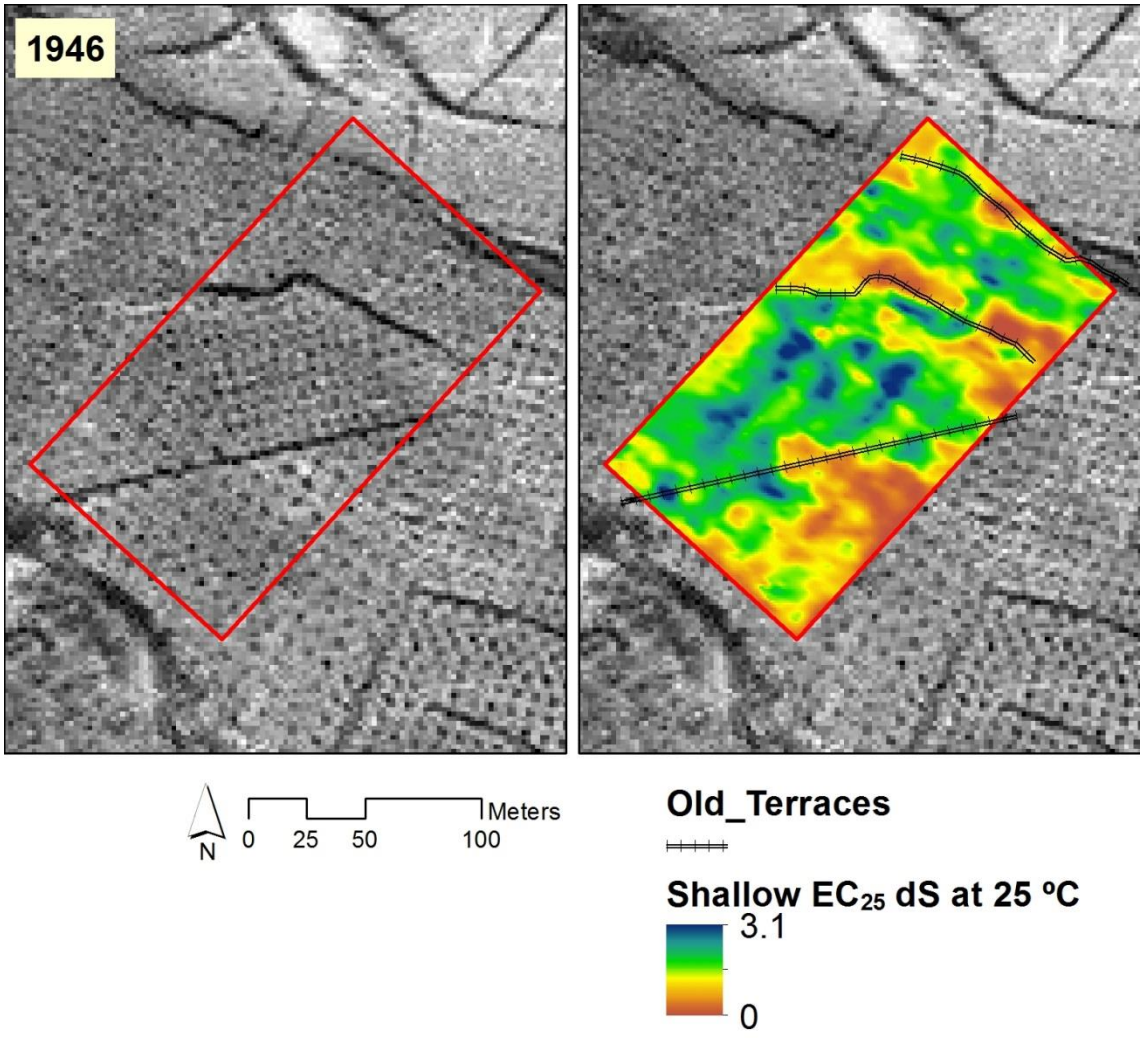

Figure 38. Comparison between the location of old stone terraces in the 1946 orthophoto and the apparent electrical conductivity surface (Shallow EC_{25} dS/m at 25 ºC) in the study plot. Source: Own elaboration. 1946 Orthophotos were downloaded from the Cartographic and Geologic Institute of Catalonia).

5.3. Normalized Difference Vegetation Index

Figure 39 shows the results of the different processing made to the airborne multispectral image acquired on May 16, 2016, with a spatial resolution of 0.25 m. As result, 1816 peach trees were identified in the study plot. The polygon cover created after masking the NDVI image by reclassifying according to the threshold of 0.5, allowed to know the tree canopy area per tree. It ranged from 0.625 – 5.5 m^2, with an average of 2.82±0.60 m^2. Then, the zonal statistics operation between the tree canopy area and the NDVI image allowed the calculation of the basic statistics of the NDVI per tree. The average NDVI values per tree ranged from 0.40 – 0.75±0.04. In Figure 39, one can observe the spatial distribution of these values in the plot. Two main zones can be distinguished: one with high NDVI values, in the NW of the plot, and one with low NDVI values, in the SE of the plot.

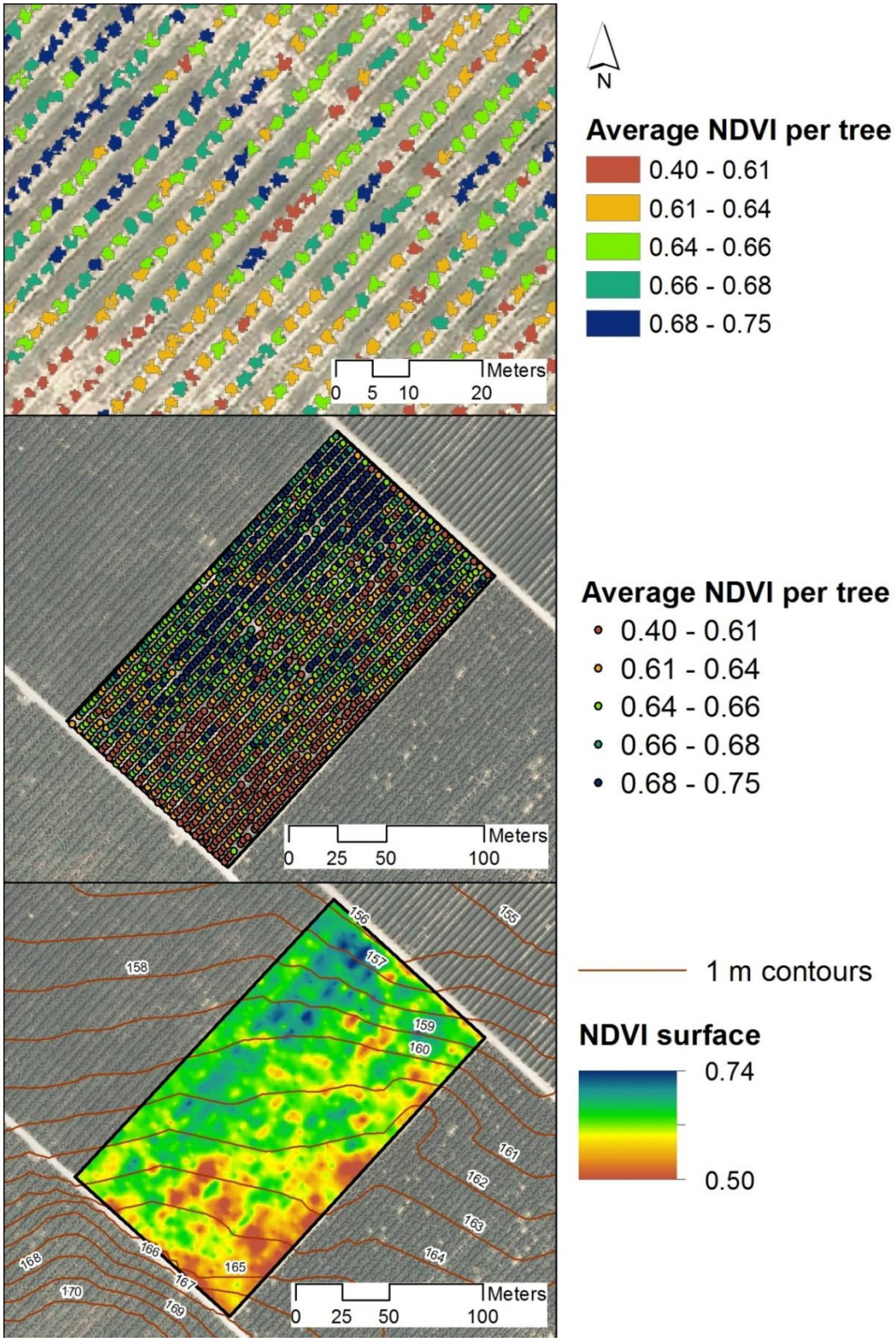

Figure 39. Top: Detail of the tree canopy area coloured by the average NDVI per tree as a result of the reclassification of the NDVI according to the 0.5 threshold. Middle: Trees represented as points as result of the computation of the centroid of the tree canopy area. The points are coloured by the average NDVI. Bottom: NDVI surface as result of the interpolation by the kriging method. Contours are overlaid.

According to Figure 39, the spatial distribution of NDVI seems to follow a gradient from the south to the north of the plot. Zones with higher elevation have a lower NDVI value than the lower zones. To some extent, the pattern is similar to the EC_{25} one (Figure 36 and Figure 38). Nevertheless, there are some differences. NDVI shows a more continuous distribution from south to north, without big changes where the old terraces were located (Figure 40).

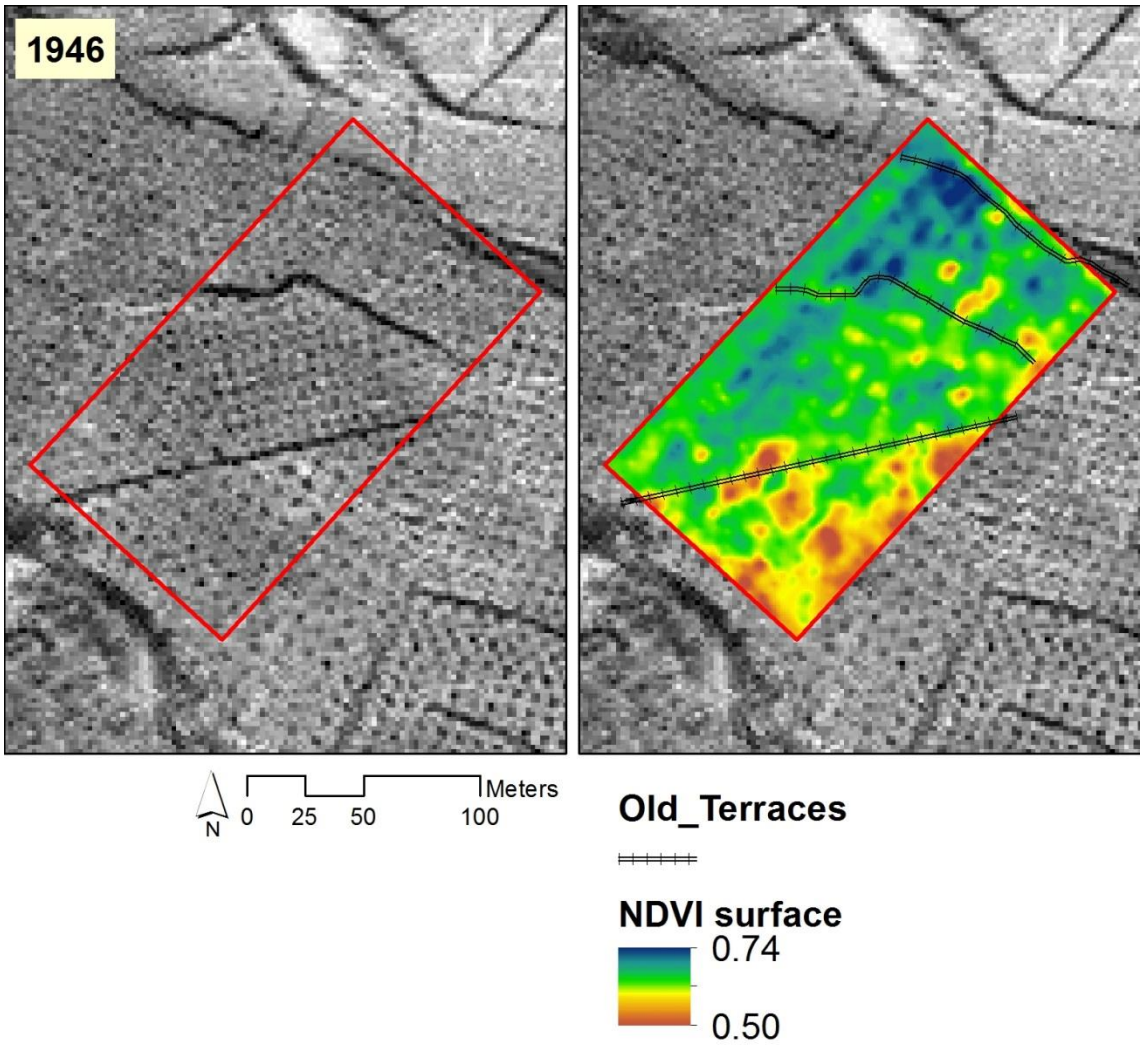

Figure 40. Comparison between the location of old stone terraces in the 1946 orthophoto and the NDVI surface in the study plot. Source: Own elaboration. 1946 Orthophotos were downloaded from the Cartographic and Geologic Institute of Catalonia).

5.4. Relationship between soil properties, EC_{25} and NDVI values and zones

5.4.1. Soil properties and EC_{25}

Apparent soil electrical conductivity is a complex measurement that requires knowledge and experience to interpret (Corwin and Lesch, 2005). Ground-truth soil samples are obligatory to be able to understand and interpret spatial measurements of ECa.

Table 14 shows the correlation coefficients and significance level of the relationships between the shallow and deep EC_{25} and soil properties for the top horizon (0-30 cm). The results indicated a positive and significant correlation of the shallow and deep EC_{25} with the $CE_{1:5}$ (p-value < 0.01) and with the WRC at -1500 kPa (p-value < 0.05). The EC_{25} values also showed a negative correlation with the coarse sand fraction. The results agree with the theoretical basis for the relationship between apparent electrical conductivity and soil properties developed by Rhoades et al. (1999). In this model, EC_{25} is a function of soil water content, the electrical conductivity of the soil water and of the soil particles and the soil bulk density.

Usually, the electrical conductivity signal primarily reflects soil moisture content and cation exchange capacity. The latter in turn depends essentially on clay content and soil organic matter (Williams and Hoey, 1987). Unexpectedly, however, in the present study there was not direct correlation with the clay content, as in research by other authors (Corwin and Lesch, 2005; Sudduth et al., 2005). These relationships are more frequent in non-saline soils, where conductivity variations are primarily a function of soil texture, moisture content, and CEC (Rhoades et al., 1999). These authors, together with Doolittle and Brevik (2014) and Scudiero et al. (2013), say that, under non-saline conditions, soil texture (more specifically clay content) and soil water content are the two predominant factors influencing ECa. In the study area, as shown in section 5.1 (soil properties), there were lightly saline soils that could be masking the relationship between EC_{25} and clay. Despite this discussion, other authors have found a lack of correlation between ECa and clay content, even in non-saline soils (Serrano et al., 2013). In their opinion, this justifies the need of further research to clarify the causes of this behaviour, in particular in shallow Mediterranean soils.

Regarding the relationship with sand, Williams and Hoey (1987) also stated the usefulness of soil conductivity systems, from the fact that sands have a low conductivity, as in the present case that showed a negative correlation with EC_{25} values.

The soil depth also showed a positive significant correlation with the shallow and deep EC_{25}. It means that deeper soils have higher EC_{25} values.

	Shallow EC_{25}	**Deep** EC_{25}
Shallow EC_{25}	1.0000	0.9097
Deep EC_{25}	0.9097	1.0000
$pH_{1:2.5}$	-0.1931	-0.1718
$CE_{1:5}$ (dS/m)	0.5472	0.4791
$CaCO_3$ (%)	-0.0864	-0.1972
CEC (meq/100g)	0.1361	0.1487
M Org (%)	0.1292	0.1128
WRC -33kPa (%)	0.2695	0.2605
WRC -1500kPa (%)	0.3370	0.3596
WRC (%)	-0.0326	-0.0853
Clay (%)	0.2071	0.1638
Coarse Silt (%)	0.0532	0.0798
Fine Silt (%)	0.1285	0.2309
Coarse Sand (%)	-0.4180	-0.3511
Fine sand (%)	-0.1600	-0.1801
Total Silt (%)	0.1230	0.2156
Total Sand (%)	-0.1972	-0.2110
Soil depth (cm)	0,4399	0,4765

p-value < 0.01; p-value < 0.05

Table 14. Correlation coefficients between Shallow and Deep EC $_{25}$ and soil properties of the top horizon (0-30 cm), N = 40.

5.4.2. Soil properties and EC_{25} zones

Table 15 shows the results of the ANOVA tests between the EC_{25} zones (shallow or deep) and the soil properties. Figure 41 shows the spatial distribution of the zones with the soil sampling points overlaid. The objective was to prove the correspondence of EC_{25} zones (2 zones in this case) with the measured soil properties, and see if in each zone there were significant different means of the properties. The results confirm the relationships found between the continuous values of the shallow and deep EC_{25} and soil properties (section 5.4.1), but there were also other properties that could be distinguished in the shallow EC_{25} zones. This was the case of pH, which was negatively correlated, and also WRC -33 kPa. In addition, the clay content of the top horizon could be differentiated by zones of shallow EC_{25}, with a positive relationship (the higher the EC_{25} the higher the clay content). This is in agreement with the theoretical background about the nature of the ECa signal exposed above, although the direct relationship between clay content and EC_{25} was not significant, possibly because of the salinity of the soils.

The results did not improve significantly in the case of the deep EC_{25} zones, but this was expected because the analyzed soil properties corresponded to the top horizon (0-30 cm). Soil depth also showed a clear distinction between the two types of zones, with similar averages either if the zoning was done with the shallow or deep EC_{25}.

	Shallow EC_{25} Zone		**Deep EC_{25} Zone**	
	Low (N=19)	High (N=20)	Low (N=18)	High (N=21)
Shallow EC_{25}	0.97 b	2.07 a	0.98 b	2.01 a
Deep EC_{25}	0.86 b	1.59 a	0.78 b	1.62 a
$pH_{1:2.5}$	8.24 a	8.14 b	8.21 a	8.16 a
$CE_{1:5}$ (dS/m)	1.13 b	1.94 a	1.16 b	1.87 a
$CaCO_3$ (%)	33.96 a	33.01 a	34.38 a	32.70 a
CEC (meq/100g)	10.24 a	10.61 a	9.94 a	10.84 a
M Org (%)	2.05 a	2.28 a	2.09 a	2.25 a
WRC -33kPa (%)	21.90 b	23.96 a	22.06 a	23.44 a
WRC -1500kPa (%)	12.29 a	13.67 a	12.12 b	13.74 a
WRC (%)	9.59 a	9.99 a	9.62 a	9.99 a
Clay (%)	22.16 b	25.90 a	23.01 a	25.00 a
Coarse Silt (%)	12.40 a	12.36 a	12.18 a	12.54 a
Fine Silt (%)	26.18 a	27.12 a	24.82 a	28.24 a
Coarse Sand (%)	2.92 b	2.18 a	2.91 a	2.22 b
Fine Sand (%)	33.47 a	30.35 a	33.96 a	30.07 a
Silt (%)	38.60 a	39.49 a	37.03 a	40.08 a
Sand (%)	36.38 a	32.52 a	36.86 a	32.92 a
Soil depth (cm)	51.57 a	70.25 b	49.16 b	71.42 a

p-value < 0.1, p-value < 0.05, p-value < 0.01

Table 15. ANOVA tests between the Shallow or Deep EC_{25} (2 zones or clusters) and soil properties. The letters "a" and "b" indicate different statistical significant groups.

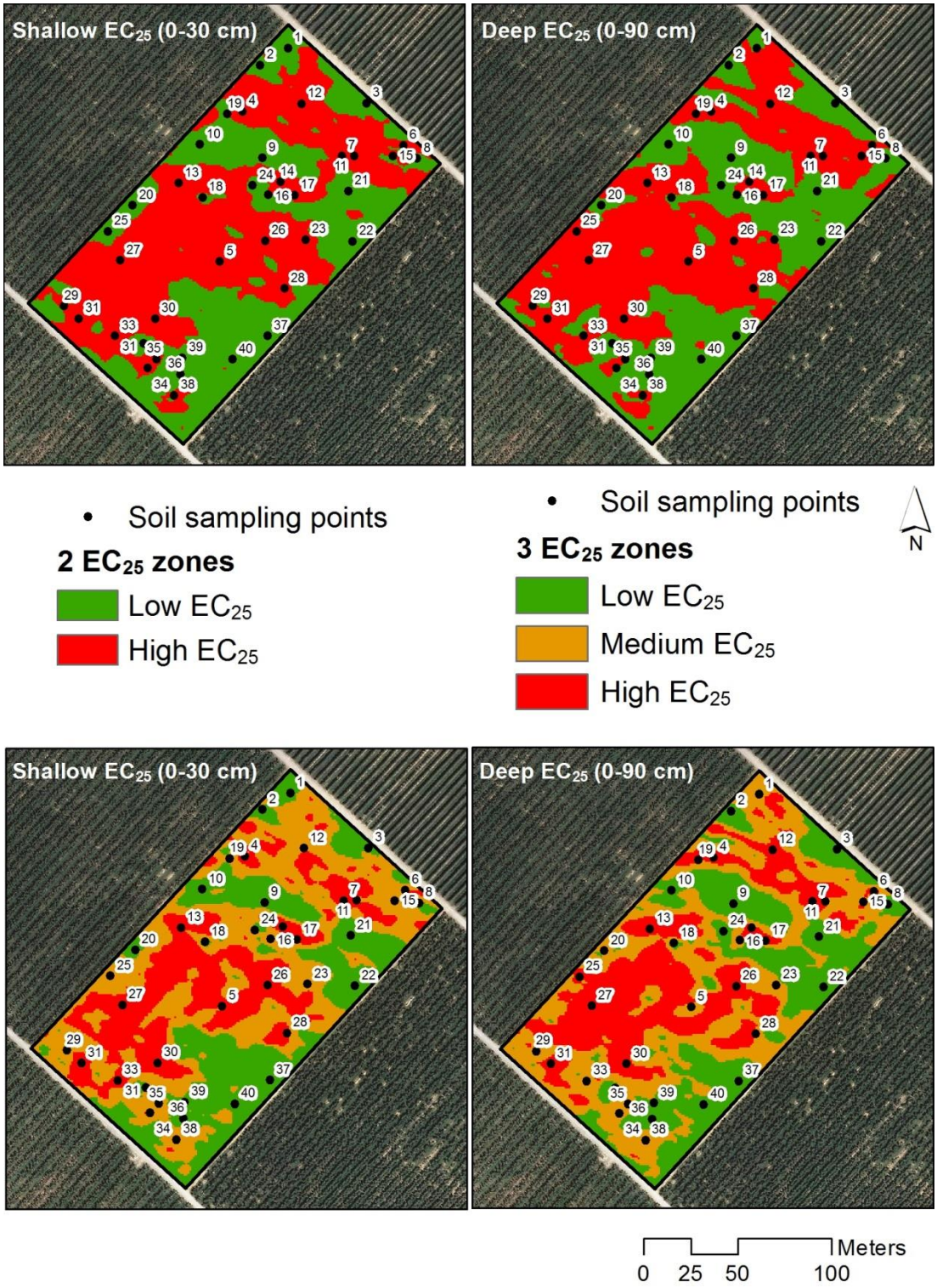

Figure 41. 2 (top) or 3 (bottom) zones of Shallow or Deep EC_{25} as result of the Isodata unsupervised classification. The soil sampling points are overlaid.

Table 16 shows the results of the ANOVA tests between the EC_{25} zones (shallow or deep) and the soil properties: in this case 3 zones were considered. The relationships between the continuous values of the shallow and deep EC_{25} were confirmed as well as in the previous case, but some of the properties differ from the two zones analysis. In the case

of the 3 zones, pH, WRC -33 kPa, clay and coarse sand content had not a significant statistic correlation with the shallow EC_{25} zones. Also, in this case, $EC_{1:5}$ preserved a positive relation, with a p-value < 0.01 for the shallow zones, but with a p-value < 0.05 for the deep zones. Opposite than in the 2 zones analysis, WRC -1500 kPa (%) presented only a tendency for the shallow zones, and a positive correlation with the deep zones (p-value < 0.05). The fine silt tendency was evidenced again. Nevertheless, although the ANOVA analysis found significant differences in the above mentioned properties, only two different groups (but not 3) could be distinguished. This could indicate that the 2 zone EC_{25} maps would be better than the 3 zone maps to distinguish areas with different soil properties.

	Shallow EC_{25} Zone			**Deep EC_{25} Zone**		
	Low (N=16)	Medium (N=10)	High (N=13)	Low (N=14)	Medium (N=12)	High (N=13)
Shallow EC_{25}	0.89 c	1.62 b	2.26 a	0.86 c	1.65 b	2.15 a
Deep EC_{25}	0.73 c	1.43 b	1.70 a	0.67 c	1.33 b	1.76 a
$pH_{1:2.5}$	8.23 a	8.12 a	8.19 a	8.22 a	8.14 a	8.19 a
$CE_{1:5}$ (dS/m)	1.09 b	1.56 ab	2.08 a	1.08 b	1.65 ab	1.93 a
$CaCO_3$ (%)	34.62 a	31.54 a	33.55 a	34.85 a	31.65 a	33.66 a
CEC (meq/100g)	9.94 a	11.37 a	10.30 a	9.92 a	10.30 a	11.09 a
M Org (%)	2.07 a	2.37 a	2.14 a	2.02 a	2.17 a	2.34 a
WRC -33kPa (%)	21.98 a	23.32 a	23.42 a	21.83 a	22.98 a	23.68 a
WRC -1500kPa (%)	11.99 a	14.08 a	13.40 a	11.82 b	13.35 a	13.93 a
WRC (%)	9.97 a	9.24 a	10.01 a	9.99 a	9.63 a	9.74 a
Clay (%)	22.87 a	24.97 a	24.89 a	22.66 a	25.22 a	24.56 a
Coarse Silt (%)	12.21 a	12.60 a	12.42 a	11.72 a	12.87 a	12.63 a
Fine Silt (%)	24.92 a	28.92 a	27.07 a	24.90 a	25.29 a	29.83 a
Coarse Sand (%)	2.91 a	2.40 a	2.20 a	2.88 a	2.40 a	2.30 a
Fine Sand (%)	34.08 a	29.89 a	30.66 a	34.35 a	32.61 a	28.51 a
Silt (%)	37.15 a	41.54 a	39.50 a	41.43 a	38.18 a	42.46 a
Sand (%)	36.98 a	32.28 a	32.86 a	37.22 a	35.00 a	30.81 a
Soil depth (cm)	46.87 b	75.50 a	67.69 a	44.28 b	75.83 a	65.76 a

p-value < 0.1, p-value < 0.05, p-value < 0.01

Table 16. ANOVA tests between the Shallow or Deep EC_{25} (3 zones or clusters) and soil properties. The values are the average of each soil property in each EC_{25} zone. The letters "a", "b" and "c" indicate different statistical significant groups.

Table 17 shows the results of the ANOVA tests between the 2 zones of shallow and deep EC_{25} (clustered together) with the soil properties. Figure 42 shows the spatial distribution of the shallow-deep zones with the soil sampling points overlaid. Shallow EC_{25}, deep EC_{25} (dS/m) and $CE_{1:5}$ (dS/m) were the only properties correlated with a p-value < 0.01. Other properties that presented some degree of relationship with the EC_{25} zones were the WRC -1500 kPa (positive correlation) and the coarse sand (negative correlation).

In comparison with the shallow and deep EC_{25} clustered by separate, the zones of the same variables clustered together resulted in lower number of related soil properties (Table 15 versus Table 17).

	Shallow-Deep ECa Zone	
	Low (N=17)	High (N=22)
Shallow EC_{25}	0.93 b	2.00 a
Deep EC_{25}	0.76 b	1.60 a
$pH_{1:2.5}$	8.22 a	8.16 a
$CE_{1:5}$ (dS/m)	1.08 b	1.89 a
$CaCO_3$ (%)	34.50 a	32.68 a
CEC (meq/100g)	10.10 a	10.68 a
M Org (%)	2.12 a	2.21 a
WRC -33kPa (%)	22.06 a	23.37 a
WRC -1500kPa (%)	12.13 b	13.66 a
WRC (%)	9.91 a	9.70 a
Clay (%)	23.17 a	24.78 a
Coarse Silt (%)	12.21 a	12.51 a
Fine Silt (%)	25.05 a	27.91 a
Coarse Sand (%)	2.94 a	2.23 b
Fine Sand (%)	33.58 a	30.54 a
Silt (%)	37.28 a	40.43 a
Sand (%)	36.52 a	32.76 a
Soil depth (cm)	46.76 b	72.27 a

p-value < 0.1, p-value < 0.05, p-value < 0.01

Table 17. ANOVA tests between the Shallow and Deep EC_{25} (2 zones or clusters) and soil properties. The values are the average of each soil property in each EC_{25} zone. The letters "a" and "b" indicate different statistical significant groups.

Table 18 shows the results of the ANOVA tests between the 3 EC_{25} zones of shallow and deep (clustered together) with the soil properties. As in the previous case, only the shallow EC_{25}, the deep EC_{25} (dS/m) and the $CE_{1:5}$ (dS/m) were significantly correlated. Other soil properties, such as the WRC -33kPa (%) and WRC -1500kPa (%), only showed a certain tendency. There were not correlations with physical properties.

In the previous 3 zones case (Table 16), the shallow and deep EC_{25} clustered by separate, produced better results with respect soil properties differentiation than when the EC_{25} variables were clustered together.

	Shallow-Deep ECa Zone		
	Low (N=15)	Medium (N=10)	High (N=14)
Shallow EC_{25}	0.87 c	1.56 b	2.23 a
Deep EC_{25}	0.70 c	1.36 b	1.72 a
$pH_{1:2.5}$	8.23 a	8.14 a	8.17 a
$CE_{1:5}$ (dS/m)	1.05 b	1.53 ab	2.08 a
$CaCO_3$ (%)	34.64 a	31.17 a	33.87 a
CEC (meq/100g)	10.03 a	10.33 a	10.92 a
M Org (%)	2.10 a	2.01 a	2.37 a
WRC -33kPa (%)	22.08 a	22.06 a	24.10 a
WRC -1500kPa (%)	12.00 b	13.04 ab	14.03 a
WRC (%)	10.06 a	9.02 a	10.07 a
Clay (%)	22.91 a	23.00 a	26.11 a
Coarse Silt (%)	12.18 a	12.59 a	12.45 a
Fine Silt (%)	25.27 a	26.35 a	28.38 a
Coarse Sand (%)	2.78 a	2.73 a	2.15 a
Fine Sand (%)	33.93 a	33.76 a	28.31 a
Silt (%)	40.84 a	38.95 a	37.47 a
Sand (%)	36.70 a	36.48 a	30.46 a
Soil depth (cm)	47.33 b	70.50 a	69.28 a

p-value < 0.1, p-value < 0.05, p-value < 0.01

Table 18. ANOVA tests between the Shallow and Deep EC_{25} (3 zones or clusters) and soil properties. The values are the average of each soil property in each EC_{25} zone. The letters "a", "b" and "c" indicate different statistical significant groups.

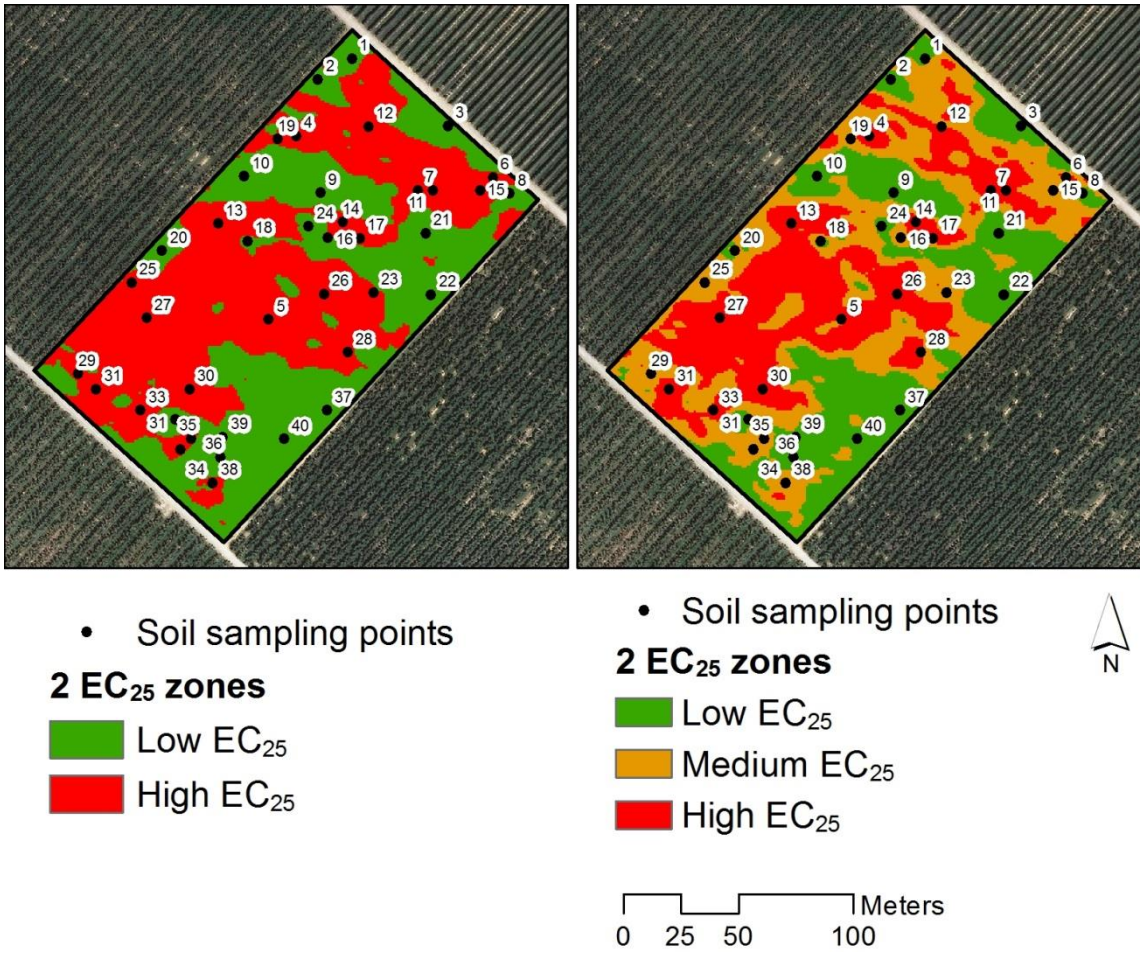

Figure 42. Shallow and Deep EC_{25} (2 and 3 zones) and soil sample points.

5.4.3. Soil properties and NDVI

The analysis of correlation between soil properties of the top horizon and NDVI is presented in Table 19. Differently from the relationships with the EC_{25} (section 5.4.1), the NDVI was not related to properties as $EC_{1:5}$, water retention capacity or soil depth. In this case, only the textural fractions coarser than clay were correlated. The CEC also showed a certain positive tendency.

The NDVI was not either correlated to the apparent electrical conductivity measured with Veris 3100 or measured at laboratory ($EC_{1:5}$). Regarding this lack of relationship, (Fortes et al., 2013) state that NDVI is a measure of the plant status, while ECa is related to some soil properties. These related soil properties may help to explain the potential plant status but that also depend on other parameters, which are difficult to estimate. Because of that,

although there could be a relationship between ECa and yield (Kitchen et al., 1999) or between NDVI and yield (Martínez-Casasnovas et al., 2012), it could not be a direct relationship between ECa and NDVI. The cause could be the type of irrigation system (drip irrigation), which maintains the root area free of salts (Figure 32). It allows the growing of the trees without affection by salts or maintaining the soil with certain levels of salts that are tolerated by the peach trees.

	NDVI
Shallow CE_{25} (dS/m)	0.0712
Deep CE_{25} (dS/m)	0.2066
$pH_{1:2.5}$	0.1102
$CE_{1:5}$ (dS/m)	0.0759
$CaCO_3$ (%)	0.1197
CEC (meq/100g)	0.2847
M Org (%)	0.0979
WRC -33kPa (%)	0.1677
WRC -1500kPa (%)	0.2414
WRC (%)	-0.0765
Clay (%)	0.0480
Coarse Silt (%)	0.5856
Fine Silt (%)	0.3743
Coarse Sand (%)	0.0897
Fine sand (%)	-0.3796
Total Silt (%)	0.5233
Total Sand (%)	-0.3659
Soil depth (cm)	0.0775

p-value < 0.1, p-value < 0.05, p-value < 0.01

Table 19. Correlation coefficients between NDVI surface and soil properties of the top horizon (0-30 cm), N = 40.

5.4.4. Soil properties and NDVI zones

Table 20 shows the results of the ANOVA tests of sampled soil properties checking the possible effect of NDVI classes (factor under analysis). Figure 43 shows the spatial distribution of the zones with the soil sampling points overlaid. In this case, 2 NDVI zones were considered. As it can be observed, only a correlation with some texture fractions

was found. In particular, the relationship was with coarse silt and total silt (p-value <0.01); and with fine silt, fine sand and, consequently, with total sand (p-value <0.05). However, possible expected relationships between the NDVI zones and the EC_{25} or $EC_{1:5}$ were not found. Neither with the soil depth at the sampling points, which had been a logical relationship, since higher vigor trees would be located in deeper soils.

	NDVI Zone	
	Low (N=12)	High (N=27)
Shallow EC_{25}	1.36 a	1.61 a
Deep EC_{25}	1.04 a	1.32 a
$pH_{1:2.5}$	8.19 a	8.17 a
$CE_{1:5}$ (dS/m)	1.41 a	1.61 a
$CaCO_3$ (%)	32.38 a	33.96 a
CEC (meq/100g)	9.67 a	10.76 a
M Org (%)	2.10 a	2.21 a
WRC -33kPa (%)	22.18 a	23.08 a
WRC -1500kPa (%)	12.25 a	13.32 a
WRC (%)	9.93 a	9.74 a
Clay (%)	23.20 a	24.47 a
Coarse Silt (%)	10.65 b	13.15 a
Fine Silt (%)	23.66 b	28.00 a
Coarse Sand (%)	2.4 a	2.6 a
Fine Sand (%)	37.06 a	29.56 b
Silt (%)	34.32 b	41.16 a
Sand (%)	39.44 a	32.16 b
Soil depth (cm)	60.00 a	61.66 a

p-value < 0.1, p-value < 0.05, p-value < 0.01

Table 20. ANOVA tests between the NDVI (2 zones or clusters) and soil properties. The values are the average of each soil property in each NDVI zone. The letters "a" and "b" indicate different statistical significant groups.

The results of the ANOVA tests of sampled soil properties checking the possible effect of NDVI classes (factor under analysis). are shown in Table 21. In this case, another soil property could be separated per zones. This was the cation exchange capacity (p-value <0.05). Moreover, the relationship between NDVI zones and soil texture was maintained. In fact, coarse and fine silt presented a strong correlation with NDVI (p-value <0.01) (and consequently also for the total silt). The same for total sand (p-value <0.01), although the

fine sand with a p-value <0.05 and none relation with coarse sand. As in the NDVI 2-zones, the soil depth could not be differentiated.

As in the case of the EC_{25} zones, although the ANOVA analysis found significant differences in the above mentioned properties, only two different groups (but not 3) could be distinguished. This would be an indication that the medium zone is to some extent ambiguous, and can either belong to the low or high group.

	NDVI Zone		
	Low (N=5)	Medium (N=17)	High (N=17)
Shallow EC_{25}	1.46 a	1.56 a	1.53 a
Deep EC_{25}	1.15 a	1.16 a	1.33 a
$pH_{1:2.5}$	8.18 a	8.15 a	8.22 a
$CE_{1:5}$ (dS/m)	1.35 a	1.58 a	1.56 a
$CaCO_3$ (%)	31.20 a	33.61 a	34.00 a
CEC (meq/100g)	10.24 ab	9.54 b	11.37 a
M Org (%)	2.44 a	2.02 a	2.24 a
WRC -33kPa (%)	23.48 a	21.78 a	23.62 a
WRC -1500kPa (%)	12.84 a	12.44 a	13.60 a
WRC (%)	10.64 a	9.34 a	10.01 a
Clay (%)	26.78 a	22.43 a	24.94 a
Coarse Silt (%)	9.74 b	11.58 b	13.95 a
Fine Silt (%)	26.24 ab	22.93b	30.52 a
Coarse Sand (%)	2.12 a	2.81 a	2.39 a
Fine Sand (%)	33.40 ab	36.31 a	26.98 b
Silt (%)	35.96 b	34.54 b	44.49 a
Sand (%)	35.50 ab	39.11 a	29.37 b
Soil depth (cm)	60.00 a	58.52 a	64.11 a

p-value < 0.1, p-value < 0.05, p-value < 0.01

Table 21. ANOVA tests between the NDVI (3 zones or clusters) and soil properties. The values are the average of each soil property in each NDVI zone. The letters "a", "b" and "c" indicate different statistical significant groups.

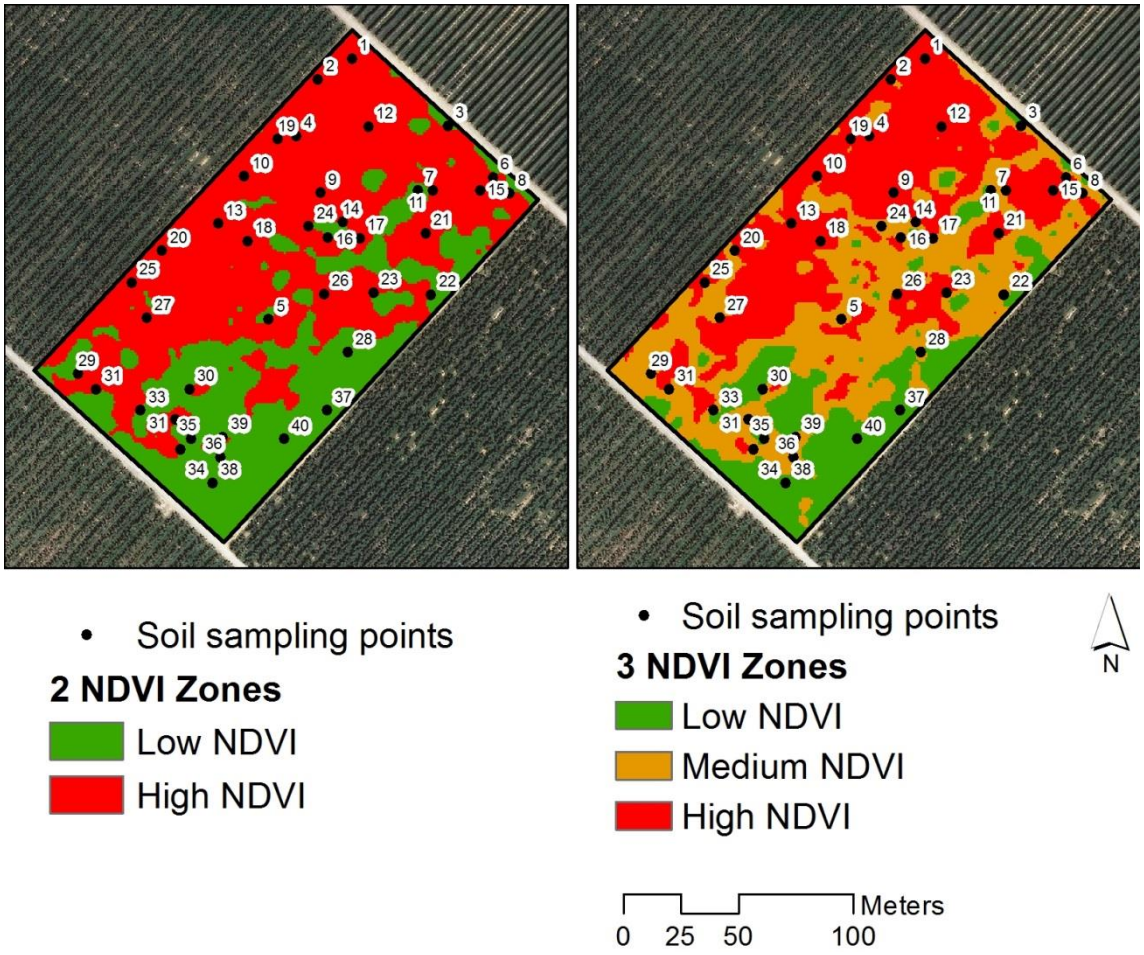

Figure 43. 2 (left) or 3 (right) zones of NDVI as result of the Isodata unsupervised classification. The soil sampling points are overlaid.

5.4.5. Summary of ANOVA

As summary, Table 22 presents the counting of the number of soil properties that had different average values either in EC_{25} or NDVI zones. The Shallow and Deep EC_{25}-2 Zones were the classes that served to distinguish more soil properties (7 or 6, respectively). Two zones of EC_{25} were always better than 3 zones, since the number of properties that could be differentiated was lower (4 in both cases). The zoning based on Shallow and Deep EC_{25} together, did not improve the results either. Regarding the soil properties that could be differentiated by the NDVI classes, were almost the same in number as for the 2 zones of Shallow or Deep EC_{25}. Nevertheless, the properties were different in both cases. While the Shallow or Deep EC_{25} were more related to $CE_{1:5}$, water

retention capacity, sand content and soil depth; the NDVI was more related with finer textural fractions (silt and fine sand) and the cation exchange capacity, but not with depth.

Variable	Soil properties with p-value < 0.05	Soil properties with p-value < 0.1	Total
Shallow EC_{25}-2 Zones	6	1	7
Deep EC_{25}-2 Zones	5	1	6
Shallow EC_{25}-3 Zones	2	1	3
Deep EC_{25}-3 Zones	3	1	4
Shallow-Deep EC_{25} 2 Zones	4	0	4
Shallow-Deep EC_{25} 3 Zones	2	2	4
NDVI-2 Zones	5	0	5
NDVI-3 Zones	6	0	6

Table 22. Summary of ANOVA test between EC_{25} or NDVI zones and soil properties of the top soil layer (0-30 cm).

In summary, as shown in Table 22, the ANOVA tests performed better for the 2 Shallow EC_{25} zones. For the NDVI 3 zones were apparently better than 2. Nevertheless, in the case of these 3 different groups, there were only “a”, “b” or “ab” groups, but not “a”, “b” and “c” distinct groups. Because of that, here it will be proposed to do different actions in 2 NDVI zones instead of 3.

5.4.6. Differences between shallow EC_{25} and NDVI 2-zones

One question that arises from the above results is that the shallow EC_{25} zones were not able to differentiate NDVI values or the NDVI zones were not able to differentiate EC_{25} values within the zones. However, both types of zones were related to some soil textural fractions in the same way. This suggest that part of the EC_{25} zones may be coincident with the NDVI zones but there could be something altering the relationship that makes that it is not significant.

To look for the possible explanation of this lack of relationship, a combined map with the shallow EC_{25} zones and the NDVI zones was created (Figure 44). It can be observed that there were coincident areas between low EC_{25} and low NDVI or high EC_{25} zones and high NDVI, and those represent the major part of the study plot (approximately 63.7% of the area, see the green colors). The main different zones were located where the old terraces had been in the past, before the land transformation. The removing of the terraces and the leveling have influenced (or broken) the continuity of the soil properties. This can be seen in the main brownish colored areas of the figure. Because of this and of the drip irrigation system, there was not a total or majoritarian coincidence of the zones, since in the low EC_{25} zone the trees are well maintained thanks to the irrigation system.

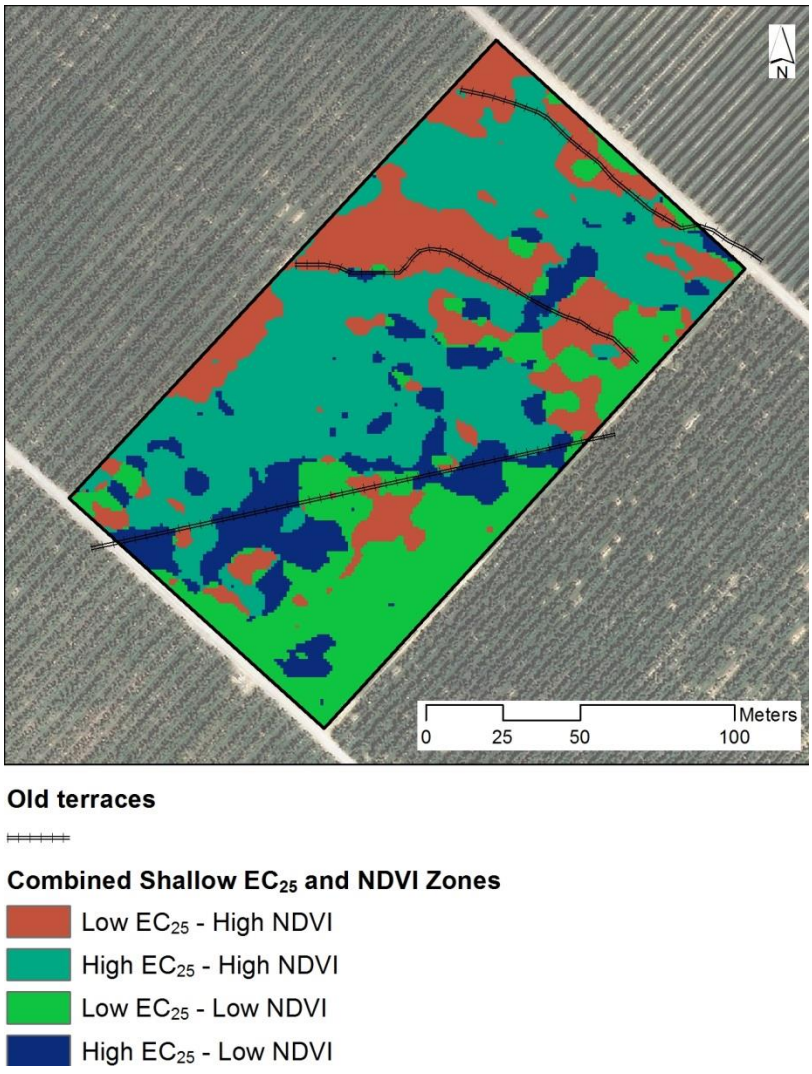

Figure 44. Combination of the shallow EC_{25} and NDVI 2-zones with old terraces overlaid.

5.5. Relationship between NDVI and measured vigor parameters

This section presents the results of the relationships between the NDVI per tree, obtained from the multispectral image and some vegetation parameters indicative of the vigor of the trees (trunk diameter and tree canopy area). The trunk diameter was measured in the peach plantation in 103 trees and the tree canopy area was derived from the reclassification of the NDVI image according to the 0.50 threshold.

5.5.1. NDVI and trunk diameter

As expected, a positive and significant relationship (p-value < 0.01) between NDVI and trunk diameter was found in the peach plantation. Trees with bigger trunk diameter had higher NDVI values (Figure 45). In this figure, also the linear regression equation is presented. The coefficient of determination (R^2) was relatively low (0.377).

The low variance explained in this relationship could be influenced by the tree canopy area. In some cases, trees relatively small (with lower trunk diameter values) also presented high NDVI values. This occurred in the case of young trees that were replanted because of the failure of the original ones. In these cases the trees present a good development, with high vigor, but the diameter was still lower than those originally planted. Because of that, a tree canopy area coefficient was considered to correct the NDVI depending on their canopy area, which is presented and discussed here below.

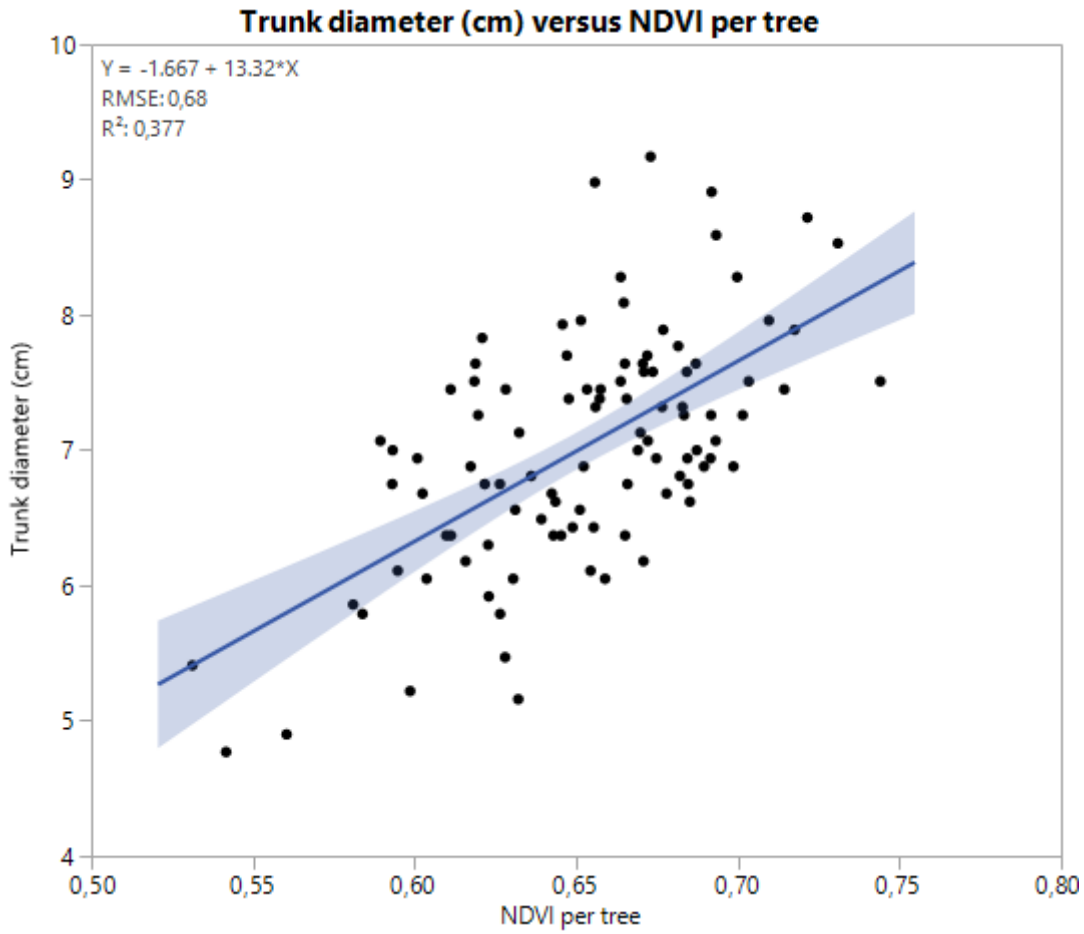

Figure 45. Linear regression analysis between the trunk diameter and the NDVI per tree measured from the multispectral airborne image. N = 100 (3 outliers were excluded from the original 103 sampled trees).

Similar relationships have been found by other researchers. According to Wang et al. (2010), tree ring radius and diameter increase are strongly correlated with NDVI of the same growing season. Probably, higher vigor is determined by better soil conditions and by an adequate irrigation, which is reflected in a higher trunk diameter.

5.5.2. NDVI and corrected tree canopy area

NDVI was corrected according to a tree canopy area coefficient, with the following formula (Equation 5), to compensate the influence of the canopy area in the relationship with the trunk diameter:

Equation 5

$$\mathbf{NDVI_i} \cdot \frac{\mathbf{TCA_i}}{\mathbf{TCA_{max}}}$$

where $NDVI_i$ is the NDVI of a specific tree, TCAi is the tree canopy area of that specific tree and TCA_{max} is the maximum tree canopy area in the plantation (5.5 m^2 in the present case).

The result of the linear regression analysis can be seen in Figure 46. It shows how the relationship with the trunk diameter improved with respect the previous case, with R^2 = 0.469. Therefore, the corrected NDVI would be better in predicting the trunk diameter than the NDVI without correction in the case of tree plantations.

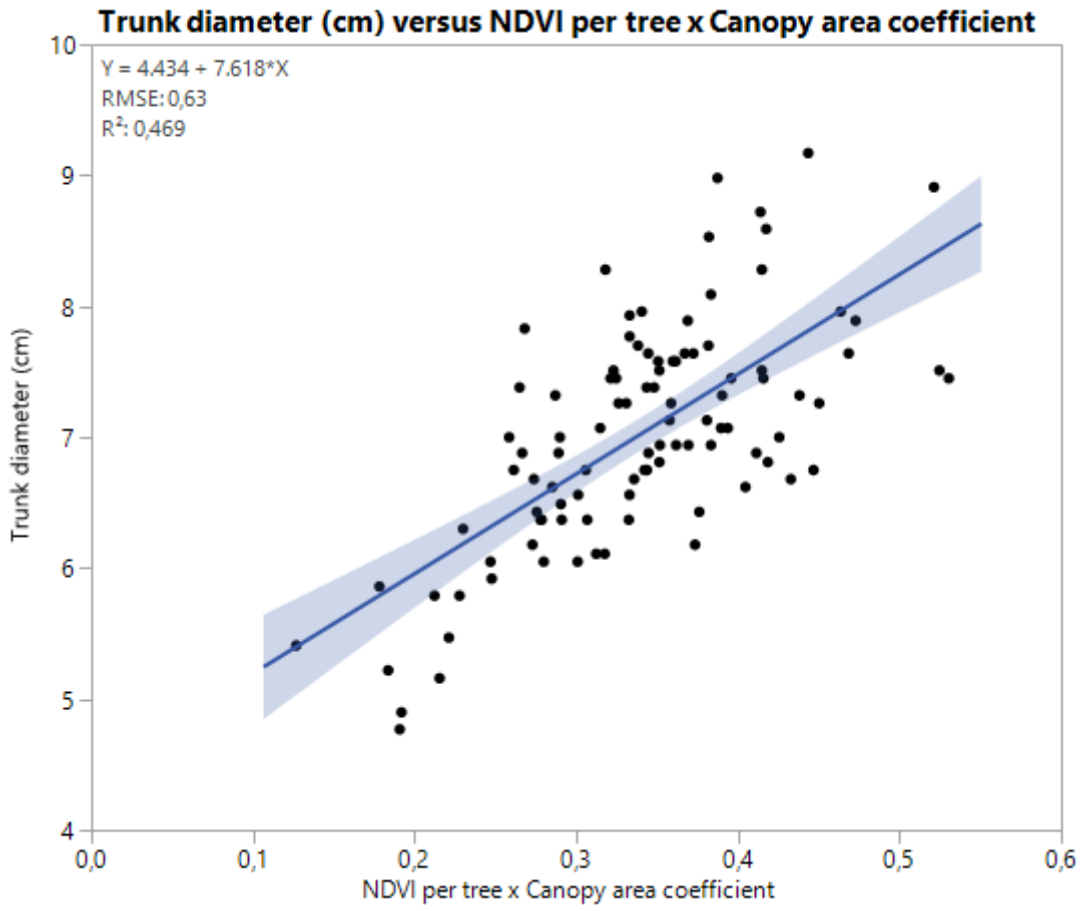

Figure 46. Linear regression analysis between the trunk diameter and the NDVI per tree corrected by the tree canopy area. N = 100 (3 outliers were excluded from the original 103 sampled trees).

5.5.3. NDVI and number of fruits

The result of the linear regression between the NDVI corrected by the area coefficient and the number of fruits can be seen in Figure 47. It shows that there was a linear relationship between the variables (p-value < 0.01) but it was weak $R^2 = 0.227$. This weak relationship could be due to the manual thinning of the fruits, which was done at the beginning of May 2016. In this case, the workers estimate the number of fruits to thin according to their experience, and cannot be directly related to the vigor of the tree. Then, although a linear relationship was found, it was considered weak to estimate the final number of fruits in the whole peach plantation without a considerable error.

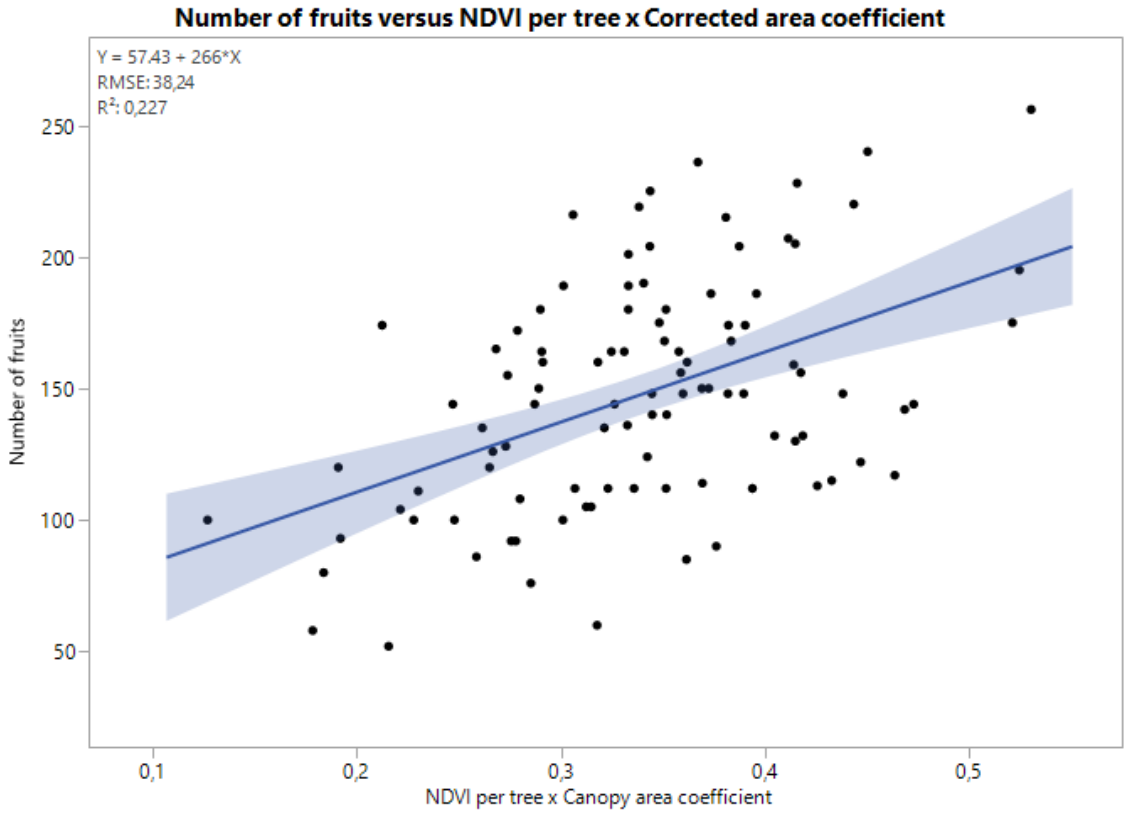

Figure 47. Linear regression analysis between the number of fruits and the NDVI per tree corrected by the tree canopy area. N = 100 (3 outliers were excluded from the original 103 sampled trees).

5.5.4. Trunk diameter and tree canopy area

Finally, the relationship between the trunk diameter and the tree canopy area was calculated. The results are presented in Figure 48. The relationship was similar to the previous one between the corrected NDVI and the trunk diameter. This was expected, because the tree canopy area was derived from the NDVI by reclassification according to a threshold. Also, trees with higher diameter were expected to have higher canopy area and higher vigor as well.

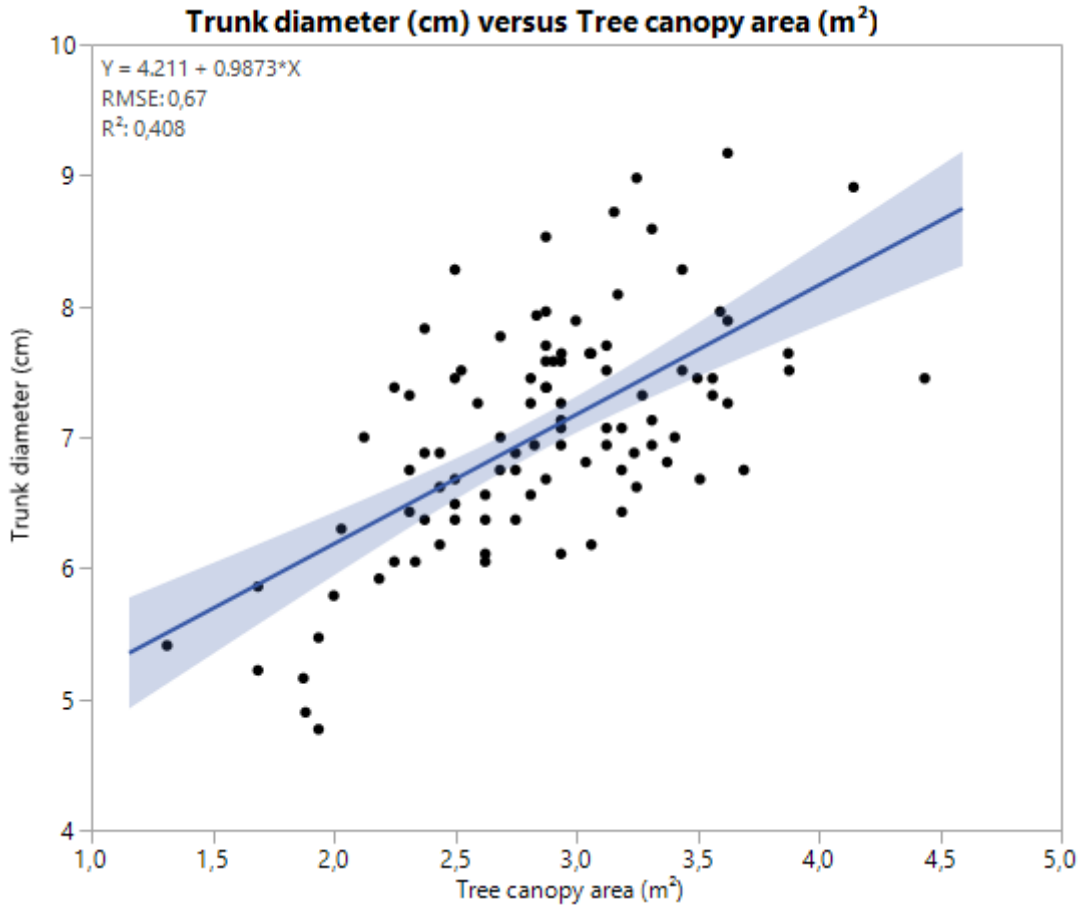

Figure 48. Linear regression analysis between the trunk diameter and the tree canopy area. N = 100 (3 outliers were excluded from the original 103 sampled trees).

5.6. Proposal of differential management actions

At present, the case study peach plantation is uniformly managed, without applying differential management according to precision agriculture directives. It means that the same amount of fertilizers, iron chelates, pesticides, irrigation water and other inputs are applied in whole the plot. Also other actions such as pruning or fruit thinning are done more or less uniformly, according to the experience of the workers.

In this work, spatial variability of soil properties through the ECa and of vegetation vigor of the peach trees through the NDVI were analyzed and confirmed. The results of the analysis could serve to propose different management actions to improve the productivity of the orchard. The different actions are proposed here below.

5.6.1. Delineation of management zones based on Shallow EC_{25}

According to the results of the research, the best variable to define possible management zones in the orchard is the shallow EC_{25} in 2 zones (Table 22). As stated above (section 5.4.2), the soil properties explaining the EC_{25} signal would be pH, $EC_{1:5}$, WRC -33kPa, WRC -1500kPa, clay content, coarse sand and soil depth. The EC_{25} zones clearly differentiate soil properties related to salts content, water retention capacity, texture and soil depth.

In this case, the actions that could be proposed in the shallow EC_{25} zones would be:

- **Low EC_{25} zone**: Here there is a lower water retention capacity and higher sand content. The proposed action is to carry out organic matter amendment to increase the water retention capacity of the soils. This action will also favor the improvement of soil structure.

  The irrigation system also could be modified in this zone by changing the distance between the drips in the drip lines, in order to supply more water to compensate for the lower water retention capacity and shallower soils.

- **High EC_{25} zone**: Here there is a higher salt content. The proposed action is to carry out a subsoiling to favor natural drainage with rainfall. This is because with the drip irrigation system in the plantation is difficult to leach the excess of salts. Although these salts are mainly out of the irrigation bulb, it would favor the leaching from the plot.

One of the necessary and costly inputs in the peach plantation is the iron chelates. It had been interesting to adjust the doses according to the zones. However, the calcium carbonate is very high in the whole plot, without distinction between the EC_{25} zones, and because of that different doses cannot be recommended in the low or high EC_{25} zones.

5.6.2. Delineation of management zones based on NDVI

According to the expressed in the section 5.4.5, the actions that could be proposed in the NDVI 2-zones would be:

- **Low NDVI zone**: It corresponds with textures of higher sand content, and lower CEC (poorer fertility) which would require amendment with organic matter. This zone would also require more frequent application of fertilizers. Trees in this zone would require less fruit thinning and pruning intensity. In this zone a higher irrigation frequency could be established.

- **High NDVI zone**: It corresponds with lower content of sand and higher of silt, and with higher CEC. Trees in this zone have a higher development that could be regulated with growth regulators or higher intensity pruning. Also trees can require a more intensive fruit thinning.

6. Conclusions

The present work constitutes a contribution to the application of precision agriculture (PA) techniques in fructiculture, which was found that are not so extensively used as in arable crops. In this respect, it was demonstrated that in a relatively small orchard it can exist an important spatial variation of soil properties and plant vigor, which can justify the application of PA techniques.

The results of the research showed that the land transformation carried out starting in the 1980 decade to enlarge fields to favor the design and mechanization of orchards, have altered the spatial distribution and continuity of soil properties. This was mainly due to the removing of terraces and levelling works. In this respect, the ECa survey carried with the Veris 3100 sensor allowed to map these discontinuities.

Although a relationship between apparent electrical conductivity and peach tree vigor could be expected, in the present case study it was not found, even in the case of trees in soils with salt content above the tolerance. This could be due to drip irrigation (and fertirrigation) system in the plot, which maintains the trees free of high saline contents.

Because of the lack of relationship between EC_{25} and NDVI, it is better to propose two types of management zones, depending on the objective of the differential management action to carry out. In any case, 2 zones of EC_{25} or NDVI are better than 3 zones, because one of the 3 is always ambiguous. Regarding shallow or deep EC_{25} zones, the shallow zones were better than the deep since only the soil properties of the top horizon (0-30 cm) could be analyzed.

- The Shallow EC_{25} zones would serve mainly to improve the water retention capacity through amendments with organic matter and more frequent irrigation; and to improve natural drainage.
- The NDVI zones would serve as reference to regulate tree vigor and yield through different actions as pruning, growth regulators or fruit thinning.

To reduce the salt content it could be necessary to change the irrigation system to allow a leaching water fraction. Nevertheless, this is not possible at present and because of that

here some actions as subsoiling have been proposed to improve the natural drainage of the plot.

The results also served to confirm the expected relationships between NDVI and trunk diameter, tree canopy area and number of fruits. The NDVI corrected by the canopy area coefficient performed better than the NDVI by itself. However, other expected relationships, as the one between EC_{25} and clay content, were not found. This could be probably due to the mask effect of the salts in the ECa signal.

Finally, further research is necessary to explore other possible relationships between soil properties in deeper horizons and the ECa signal and/or NDVI, since these could not be carried out in the present work because the lack of time to analyze them. These data will be analyzed in the frame of the research project that is carried out in the study area, in which complementary experiments are being done (e.g. Lidar data acquisition, LAI, red-edge vegetation index, canopy temperature and yield).

7. Bibliographic references

Boelman, N.T., Stieglitz, M., Rueth, H.M., Sommerkorn, M., Griffin, K.L., Shaver, G.R., Gamon, J.A., 2003. Response of NDVI, biomass, and ecosystem gas exchange to long-term warming and fertilization in wet sedge tundra. Oecologia, 135, 414–421.

Bonfante, A., Agrillo, A., Albrizio, R., Basile, A., Buonomo, R., De Mascellis, R., et al. 2015. Functional homogeneous zones (fHZs) in viticultural zoning procedure: An Italian case study on Aglianico vine. SOIL, 1, 427–441.

Brevik, E., Fenton, T., Lazari, A., 2006. Soil electrical conductivity as a function of soil water content and implications for soil mapping. Precision Agriculture, 7, 393–404.

Bronson, K., Booker, J., Officer, S., Lascano, R., Maas, S., Searcy, S., et al., 2005. Apparent electrical conductivity, soil properties and spatial covariance in the U.S. southern high plains. Precision Agriculture, 6, 297–311.

Burger, H.R., 1992. Exploration Geophysics of the Shallow Subsurface. Prentice Hall PTR, Upper Saddle River, NJ.

Buurman, P., van Lagen, B., Velthorst, E.J., 1996. Manual for soil and water analysis. Leiden, Backhuys.

Corwin, D.L., Hendrickx, J.M.H., 2002. Solute content and concentration – indirect measurement of solute concentration – electrical resistivity: Wenner array. In: Dane, J.H., Topp, G.C. (Eds.), Methods of Soil Analysis, Part 4 – Physical Methods. Soil Science Society of America, Madison, WI, USA, 1282–1287.

Corwin, D.L., Lesch, S.M., 2003. Application of soil electrical conductivity to precision agriculture: theory, principles and guidelines. Agronomy Journal, 95, 455–471.

Corwin, D.L., Lesch, S.M., 2005. Characterizing soil spatial variability with apparent soil electrical conductivity. Part II. Case study. Computers and Electronics in Agriculture, 46, 135–152.

Corwin, D.L., Lesch, S.M., 2005a. Characterizing soil spatial variability with apparent soil electrical conductivity: I Survey protocols. Computers and Electronics in Agriculture, 46, 103–133.

Dirección General de Política Alimentaria (Espanya), 1986. Métodos oficiales de análisis, Tomo 3. Madrid: Ministerio de Agricultura, Pesca y Alimentación.

Dobrin, M.B., 1960. Introduction to Geophysical Prospecting. McGraw-Hill, New York, USA.

Domsch, H., Giebel, A., 2004. Estimation of soil textural features from soil electrical conductivity recorded using the EM38. Precision Agriculture, 5, 389–409.

Doolittle, J.A., Brevik, E.C., 2014. The use of electromagnetic induction techniques in soils studies. Geoderma, 33–45.

Fortes, R., Prieto, M.H., Terrón, J.M., Blanco, J., Millán, S., Campillo, C., 2013. Using apparent electric conductivity and NDVI measurements for yield estimation of processing tomato crop. American Society of Agricultural and Biological Engineers, 57, 827-835.

Gomez, C., Viscarra Rossel, R.A., McBratney, A.B., 2008. Soil organic carbon prediction by hyperspectral remote sensing and field vis-NIR spectroscopy: an Australian case study. Geoderma, 146, 403–411.

Guo, W., Maas, S.J., Bronson, K.F., 2012. Relationship between cotton yield and soil electrical conductivity, topography, and Landsat imagery. Precision Agriculture, 13, 678–692.

Hanson, B.R., Kaita, K., 1997. Response of electromagnetic conductivity meter to soil salinity and soil-water content. Journal of irrigation and drainage engineering, 123, 141–143.

Ilaco, BV., 1985. Agricultural compendium for rural development in the tropics and subtropics. Elsevier Science Publisher, Amsterdam.

IUSS Working group WRB, 2007. World Reference Base for Soil Resources. World Soil Resources Reports, 103, FAO, Rome.

Jensen, JR., 1996. Introductory digital image processing: remote sensing perspective. 2nd ed. Prentice-Hall, Englewood Cliffs, NJ, USA.

Johnson, C.K., Eskridge, K., Corwin, D.L., 2005. Apparent soil electrical conductivity: applications for designing and evaluating field-scale experiments. Computers and Electronics in Agriculture, 46, 181–202.

Johnson, C.K., Nortensen, D.A., Wienhold, B.J., Shanahan, J.F., Doran, J.W., 2003. Site-specific management zones based on soil electrical conductivity in a semiarid cropping system. Agronomy Journal, 95, 303-315.

Kalra, Y.P., Maynard, D.G., 1991. Analytical Services Labortory, Methods manual for forest soil and plant analysis. Edmonton, Alta: Forestry Canada, Northwest Region, Northern Forestry Centre, 17-86.

King, J., Dampney, P., Lark, R., Wheeler, H., Bradley, R., Mayr, T., 2005. Mapping potential crop management zones within fields: use of yield-map series and patterns of soil physical properties identified by electromagnetic induction sensing. Precision Agriculture, 6, 167–181.

Kitchen, N.R., Sudduth, K.A., Drummond, S.T., 1999. Soil electrical conductivity as a crop productivity measure for claypan soils. Journal of Production Agriculture, 12, 607–617.

Ma, R., McBratney, A., Whelan, B., Minasny, B., Short, M., 2010. Comparing temperature correction models for soil electrical conductivity measurement. Precision Agriculture, 12, 55–66.

Martínez, G., Vanderlinden, K., Pachepsky, Y., Espejo, A., Gira´ldez, J.V., 2012. Estimating topsoil water content of clay soils with data from time-lapse electrical conductivity surveys. Soil Science, 177, 369–376.

Martinez Casasnovas, J.A., Agelet-Fernandez, J., Arno, J., Ramos, M.C., 2012. Analysis of vineyard differential management zones and relation to vine development, grape maturity and quality. Spanish Journal of Agricultural Research, 10, 326-337.

Martínez Casasnovas, J.A., Antúnez, M., Margarit, J., 2010. Mapa Geològic de Catalunya. Geotreball IV. Mapa de Sòls. Sarroca de Lleida 416-1-1 (63-31) 1:25000. Institut Cartogràfic i Geològic de Catalunya. Barcelona.

Martínez Casasnovas, J.A., Antúnez, M., Roca, J., 1992. Mapa de suelos detallado (1:25000) y evaluación para riego del área regable por el canal de "les Baixes Garrigues" (El Segrià. Lleida). Departament de Meteorologia i Ciència del Sòl, UPC, Lleida. (Unpublished).

McCormick, S., Jordan, C., Bailey, J., 2009. Within and between-field spatial variation in soil phosphorus in permanent grassland. Precision Agriculture, 10, 262–276.

Moral, F., Terro´n, J., Marques da Silva, J., 2010. Delineation of management zones using mobile measurements of soil apparent electrical conductivity and multivariate geostatistical techniques. Soil & Tillage Research, 106, 335–343.

Osman, K.T., 2013. Soils: Principles, properties and management. Springer Science+Bussiness, Dordrectch, The Netherlands, 29, 607.

Page, A.L., Miller, R.H., Keeney, D.R., 1982. Methods of soil analysis, part 2, Madison, Wis.: American Society of Agronomy : Soil Science Society of America, 149-693.

Palmieri, A., Pirazzoli, C., 2013. Scenari futuri e opportunità di mercato per la frutticoltura italiana. Frutticoltura Journal, 9, 6-8.

Pascual, M., Urbina, V., Dalmases, J., Nolla, JM., 2006. Historia y situación actual de la fruticultura en Lleida. Fruticultura profesional, 158, 5-15.

Porta, J., López-Acevedo, M., Roquero, C., 2003. Edafología para la agricultura y el medio ambiente, 3a edition. Mundi-Prensa, Madrid.

Rhoades, J.D., Halvorson, A.D., 1977. Electrical conductivity methods for detecting and delineating saline seeps and measuring salinity in Northern Great Plains soils, ARS W-42. USDA-ARS Western Region, Berkeley, CA, USA, 1–45.

Rhoades, J.D., 1999. Soil salinity assessment: methods and interpretation of electrical conductivity measurements. FAO, Irrigation and Drainage, 57, 1–150.

Rouse, J.W., Haas, R.H., Schell, J.A., Deering, D.W., 1974. Monitoring vegetation systems in the Great Plains with ERTS, 301–317.

Saey, T., Simpson, V. H., Cockx, L., Van Meirvenne, M., 2009a. Comparing the EM38DD and DUALEM-21S sensors for depth-to-clay mapping. Soil Science Society of America Journal, 73, 7–12.

Scudiero, E., Teatini, P., Corwin, D.L, Deiana, R., Berti, A., Morari, F., 2013. Delineation of site-specific management units in a saline region at the Venice Lagoon margin, Italy, using soil reflectance and apparent electrical conductivity. Computers and Electronics in Agriculture, 99, 54–64.

Serrano, J.M, Shahidian, S., Marques da Silva, J.R., 2013. Apparent electrical conductivity in dry versus wet soil conditions in a shallow soil. Precision Agriculture 14, 99–114.

Soil Survey Staff, 1975. Soil Taxonomy – A basic System of soil classification for making and interpreting soil surveys. Agriculture Handbook 436. Soil Conservation Service, US Department of Agriculture, Washington D.C.

Soil Survey Staff, 2014. Keys to Soil Taxonomy. Twelfth Edition. US Department of Agriculture. Natural Resources Conservation Service, Washington D.C.

Stafford, J.V., 2000. Implementing precision agriculture in the 21st century. Journal of Agricultural Engineering Research, 76, 267-75.

Street, L.E., Shaver, G.R., Williams, M., van Wilk, M.T., 2007. What is the relationship between changes in canopy leaf area and changes in photosynthetic CO2 flux in arctic eco-systems. Journal of Ecology, 95,139–150.

Sudduth, K.A., Kitchen, N.R., Wiebold, W.J., Batchelor, W.D., Bollero, G.A., Bullock, D. G., et al., 2005. Relating apparent electrical conductivity to soil properties across the north-central USA. Computers and Electronics in Agriculture, 46, 263–283.

Tanji K.K., Kielen N.C., 2002. Agricultural drainage water management in arid and semi-arid areas. FAO Irrigation and Drainage, Rome, paper 61.

Taylor, J.A., McBratney, A.B., Whelan, B.M., 2007. Establishing Management Classes for Broadacre Agricultural Production. Agronomy Journal, 99, 1366-1376.

Telford, W.M., Gledart, L.P., Sheriff, R.E., 1990. Applied Geophysics, 2nd ed. Cambridge University Press, Cambridge, UK.

U.S. Department of Agriculture, Natural Resources Conservation Service,1983. National soil survey handbook, 430-VI.

van Meirvenne, M., Islam, M.M., De Smedt, P., van Meerschman, E., De Vijver, E., Saey, T., 2013. Key variables for the identification of soil management classes in the aeolian landscapes of north-west Europe. Geoderma, 199, 99–105.

van Reeuwijk, L.P., 1995. Procedures for soil analysis. Wageningenm, ISRIC, 1-9.

van Wijk, M.T., Williams, M., 2005. Optical instruments for measuring leaf area index in low vegetation: application in Arctic ecosystems. Ecological Applications, 15, 1462–1470.

Viscarra Rossel, R., Adamchuk, V., Sudduth, K.A., Mckenzie, N., Lobsey, C., 2011.Proximal soil sensing: an effective approach for soil measurements in space and time. Advances in Agronomy, 113, 237–282.

Wanga, J., Richb, P.M , Pricec, K.P, Kettled, W.D., 2010. Relations between NDVI and tree productivity in the central Great Plains. International Journal of Remote Sensing, 25, 3127-3138.

Williams, B.G., Hoey, D., 1987. The use of electromagnetic induction to detect the spatial variability of the salt and clay contents of soils. Australian Journal of Soil Research, 25, 21–27.

World Resources Institute, 1998. World Resources – A Guide to the Global Environment. Oxford University, Press, New York, USA.

Zhang, W., Wang, K., Chen, H., He, X., Zhang, J., 2012. Ancillary information improves kriging on soil organic carbon data for a typical karst peak cluster depression landscape. Journal of the Science of Food and Agriculture, 65, 1094–1102.